FHWA-NJ-2024-001

Innovative Pothole Repair Materials and Techniques
Volume I: Asphalt Pavement

FINAL REPORT

January 2024

Submitted by

Dr. Hao Wang
Professor
Rutgers University

Xiao Chen
Graduate Research Assistant
Rutgers University

NJDOT Research Project Manager
Giri Venkiteela

In cooperation with

New Jersey
Department of Transportation
Bureau of Research
And
U. S. Department of Transportation
Federal Highway Administration

DISCLAIMER STATEMENT

The contents of this report reflect the views of the author(s) who is (are) responsible for the facts and the accuracy of the data presented herein. The contents do not necessarily reflect the official views or policies of the New Jersey Department of Transportation or the Federal Highway Administration. This report does not constitute a standard, specification, or regulation.

TECHNICAL REPORT DOCUMENTATION PAGE

1. Report No. FHWA NJ-2024-001	**2. Government Accession No.**	**3. Recipient's Catalog No.**
4. Title and Subtitle Innovative Pothole Repair Materials and Techniques Volume I: Asphalt Pavement		**5. Report Date** January 2024 **6. Performing Organization Code** CAIT/Rutgers
7. Author(s) Hao Wang, PhD. and Xiao Chen		**8. Performing Organization Report No.**
9. Performing Organization Name and Address Center for Advanced Infrastructure and Transportation Rutgers, The State University of New Jersey 100 Brett Road Piscataway, NJ 08854		**10. Work Unit No.** **11. Contract or Grant No.** NJDOT TO 362
12. Sponsoring Agency Name and Address Federal Highway Administration (SPR) 1200 New Jersey Avenue, SE Washington, DC 20590 New Jersey Department of Transportation (SPR) 1035 Parkway Avenue, P.O. Box 600 Trenton, NJ 08625.0600		**13. Type of Report and Period Covered** Final Report, September 2019 – September 2023 **14. Sponsoring Agency Code** FHWA, NJDOT

15. Supplementary Notes
Conducted in cooperation with the U.S. Department of Transportation, Federal Highway Administration.

16. Abstract
Potholes in asphalt pavement surface have detrimental effects on asphalt pavement deterioration and traffic safety. Cost-effective pothole repair methods are needed for highway agencies at all levels. This project aims to identify and evaluate innovative tools, technologies and materials for pothole repair in New Jersey. The pothole repair methods that have potential to improve the cost-effectiveness of current practice at NJDOT were identified and analyzed using life-cycle cost analysis. The identified technologies and materials were further studied through analytical modeling, laboratory testing, and field implementation. The optimized heating procedures were developed considering heat source, pothole geometry, and weather condition. The effective test procedures and performance requirements on pothole repair materials to ensure good performance and bonding in the field were studied and specified. Finally, the optimized heating procedures for pothole repair and the recommended material products were developed for NJDOT.

17. Key Words Pothole repair; Cold patching; Microwave heating; Infrared heating; Recycled asphalt pavement (RAP), Numerical modeling	**18. Distribution Statement** No restrictions.

19. Security Classif. (of this report) Unclassified	**20. Security Classif. (of this page)** Unclassified	**21. No. of Pages** 100	**22. Price**

Form DOT F 1700.7 (8-72) Reproduction of completed page authorized

ACKNOWLEDGEMENTS

This project was sponsored by the New Jersey Department of Transportation (NJDOT) and the Federal Highway Administration. This project could not have been accomplished without the assistance of numerous individuals. The authors would like to express gratitude to Nicholas Colangelo, Kenrick Layne, Evanylo Jeff and Ladanza Robert from NJDOT, Dr. Thomas Bennert, Edward Wass, Edwin Hass, and Drew Tulanowski from Rutgers University for their support on the project.

TABLE OF CONTENTS

LIST OF FIGURES

LIST OF TABLES

EXECUTIVE SUMMARY

Pothole repair is one of the most important and frequent maintenance activities for highway agencies. Significant amounts of costs and resources are spent in pothole repair for material, labor, equipment, and traffic control. Cost-effective pothole repair methods can reduce or eliminate the possibility of re-patching and save future repair costs. The good condition of pothole repair with less cracking will also prevent reflective cracking when asphalt overlay is placed. Preheating the excavated pothole prior to repair has been found to improve the interface bonding between existing pavements and hot filling material, which can help enhance the overall performance of asphalt patches. The long lifespan of patch will reduce travel delay due to work zone and safety risk of highway users and workers. These will better preserve the condition of highway infrastructure and provide better service to the travel public. On the other hand, as it has been found feasible to incorporate recycled material in asphalt pavement pothole repair, the usage of recycled material can reduce the production of new material, which can contribute towards a more sustainable approach of roadway repair with economic and environmental benefits.

Preheating can be achieved using infrared radiation and microwave. The heating trial tests were performed in a test section with artificial potholes, and the heating performance of different heating methods were evaluated. The results show the infrared radiation can efficiently heat the pothole surfaces and lead to remarkable temperature increase in a short time. Compared with infrared heating, although microwave can heat both surface and internal pavement materials, its heating efficiency is lower. Therefore, infrared heating was adopted as preheating method to repair the potholes in the test section. Subsequently, laboratory analysis was conducted on field cores taken from repaired potholes to verify the effectiveness of preheating. It was found that preheating can enhance not only the interface bonding strength between patching material and surrounding pavement, but also the strength of patching materials themselves.

With the application of preheating, the feasibility of using recycled asphalt pavement (RAP) in pothole repair was investigated. Based on laboratory testing results of the HMA with 0% to 50% RAP contents, HMA with 30% RAP was selected for pothole repair in the field test section because it can lead to satisfactory performance with traditional HMA without preheating method. After repair, field cores were collected for additional laboratory analysis to evaluate the performance of asphalt patch with recycled material. The results show that with the application of preheating, asphalt patches repaired by HMA with 30% RAP can achieve comparable or better performance than that made with traditional HMA.

INTRODUCTION

Background and Motivation

Pothole is a bowl-shaped depression in asphalt pavement surface that affects both pavement deterioration and traffic safety. Potholes usually result from gradual damage caused by traffic, moisture, freeze-thaw action, poor underlying support or some combination of these factors [(1)]. The LTPP distress manual published by FHWA defines that the pothole has the minimum plane dimension of 150 mm and the severity levels of pothole depends on the depth of pothole (low: <25mm; medium: 25-50mm; high: >50mm) [(2)].

Pothole repair is one of the most important and frequent maintenance activities for highway agencies. It is generally performed either as an emergency repair under harsh conditions, or as routine maintenance scheduled for warmer and drier periods. Unprepared pothole could result in potential traffic safety problems. Highway agencies must take into consideration the level of traffic, the tolerance of traveling public, the availability of personnel, equipment and materials and so on to decide whether a pothole should be repaired temporally or permanently.

Currently, many pothole repair technologies are available, while they should be adopted under different conditions such as the weather, time, cost and so on. As reported by the NCHRP Synthesis 463 [(3)], the most common asphalt pavement patch materials are hot mix asphalt (HMA), generic stockpile, spray emulsion and aggregate and proprietary asphalt mix, as shown in Figure 1. Comparing different repair technologies and selecting an appropriate one could not only achieve the best cost-effectiveness, but also improve the safety on the road.

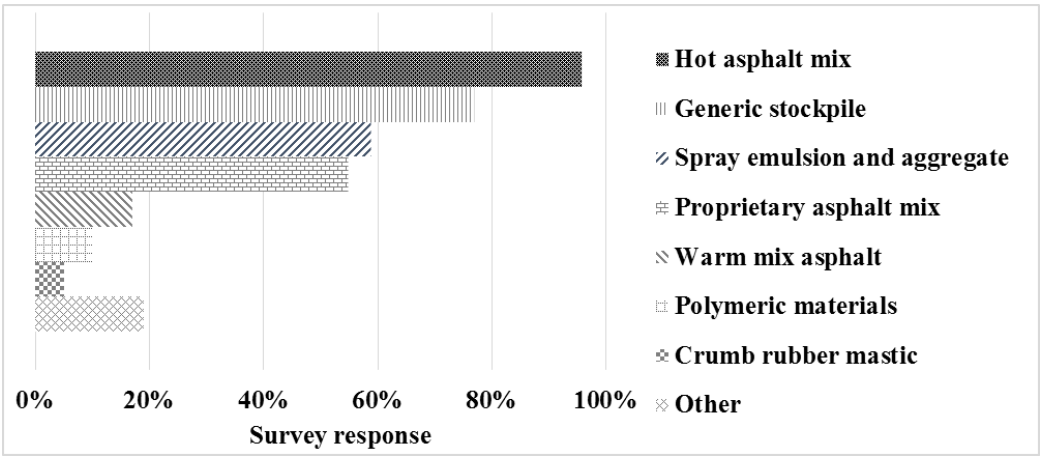

Figure 1. Materials used for asphalt pavement patches (McDaniel et al. 2014)

Although the ideal patch material is HMA that provides the best quality of pothole repair, it has limited applicability for pothole repair because of the minimum production amount and the laydown temperature constraint. Potholes are more often formed during winter seasons after freeze-thaw cycles. In this case, cold mix asphalt (CMA) is typically used with high flexibility. Small amounts of CMA could be used to repair individual potholes

with high flexibility, especially under cold weather conditions. However, the use of CMA may result in reduced adhesion to the existing pavement material and delayed strength formation in the pothole fill material, leading to cracking or depression at patches. Therefore, it is necessary to evaluate the repair effectiveness of CMA materials on the market based on standard test methods and field performance observations.

Recently, many researchers have suggested to preheat the excavated pothole before filling the hole, which could improve the interface bonding conditions between the patch materials and the surrounding pavements [4,5]. Additionally, heating can be used to remove defected material, ensuring that the temperature is sufficiently high to compact the filled hot-mix asphalt, and aid in drying the surface and pore spaces of the pothole area. However, no standard procedures of preheating methods could be followed. It is expected that the surface temperature in the pothole and host pavement are affected by the heating method, duration, pothole depth, and climate condition. The heating procedure needs to be optimized to satisfy the repair requirement and at the same time maintain high productivity without increasing additional traffic control time and labor cost significantly. In addition, the curing process of CMA involves the evaporation of water and volatile matter and the initiation of emulsion rupture. The effect of heating on the strength forming mechanism of CMA has not been studied.

Objective and Scope

The objective of this project is to identify and evaluate innovative tools, technologies and materials for repairing the potholes in New Jersey's asphalt concrete pavements. Based on the objective, an integrated research methodology composed of literature synthesis, experimental and numerical investigation, and life-cycle cost analysis is proposed. The scope of work includes:

- Conduct comprehensive literature review on 1) traditional pothole repair techniques and compare their advantages and limitations, 2) potential preheating methods and their working principles, material requirements, and heating efficiency. 3) cold mix asphalt (CMA) materials used in pothole repair, including proprietary materials and modified cold mix with different additives.

- Summarize field performance of asphalt patches repaired by traditional techniques and new heating techniques with various patching materials. Conduct life-cycle cost analysis (LCCA) of pothole repair with heating method to analyze the cost-effectiveness as compared to traditional methods.

- Investigate the performance of microwave and infrared heating methods in the test section. Adopt appropriate heating procedure to repair artificial potholes in the test section, and then conduct laboratory analysis to evaluate the effect of preheating on performance enhancement of asphalt patch.

- Evaluate the mechanical performance of different patching materials in laboratory, including bulk CMA, different commercial CMA, and hot mix asphalt (HMA) with recycled asphalt pavement (RAP). Determine the optimal RAP content for pothole

repair in the test section and conduct laboratory analysis to evaluate the feasibility of using RAP in asphalt pavement pothole repair.

- Develop microwave and infrared heating models and validate them against the field measurements. Predict the required heating time for pothole repair under different filed conditions.

The research outcome will provide recommendations for future implementation of pothole repair on the New Jersey roadway. The application preheating method can help provide the enhanced performance of asphalt patch and thereby reduce frequency of a second repair. The usage of recycled material in pothole repair will help save energy and natural resources, and reduce greenhouse gas (GHG) emission generated from producing new HMA.

LITERATURE REVIEW

Traditional Pothole Repair Technology

Throw and go

Throw and go is a widely used method adopted by many states. Although it is not considered the best pothole repair method, it is commonly used due to its high rate of production. It uses conventional HMA or CMA to fill the pothole with the initial compaction of the back face of the shovel, and the common compaction is left to the passing traffic. In most maintenance activities, the potholes are not heated, dried, or even cleaned prior due to time. The life of these repairs typically ranges from a few hours to a few weeks.

The throw and go method can be conducted based on the following steps:

1. Throw the patching material into the hole without cleaning.
2. Compact the materials with the back face of a shovel.
3. Open the repaired section to traffic as soon as maintenance workers and equipment are cleared from the area.

Throw and roll

The procedure named throw and roll is considered as a superior substitute to the traditional throw and go method. The difference between them is that some effort is made to compact the potholes with truck tires in throw and roll method. The compaction of the potholes generally takes 1-2 minutes per patch and would not significantly affect productivity.

The throw and roll method consists of the following steps:

1. Place the material into a pothole (which may or may not be filled with water or debris) as shown in
2. Figure 2(a).
3. Compact the patch using truck tires, as shown in
4. Figure 2(b).
5. Verify that the compacted patch has some crown with a height between 0.38cm to 0.64cm.
6. Open the repaired section to traffic as soon as maintenance workers and equipment are removed from the area.

(a)

(b)

Figure 2. Repair procedure of Throw and Roll: (a) Placing materials, (b) Compact using tires [1]

Semi-permanent

This procedure is considered as one of the best for repairing potholes. It is a more-involved throw and roll procedure and can be considered as a partial-depth repair. The time and effort needed to perform this procedure are thought to improve the success rates for patches. This method provides a sound area for patches and results in very tightly compacted patches.

The semi-permanent method consists of the following steps:

1. Remove all water and debris from pothole using compressed air, brooms, shovels, or other available equipment.
2. Square up the sides of the pothole until vertical sides exist in reasonably sound pavement, as shown in Figure 3(a).
3. Place the patching material into the cleaned, squared hole. The material should mound in the center and taper down to the edges so that it meets the surrounding pavement edge.
4. Compact the material starting in the center and working out toward the edges, which will cause the material to pinch into the corners. As shown in Figure 3(b), a one-man compaction device, such as a single-drum vibratory roller or vibratory plate compactor work best.
5. Open the repaired section to traffic as soon as maintenance workers and equipment are removed from the area.

(a) (b)

Figure 3. Repair procedure of Semi-permanent: (a) Straighten up pothole edges, (b) Compaction of patching materials [1]

Spray injection

The spray injection is another method that has been used for patching potholes. This technique has a high rate of productivity and lower material costs. It utilizes air pressure as the main source of compaction. The air pressure also works to dry the hole and remove water. Spray-injection patching devices are capable of producing good patches when good quality, compatible aggregate and binder are used. This procedure requires no compaction after the cover aggregate has been placed. The repair process is shown in

Figure 4.

The spray injection method consists of the following steps:

1. Clean water and debris from the pothole, as shown in Figure 4(a).
2. Spray the bottom and sides of the pothole with binder materials to act as tack coat. Subsequently, spray aggregate and binder into the pothole until the pothole is filled just above the level of the surrounding pavement, which is shown in Figure 4(b).
3. Cover the patched area with a layer of aggregate, as Figure 4(c) shows.
4. Open the repaired section to traffic as soon as maintenance workers and equipment are removed from the area.

(a) (b) (c)

Figure 4. Repair process of Spray injection: (a) Blowing water and debris, (b) Blowing patching materials, (c) Covering patch with aggregates [(1)]

Edge seal

Edge seal method is throw-and-roll procedure plus edge sealing using asphalt tack and sand on the road surface. However, this method requires a second pass through the repair area. A ribbon of asphaltic tack material is placed on the patch edge, and a layer of sand is placed on it. Although this does reduce the productivity of the procedure, the placement of the tack material prevents water from getting through the edge of the patch and can glue together pieces of the surrounding pavement, improving support for the patch.

The edge seal method consists of the following steps:

1. Place material into the pothole (no clean of water or debris is needed prior to material placement).
2. Compact the patching material using truck tires (between four and eight passes) leaving a 0.38-cm- to 0.64-cm-high crown.
3. Allow pavement and patch surfaces to dry, generally one day after the installation. Place a band of asphalt tack coat material, 10-cm- to 15-cm-wide, along the perimeter of the patch.
4. Place a layer of cover aggregate like coarse sand over the tack material to prevent tracking.
5. Open the repaired section to traffic as soon as maintenance workers and equipment are removed from the area.

Other procedures

Participating agencies in Illinois and Oregon took advantage of placing one additional material or procedure beyond the above methods. The method used by agencies in Oregon consists of the following steps [1]:

1. Remove water and debris from the pothole.
2. Place asphalt emulsion into the pothole as tack coat.
3. Heat tack coat using propane torch to get the emulsion to break faster.
4. Heat the cold mix with the propane torch to make it easier to place and to improve the mixtures compaction.
5. Compact patch with the truck (between four and eight passes) and verify that the compacted patch has some crown with a height between 0.38cm to 0.64cm.
6. Open the repaired section to traffic as soon as maintenance workers and equipment are removed from the area.

Agencies in Illinois proposed an additional repair procedure beyond throw and roll method [1]. The additional repair procedure used in Illinois before opening the traffic is to cover the entire surface of the patch by applying emulsions and crushed aggregates to prevent tracking in the day after the patches are placed.

Comparisons between pothole repair technologies

When selecting the optimal pothole repair technology, many factors need to be taken into consideration, such as the pothole size, the traffic flow, the crew experience, the required time, materials, equipment, costs and so on. Table 1 summarizes the advantages and limitations of each pothole repair technology.

Generally, throw and roll method is superior to throw and go in all sites due to its initial compaction with no significant effect on its productivity, this is especially true if the areas to be patched are separated by long distances and most of the time is spent traveling between potholes [1]. Also, edge seal has some advantages over throw and roll because it has an additional procedure to apply asphalt tack and sand on the pavement surface, preventing the water from the edge of the patch and enabling adequate bonding at patch edges; nevertheless, the second pass in edge seal may lower its productivity. Similarly, the second pass needed in the repair procedure used in Illinois discounts its advantage over throw and roll method.

Pothole patching can be performed during various weather conditions, with temperatures anywhere from to -18℃ and 38℃. When cold temperatures and precipitation happen under winter conditions, the pothole is expected to be repaired as quickly as possible; thus, semi-permanent is not recommended for use due to its increase in time required, higher labor and equipment cost, and lower productivity [6]. Alternatively, the throw and roll and spray-injection procedures could be used because they can produce high-quality repairs very quickly in all cases, which reduce the time crews spend in traffic and improve road safety [7,8]. However, the spray injection may lead to depression [4], because leaving the patch to be compacted by traffic will result in premature patch failures [1]. Thus, the throw and roll could be an appropriate technique when the time is limited.

From the pothole size perspective, shallow potholes (less than 5cm deep) that occur entirely in an asphalt layer could be repaired by spray injection as it has high productivity; while for medium depth pothole (5cm to 10cm deep) and deep potholes (greater than 10m deep), other methods are more suitable because the materials dumped in the pothole should be roughened and bonded tightly [4]. For deep potholes or potholes in wet freeze areas, it is essential to remove water and the water source itself before repair. Spray injection and semi-permanent technology provide the procedure to clean the pothole firstly; nevertheless, spray injection may make the patch deflect due to the fineness of its materials [1]; for this reason, semi-permanent technology is recommended for repairing deep potholes.

Table 1. Summary of Pothole Repair Techniques

Repair Technology	Advantages	Limitations
Throw and go	High productivity; Low cost; Most frequently used	Least longevity; No good support from surrounding pavement; No moisture and debris removal;
Throw and roll	Cost-effectiveness; High productivity; With initial compaction	Inadequate bonding at patch edges
Edge seal	Prevent water from the edge of the patch; Adequate bonding at patch edges	Lower productivity than throw and roll; The second pass required
Semi-permanent	Square up the sides of pothole; Good compaction quality	High labor and equipment cost; Low productivity; Longevity depends on material quality
Spray and injection	High productivity; Low material costs; Remove water and debris; Cost-effectiveness	Require well-trained operators and qualified materials; Depression due to no compaction; Operator exposed to flying debris; Inadequate bonding at patch edges

Preheating Method for Pothole Repair

Temperature requirement for compaction of HMA

Traditionally, the viscosity of asphalt binder is used to determine the compaction temperature requirement of HMA. The Brookfield viscometer is used to test the viscosity of asphalt binder at high temperature and the viscosity requirement for compaction is stated in Superpave mix design procedure. Goh et al. (2007) summarized the range of compaction temperature for HMA, warm mix asphalt and CMA, as shown in Figure 5 [9]. Specifically, the common compaction temperature for unmodified HMA could be from 135℃ to 148℃, while the typical laydown temperature is 140℃ to 160℃ for polymer modified HMA [10].

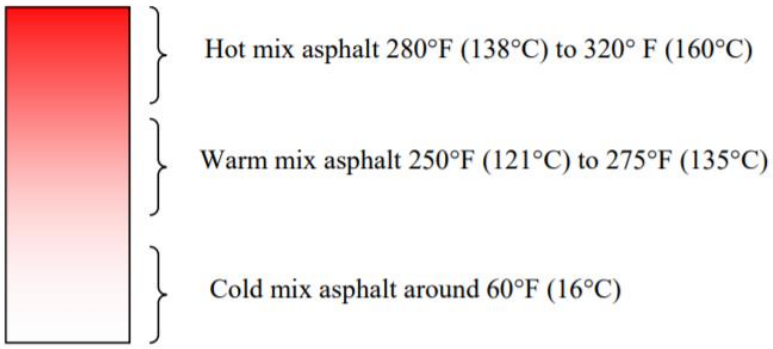

Figure 5. Typical compaction temperature ranges of asphalt mixtures [9]

During the compaction process of HMA, as the temperature decreases, asphalt binder becomes more viscous and resistant to shear deformation, which results in smaller reduction in air voids for a given compaction energy. Given that the optimal compaction temperature is determined through the relationship between the viscosity and temperature as recommended in Superpave mix design procedure, previous researchers have developed tools to predict the temperature window suitable for compaction, including the starting and ending temperature to compact HMA [11,12,13].

PaveCool was the first generation of computer program to predict cooling rate of HMA during compaction developed for the Minnesota Department of Transportation, but it was limited to one lift of paving as opposed to multiple lifts. Later on, CalTool was developed for temperature prediction of multi-layer asphalt pavement during construction [14]. It is noted that the increased discrepancies between model predictions and field measurements were observed in the multi-layer cases. Vasenev et al. (2012) used automated temperature unit (ATU) to provide real-time surface and in-asphalt temperature measurements to roller operators for better compaction of HMA [15]. The general form of the temperature cooling curve is schematically represented in Figure 6 as a function of time. For different mixtures and environmental conditions, the ideal compaction window shifts along the timescale. The compaction temperature would decrease as time goes by, and its cooling rate would gradually slow down after laydown.

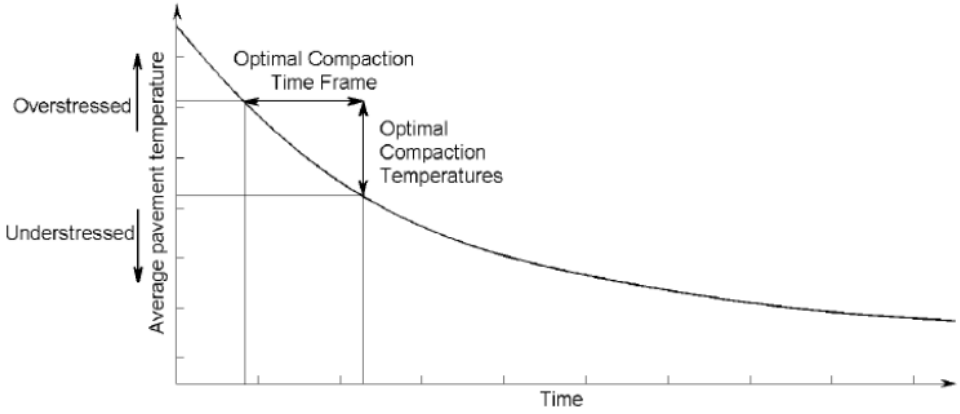

Figure 6. General form of the temperature cooling curve during compaction [15]

Mechanism and effects of different heating methods

Direct heating

Recent research studies have suggested preheating the excavated pothole before repairing to strength interface bonding between existing pavements and hot patching materials [4,5]. Heating can also be used to remove defected material around the pothole, ensuring the temperature is high enough for patching materials to be compacted. Simultaneously, heating could remove the water in the surface and pore space of the pothole area. Currently, different heating methods are available, such as direct heating, infrared heating, microwave heating, and induction heating.

In direct heating, the propane torch is often used to heat asphalt emulsion to get emulsion brake faster [16]. However, it was reported that direct heating methods like hot compressed air burning and excess oxygen burning may overheat the pavement and burn the asphalt, leading to asphalt aging [17].

Infrared heating

Infrared heating is a straightforward heating method for pothole repair [4,18,19]. The heating plate can emit thermal radiation towards the pavement so that the pavement can be heated from the surface downwards to layers below. The energy transmitted by an infrared heater is proportional to its temperature. The higher the temperature, the shorter the wavelength and the higher the amount of energy radiated. When the transmitted radiation energy of the heater hits the asphalt surface, then infrared heat transfer occurs. Heat could only transfer from the surface to the sublayers through conduction, and the depth of heat penetration could be less than 5cm [18]. Since the infrared radiation cannot penetrate the pavement directly and generate heat inside the pavement structure, the time consumption can be considerable especially in winter [5].

Some researchers studied the effect of infrared heater and found that the use of infrared heater could improve the performance of patched pavement. It could improve the bonding condition at interface and therefore repair durability over time. Daniel (2006) found that preheating the longitudinal joint of HMA pavement could improve the strength of material in the joint area [20]. The average strength of the heated material obtained from indirect tensile strength (IDT) test was higher than those without preheating, while not having statistical differences. Also, Huang et al. (2010) proposed that using infrared heater to preheat the patch material could increase IDT strength because preheating increased compaction degree and density, and it was effective in reducing air void content and water permeability [21]. Byzyka (2018) studied the dynamic infrared heating method in the laboratory and found that dynamic heating for approximately 10 minutes would yield better heat distribution while minimizing the possibility of asphalt overheating and long pre-heating time [19]. The temperature increase rate inside the slab made by CMA was higher for the first 10 minutes of heating than that between 10 min and 30 min of heating, because the thermal conductivity decreased as the mixture temperature increased. Therefore, the first 10-12 min dynamic heating could ensure heating of pavement surfaces and asphalt mixture of existing pavement without burning or overheating asphalt.

Microwave heating

Microwave heating uses electromagnetic radiation in the microwave frequency range to heat the pavement [5, 22, 23]. Unlike infrared heating, microwave heating associates with a mutual coupled process of electric field and thermal field, therefore the released heat can be directly absorbed by the internal pavement structure [5]. However, asphalt binder is nonmagnetic and almost unresponsive to microwave energy. The heat-up of asphalt pavement primarily depends on aggregates to absorb the energy and transfer it to asphalt. Specified aggregate such as taconite rock or steel slag can be used in order to enhance the microwave heating effect [5,22]. Liu et al. (2017) also found the heating transfer becomes apparent as the aggregate size decreases [22].

Many researchers have conducted laboratory tests to evaluate the performance of asphalt mixtures after microwave heating. Nieftagodien (2013) found that the tensile strength of the microwave-heated half-warm asphalt mixtures could not meet the minimum criteria, as well as the mixtures containing high contents of recycled asphalt [24]. However, the microwave-heated mixtures with 20 % recycled asphalt showed much higher tensile strength, which indicated better bonds between aggregate and asphalt binder. Comparing the triaxial test results of asphalt mixture in the work by Jenkins (2000) and Nieftagodien (2013) [24,25], microwave preheating could reduce energy gradient between hot formed asphalt and warm aggregates when producing half-warm foamed asphalt mixtures, which could increase the heating rate, improve the aggregate particle coating, and ensure significant increase in the cohesion. Liu et al. (2018) found although microwave heating could increase the self-healing capacity for damaged asphalt concrete, interface defects still existed [26].

Induction heating

Induction heating is another fast heating method. Pavement structure containing electrically conductive fibers or powders can be heated by simply applying an external varying electromagnetic field, which induces micro-currents and heats the particles through the Joule's effect [27]. Heat during induction is generated by Joule losses, dielectric hysteresis and contact resistance [28]. Among them, contact resistance heating is the dominant mechanism for heat generation. Since conductive fibers were added to asphalt, the heat was applied directly into asphalt [29]. Therefore, this method was found to be very efficient for asphalt heating and consumed less energy [30]. As a consequence, the temperature would be higher in test samples with the higher number of fibers [31]. However, since induction heating cannot be directly applied to aggregates, this method is usually used for enhancing self-healing ability of asphalt mixture [See references 27,28,30,32 and 33]. When induction heating is used for pothole repair, the prefabricated asphalt tile should be used, and the adhesive layer needs to be modified with conductive fibers. As a result, the induction heating actually heats the adhesive layer rather than the patch or the surrounding asphalt pavement [34].

Some effects of the induction heating on material performances have been found. As steel fibers are simply heating elements that do not provide much mechanical strength to asphalt mixtures [35], the induction heating would lead to the material with fewer open areas of loose fibers having higher strength. On the other hand, if excess fibers were

used in the bonding layer, the induction heating would make the fibers absorb asphalt in the remaining space under high temperature and asphalt could not coat aggregates anymore. Therefore, the bonding condition between the patch and old pavement would be in question and the strength of the mixture would decrease. Moreover, Obaidi et al. (2017) found that the induction heating time would not increase or decrease the total strength of the material when using loose steel fibers, while the strength would increase with the open area of steel fiber in form of chicken wire [34].

Comparisons between heating methods

Different heating methods have different heating mechanisms and effects on material performances. When applying them as preheating methods in pothole repair, the advantages and disadvantages of each method are summarized in Table 2. Direct heating method is the most convenient heating method, which could directly heat the boundary of the materials with cheap equipment [14]. However, it may overheat the binder, leading to binder aging. For infrared heating method, its radiation cannot penetrate the pavement directly and generate heat inside the pavement structure, thus, it needs to take more time in patching [18] and its productivity in winter is low [5]. However, the materials after infrared heating could be improved in interface bonding and therefore have a better durability over time. For microwave heating method, it is more efficient than infrared heating because its released heat can be directly absorbed by the internal pavement structure, which reduces the heating time and provides excellent bond at the interface between the patch and surrounding structures. Nevertheless, common patch materials are almost unresponsive to microwave energy and specified aggregates should be used. Additionally, the microwave would impact asphaltene molecules and has the potential to decrease the viscosity of the asphalt. Contrary to microwave heating, induction heating could heat directly into the asphalt, which is more efficient. The fibers could act as the reinforcement and improve the strength of the materials. Nevertheless, the materials requiring electrically conductive fibers or powder in asphalt mixtures also becomes the disadvantage of induction heating.

Table 2. Summary of preheating methods

Heating methods	Advantages	Disadvantages
Direct heat (torch)	Cheap equipment	Overheating potential
Infrared heating	Improve interface bonding	Lower productivity, especially in winter; Time increase in traffic control
Microwave heating	Least temperature-dependent, effective under very cold condition; Good bond at edges	Common material is almost unresponsive to microwave; Potential effect on decreasing asphalt viscosity
Induction heating	Applies heat directly into the asphalt; more efficient; less energy input; Fiber acts as reinforcement	Need have electrically conductive fibers or powder in asphalt mixture

Cold Mix Asphalt as Patch Material

Currently, the most common asphalt pavement patch material is HMA [3]. It has the best quality to repair the pothole, while the requirement of minimum mixing batches and high construction temperature limit its applicability. It was found that HMA has better quality but limited applicability under different weather conditions while cold asphalt mixtures have lower quality but are workable under most weather conditions. On the other hand, potholes are usually generated in winter after freeze-thaw cycles, and in most maintenance activities, potholes are not heated due to time and costs. Thus, cold mix asphalt (CMA) is typically used with high flexibility. Small amounts of CMA can be used to repair individual potholes under cold weather conditions.

There are three types of cold mixes available for pothole repair. The first type is proprietary cold mix that usually uses specially formulated binders. The second type is cold mix produced according to specifications proposed by the agencies. It is produced by a local asphalt plant using the available aggregate and binder, usually without an opportunity to consider compatibility or expected performance. The third type is modified CMA with different additives, such as polymer, resin, fiber, or cementitious material.

Effect of curing on CMA

In the field, CMA would reach their mature level of properties after a period of time. During the curing process, the emulsified asphalt would break and the bonding condition at the interface between the patch and surrounding pavement would be improved. However, the curing time may be longer if the climate is cooler or more humid or the traffic is lighter.

To make the patch material form stable condition quickly, many researchers have studied the accelerated curing process of CMA using laboratory tests. Serfass et al. (2004) found that when curing CMA under 18℃ or 35℃, the unconfined compressive strength and IDT strength would increase as the curing time increased, and a higher temperature remarkably had an accelerating effect on curing process due to the increased compactness and reduced moisture content [36]. Similar results were found from the research conducted by Gandi et al. (2019) [37]. The Marshall stability and IDT strength of CMA increased as the curing time increased, and the increase was more significant as the curing temperature increased. Serfass et al. (2004) also found that the asphalt content of cold mix increased after curing, which reduced the penetration and increased the viscosity [36]. It means that curing CMA could potentially enhance the bonding strength between the patch material and the existing pavement.

Proprietary CMA

<u>UPM High-Performance Cold Mix</u>

The UPM High-Performance Cold Mix is a proprietary cold mix material produced using a specially formulated liquid asphalt binder and aggregate available in the vicinity of the plant producing the mix. It can be placed at sub-freezing temperatures or warmer temperatures. Both open-graded or dense-graded mixtures are available. It can be applied in rapid pothole procedures, edge seal and semi-permanent procedures.

Perma-Patch

Perma-patch is a uniform mixture of compatible mineral aggregate and asphalt material. It is also a proprietary material made with a specially formulated binder named perma-patch liquid. This material could be produced at any asphalt plant using the local aggregate in much the same way that the UPM mix is produced. This type of material is usually used in rapid pothole repair procedures like throw and roll or throw and go.

Quality Pavement Repair (QPR) 2000

QPR 2000 is a ready-to-use, pre-mixed asphalt patch material made from selected aggregate, asphalt with chemical solvents, and additives. It can be applied to either wet or dry surfaces and either hot or subfreezing temperatures. This material could be produced at any asphalt plant using local aggregate in much the same way that the UPM mix is produced. It is often used in rapid pothole repair procedures. In addition, it can be opened to traffic immediately after placement and can be stored in a stockpile for up to a year.

HFMS-2

The modified HFMS-2 material is produced using a high-float, medium-setting emulsion that has styrene butadiene (trade name Styrelf) added. It is often used in rapid pothole repair procedures.

Instant Road repair

Instant Road Repair is a rapid-curing, cold-mix patch material for asphalt pavements. It is widely used in United States and other countries. The asphalt used is a rapid-curing proprietary blend of cutback asphalt cements with polymer and antistrip agents, which meets or exceeds the ASTM requirements. Instant road repair is deemed as permanent pothole repair materials, which could be used successfully in any geographical region. The aggregate is a relatively dense-graded crushed limestone.

Optimix

Optimix is a cold-mix binder of patch material for asphalt pavements. It is composed of Optimix liquid asphalt blend, which is a proprietary blend of asphalt with different antistrip and high-adhesion additives. Different from instant road repair, the property of the Optimix liquid asphalt binder varied to meet the requirements, which depends on the geographical region. The open-graded aggregates are required for blending with the asphalt binder. Optimix is marketed as a permanent pothole repair material for asphalt or concrete pavement.

SuitKote

SuitKote is a proprietary cold mix that consists of crushed aggregate and asphalt material meeting the ASTM requirements. A batch mix plant, drum mix plant, or cold mix pugmill are used for mixing. When mixing in a hot plant, the temperature is minimized so that stripping of the asphalt mixtures can be avoided.

Sylcrete-EV

Sylcrete-EV is a cold mix patch material for asphalt and concrete pavements, which is

used throughout the US, marketed as a permanent repair material. The binder is a proprietary blend of cutback asphalt cement. Open-graded mixture with Sylcrete-EV could be used for cold weather and dense-graded mixture can be applied under warm conditions. Binder can be obtained and combined with high quality crushed aggregate.

EZ Street

EZ street is polymer modified CMA with open graded aggregates. It can be used under -18℃ to 38℃, which is workable for most weather conditions. EZ-street can be heated up 50°C in a hot-box before application in winter, which could result in better patch quality.

AQUAPHALT

Aquaphalt is claimed to be a permanent eco-friendly patch material for asphalt and concrete. The binder of is a proprietary liquid blend that contains renewable natural raw materials. It is available in three size aggregates (4mm, 6mm, and 9mm) for different depths of potholes. The installation process includes pouring Aquaphalt material, spraying water, and tamping. The water amount needed is 0.5 gallon of water to 50 lbs. After water is applied, it will start to cure in 15 minutes and will be fully cured in 24 hours in most cases. AquaphaltIt does not contain toxic solvents of volatile organic compounds (VOC).

The basic information of the aforementioned proprietary materials for pothole repair is listed in Table 3.

Table 3. Basic information of proprietary materials

Manufacturer	**Product**	**Container**	**Binder Type**
Unique Paving Materials Corp	UPM	50-lb (23 kg) bag	Cutback +Additives
National Paving and Contracting	Perma-Patch	60-lb (27 kg) bag	Cutback
Quality Pavement Repair	QPR-2000	50-lb (23 kg) bag	Cutback
Russell Standard	HFMS-2	N/A	Proprietary Liquid Asphalt
Roadway Research Inter.	Instant Road Repair	50-lb (23 kg) pail	Proprietary Cutback
Optimix Inc.	Optimix	5-gal (20 L) bucket	Cutback
SuitKote Corp.	SuitKote	N/A	Emulsified Asphalt
Sylcrete Corp.	Sylcrete-EV	4-gal (15L) bucket	Proprietary Liquid Asphalt
EZ-Street Co.	EZ Street	35-lb (16 kg) bag	Cutback
RoadStone Production LLC	AQUAPHALT	50 lb. bucket	Proprietary Liquid Asphalt

Cold mix produced under specifications

The PennDOT 485/486 material was produced by an asphalt plant in Pennsylvania according to Specification 485/486, which lists acceptable asphalt binders and additives, as well as fine and coarse aggregate. Gradations for the combined fine and coarse aggregate are also given, along with guidelines for the percent of residue of asphalt cement based on the absorption of the aggregate used. Additional requirements for the actual mixing of the materials and acceptance testing are specified. The major difference between the 485 and 486 specifications is the addition of polypropylene or polyester fibers in the 486 materials.

Local cold mix materials

The local cold mix materials are usually cheap and made of rounded aggregate and very little binder, resulting in a dry-looking material. However, in some instances, local crews used high-quality, proprietary cold mixes rather than the inexpensive ones.

Modified Cold Mix Asphalt

Modification of CMA is most often applied in pavement rehabilitation and recycling. Modified CMA has several advantages. For instance, emulsion systems need minimal changes, modification temperature is lower than hot modification, and modified asphalt emulsion shows high stability.

Polymer modification of asphalt binders has increasingly become popular in building optimally performing pavements. Pavement with polymer modification exhibits greater resistance to rutting and thermal cracking, and decreases fatigue damage, stripping and temperature susceptibility. Subsequently, the use of polymer modified CMA for pothole repair has been studied by many researchers. Yuan et al. (2012) identified a polymeric material, dicyclopentadiene (DCPD) nano molecular resin, which could be used to infiltrate porous asphalt mix and cure as a reinforcement and binder for the asphalt-aggregate pothole repair materials [(38)]. The reinforcement of DCPD and its bonding strength improvement was researched, the results show that DCPC material could strongly hole the CMA and increase its tension strength, compared to fully compacted HMA. And the DCPD greatly improved the bonding strength between cold patch materials and the surrounding pavements. Chavez-Valencia et al. (2007) used polyvinyl acetate to modify asphalt emulsion and mixed it with aggregates [(39)]. It was found that the adherence between the aggregate and the asphalt would be promoted because the polyvinyl acetate (PVA) is a thermoplastic synthetic adhesive, and as a result of this, the compressive strength was improved in 31% relative to the unmodified CMA. Therefore, a pavement patched by this modified CMA might show improved resistance to the rutting and fatigue, caused by the heavy traffic loads. Abd et al. (2017) evaluated the performance of asphalt emulsion modified using polyvinyl acetate [(40)]. The results showed that asphalt emulsion modified with PVA had satisfactory performance in terms of fuel and acid resistance.

Waterborne epoxy resin emulsified asphalt (WEREA) is a newly developed material because of its advantages in emulsifying capacity, hydrophile lipophile balance and

shorter curing time. Many researchers have studied the combinations of different epoxy resins and asphalt binder to evaluate their improved performances or weaknesses on mixtures for patching. Liu et al. (2018) found that the cohesion strength of waterborne epoxy emulsified was greater than that of matrix asphalt and SBS modified asphalt [26]. The components and network microstructure of WEREA enhance the cohesion property of interlayer and improve the material viscoelasticity, which could in turn improve the shear strength and pullout strength performance of the CMA. In the field test of asphalt pavement made with WEREA, although the shear strength of field cores might be smaller than those of laboratory samples, the shear and pullout strengths were still larger than the asphalt mixtures with SBS modified asphalt [41]. In addition, WEREA also showed strong waterproof performance for pothole repair as tack coat. However, in the construction of asphalt pavement with WEREA, the curing time of the road was found to have important influence on field performance (like raveling), which depended on the surrounding environment [41]. Zhang et al. (2017) blended waterborne epoxy resin with styrene-butadiene rubber (SBR) to prepare epoxy SBR modified emulsified asphalt [42]. The results show that the addition of SBR latex and epoxy improves the high and low temperature properties and shear strength of asphalt significantly.

Magnesium phosphate cement (MPC), a particular type of cementitious binder, has been used as a rapid concrete patch material since 1976 due to its fast strength growth [43], strong bonding with the substrate, low shrinkage, slow aging and ease of construction [See references 44,45,46 and 47]. MPC can be constructed in low temperature conditions and embody the smaller carbon footprint during production [44]. However, limited research has been conducted on applying MPC for rapid repair of asphalt pavement. Li et al. (2014) evaluated the performance of magnesium phosphate cement and emulsified asphalt combination (MPC–EA) and found that as the dosage of emulsified asphalt with MPC increased, the fluidity, toughness, bonding strength and permeability of the MPC–EA composite were enhanced [47]. However, a reduction of compressive strength, flexural strength and abrasion resistance were found due to the released water from emulsified asphalt. Issa et al. (2001) found that adding Portland cement is an efficient way to consume water in the emulsified or foamed asphalt and form a stronger and denser skeleton in the cold recycled asphalt mixture [48]. Ma et al. (2015) investigated the performances of the reclaimed asphalt mixture, which was composed of 4% emulsified asphalt, 1.5% ordinary Portland cement with grade 32.5, 5.4% water and aggregates with 75% RAP [49]. The results show that cement is an efficient additive to improve the strength of cold recycled asphalt mixtures by promoting demulsification of emulsified asphalt and producing cement hydrates, while its effect is limited by RAP.

Additionally, Ferrotti et al. (2014) found that the cold mix with 0.15% cellulose fibers provided similar or even higher performance than standard mixture (without fibers) and mixtures with glass–cellulose, nylon–polyester–cellulose [50]. The cellulose-fiber-reinforced material showed enhanced Marshall stability and IDT strength, allowing the conclusion that they could be more successfully used in pothole maintenance activities. From the field observation, the emulsified asphalt pavement with cellulose fibers showed good abrasive resistance, waterproof, and ease of construction. The traffic could be opened in a short time after the construction [51]. Shanbara et al. (2018) studied the

performance of CMA mixtures reinforced with natural and synthetic fibers [52]. Both types of fibers were found to have significant resistance to rutting in wheel track tests at high temperatures and resistance to crack propagation. On the other hand, Bueno et al. (2003) added both fibrillated fibers (FFs) and slit film fibers (SFFs) into the emulsified asphalt binder, and the aggregates used consisted of a well graded mixture of crushed gneiss stones, clean river sand, and filler that lies [53]. The FFs & SFFs-fiber-reinforced material shows substantial drops in the mixture resilient moduli when compared to plain mixtures. The addition of fibers to cold densely graded emulsified asphalt mixes was found to reduce the dry density and Marshall stability as well as cause small variations in the mixture shear strength triaxial parameters.

FIELD PERFORMANCE OF ASPHATL PATCH

Failure Mechanism and Distress of Asphalt Patch

Many researchers have studied the distresses of the pothole materials and found that the most common ones are shoving, raveling, dishing, debonding, bleeding, poor skid resistance, freeze-thaw and so on. The mechanism of each type of failure is described as follows:

• ***Shoving*** under the traffic could be resulted from a number of factors which reduce the stability of the mixtures. Materials with excess or insufficient binder may lead to shoving, as well as improper compaction which makes aggregate interlock undeveloped.
• ***Raveling*** is the loss of aggregates from the patch materials due to the inadequate cohesion of the mix. It could be because of the excess binder, poor aggregate interlock and poor compaction, which reduce the cohesion between materials. Some factors leading to shoving could also contribute to raveling.
• ***Dishing*** is the formation of a depression within the repair due to compaction by traffic. Inadequate compaction of the patch materials often leads to the instability of the materials, which in turn causes dishing after opening the traffic.
• ***Debonding*** is the loosening of the patch material from the surrounding pavement. Insufficient cohesion between patch materials and surrounding pavement can lead to debonding. In most cases, moisture or debris in the pothole without cleaning may contribute to debonding.
• ***Bleeding*** is the flushing of asphalt binder onto the patch surface, which may be caused by a combination of traffic load, inadequate voids and excessive binder in the mixture. Bleeding usually happens to materials with poor design and would further cause poor skid resistance.
• ***Poor skid resistance*** often results from bleeding surface or polished aggregates. Poor mixture design is the main reason for causing poor skid resistance.
• ***Freeze-Thaw*** is the delamination of the patch from the original pavement. Due to the water remaining at the bottom of the hole, the adhesion between patch materials and surrounding pavements are impacted, as well as the compaction quality. In winter, the water freezes and leads to the delamination of the patch materials.

Field Performance of Pothole Repair without Heating

SHRP H-106 project

During SHRP H-106 project [54], 1250 pothole patches were placed at eight test sites across the United States and Canada in 1991. These patches were placed using different proprietary, state-specified, and local cold-mix patching materials. Several different installation techniques were applied in an effort to determine the optimum combination of materials and procedures for improving the cost-effectiveness of patching operations.

Time required for different repair procedures

Table 4 shows the summary of repair time using different pothole repair methods obtained from various field sites. The time required for patch mainly depends on repair procedure and pothole size. Generally, the time required for each procedure would increase as the

pothole size increases. Therefore, the repair time for comparison is normalized as minutes per one cubic feet pothole. The data show large variations of repair time among various sites. The repair time is relatively longer for the sites in northern states; however, the trend is not consistent. Figure 7 shows the average time using different pothole repair methods. The results indicate that the semi-permanent procedure needs the longest time. The time needed for throw and roll and edge seal are comparable, and spray injection needs the shortest time. This is reasonable since spray injection has no compaction time, and semi-permanent needs some preparation time to clean the water and debris and square up the sides.

Table 4. Summary of repair time using different pothole repair methods at various field sites (minutes per one cubic feet pothole) [3,54]

Procedure	Components	Field sites								Range	Average
		CA	IL	NM	OR	TX	UT	VT	ON		
Throw and roll	Total	1.8	3.6	2.9	3	1.5	1.6	1.8	5.6	1.5-5.6	2.7
	Placement	1.2	2.2	2.2	2.4	1.1	1.2	1.5	4.3	-	2
	Compaction	0.6	1.4	0.7	0.6	0.4	0.4	0.3	1.3	-	0.7
Edge-seal	Total	1.7	2.4	4.8	6.5	2.3	2	1.7	-	1.7-6.5	3
	Placement	0.7	1.3	2.6	3	1.3	0.9	0.8	-	-	1.5
	Compaction	0.5	0.7	0.9	1	0.3	0.3	0.3	-	-	0.6
	Seal	0.5	0.4	1.3	2.5	0.7	0.8	0.6	-	-	1
Semi-permanent	Total	3.9	9.8	4.9	*33.8**	4.9	6.1	4.2	8.4	3.9-9.8	6
	Preparation	1.6	6.9	1	*30.4**	3.3	3.6	2.7	4	-	3.3
	Placement	0.9	1.8	2.8	1.8	1.3	1.8	0.8	2.2	-	1.7
	Compaction	1.4	1.1	1.1	1.6	0.3	0.7	0.7	2.2	-	1.1
Spray injection	Placement	1.4	2.2	2.3	-	1.1	2.4	1.8	*11.5**	1.1-2.4	2.2

1. * means outlier and not included in the analysis.

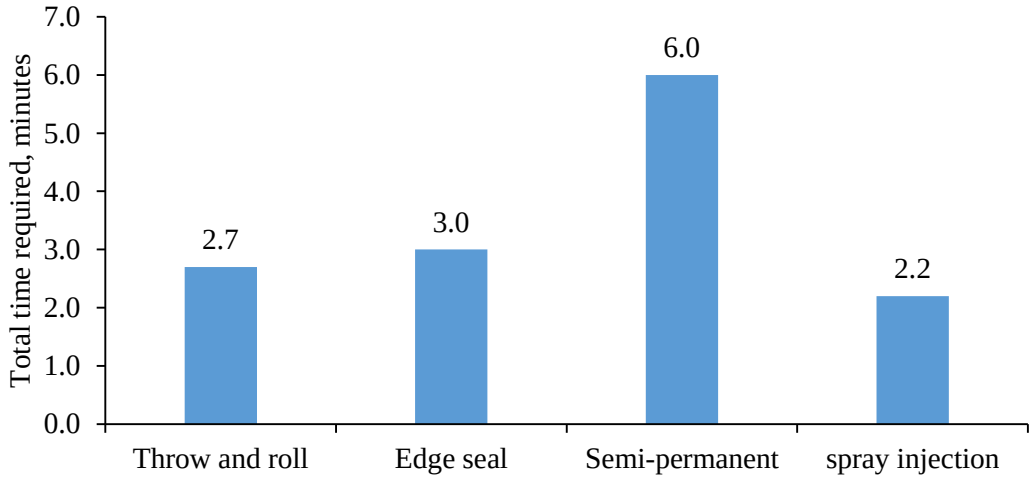

Figure 7. Repair time using different pothole repair methods (minutes per one cubic feet pothole)

Cold patch performance at different conditions

Wilson and Romine (1993) conducted a comprehensive survey on pothole repair and the surviving rate of potholes repaired with CMA [54]. The performance of repaired pothole was evaluated based on the rating of pavement distresses, including bleeding, shoveling, dishing, edge disintegration, missing patch, raveling and cracking. Figure 8 shows the performance criteria corresponding to the rating score (0-10). The definition of failure was when the rating was below zero.

DISTRESS	ESTIMATED QUANTITY	RATING										
		10	9	8	7	6	5	4	3	2	1	0
Bleeding	Percent of area	0	0 - 10	10 - 20	20 - 30	30 - 40	40 - 50	50 - 60	60 - 70	70 - 80	80 - 90	90 - 100
Cracking	Quantity of cracks	0	< 6-in	< 12-in	> 12-in	< 6-in	< 12-in	> 12-in	< 6-in	< 12-in	> 12-in	> 12-in
	Width of cracks	0	crack width < 0.0625-in			crack width < 0.25-in			crack width > 0.25-in			alligator
Dishing	Depth of dishing	0	< 0.25-in			0.25-in to 0.50-in			0.50-in to 1.0-in		> 1.0-in	
	Percent of area	0	< 25%	< 50%	> 50%	< 25%	< 50%	> 50%	< 50%	> 50%	< 50%	> 50%
Edge Disintegration	Percent of perimeter	0	0 - 10	10 - 20	20 - 30	30 - 40	40 - 50	50 - 60	60 - 70	70 - 80	80 - 90	90 - 100
Missing Patch	Percent of area	0	0 - 10	10 - 20	20 - 30	30 - 40	40 - 50	50 - 60	60 - 70	70 - 80	80 - 90	90 - 100
Ravelling	Severity	None	Loss of small rocks			Loss of larger particles			Top 0.5-in gone		Top 1.0-in gone	
	Percent of area	0	< 25%	< 50%	> 50%	< 25%	< 50%	> 50%	< 50%	> 50%	< 50%	> 50%
Shoving	Height of shoving	0	< 0.25-in			0.25-in to 0.50-in			0.50-in to 1.0-in		> 1.0-in	
	Percent area	0	< 10%	< 25%	> 25%	< 10%	< 25%	> 25%	< 25%	> 25%	< 25%	> 25%

Figure 8. Summary of patch rating criteria [54]

It is expected that the surviving rate of repaired pothole is affected by many factors, such as construction temperature, average daily traffic, repair procedure, repair material and so on. Table 5 shows the surviving rate of patches repaired by throw and roll procedure with UPM material under different conditions. The patches in ON were found to have the lowest surviving rate, probably because it had the lowest construction temperature as compared to other states. Also, the average daily traffic in IL was remarkably higher than others, which could be the reason for having the second lowest surviving rate. For other states, no apparent relationship was found between construction temperature, ADT and surviving rate. Therefore, low temperature and high traffic may result in inferior patch performance.

Table 5. Surviving rates of throw and roll procedure with UPM material

States	Average temp. (℃)	Relative Humidity (%)	ADT	Weeks	Surviving rate (%)
CA	12.9	30	1000	77	78
IL	19.1	29	15000	84	50
NM	15.2	26	1700	84	100

OR	1.7	27	5400	35	100
TX	23.1	47	7500	84	77
UT	16.0	33	1500	79	94
VT	20.8	40	2100	58	56
ON	-2.2	28	4500	44	39

The effect of repair procedure and material on surviving rate of asphalt patches was evaluated using the data collected from CA, IL, NM, TX, UT and VT, where the construction environment was similar. Figure 9(a) shows surviving rates of patches repaired by different repair procedures with UPM material after about 80 weeks of installation. The surviving rate in IL was much lower than those in other states, which could be caused by its high traffic level. On the other hand, patches repaired by edge seal in IL, NM and TX showed the highest surviving rate. It indicated that the edge seal procedure produces good field performance. Figure 9(b) shows the surviving rate of spray injection in different states. It was found that after about 80 weeks of installation, the patches repaired by spray injection exhibited a high surviving rate under different traffic levels, which indicated that spray injection can lead to satisfactory field performance. However, the study from VDOT noted that experienced and well-trained operators should be used for spray injection in order to ensure quality patches and keep the equipment in good operating order [8].

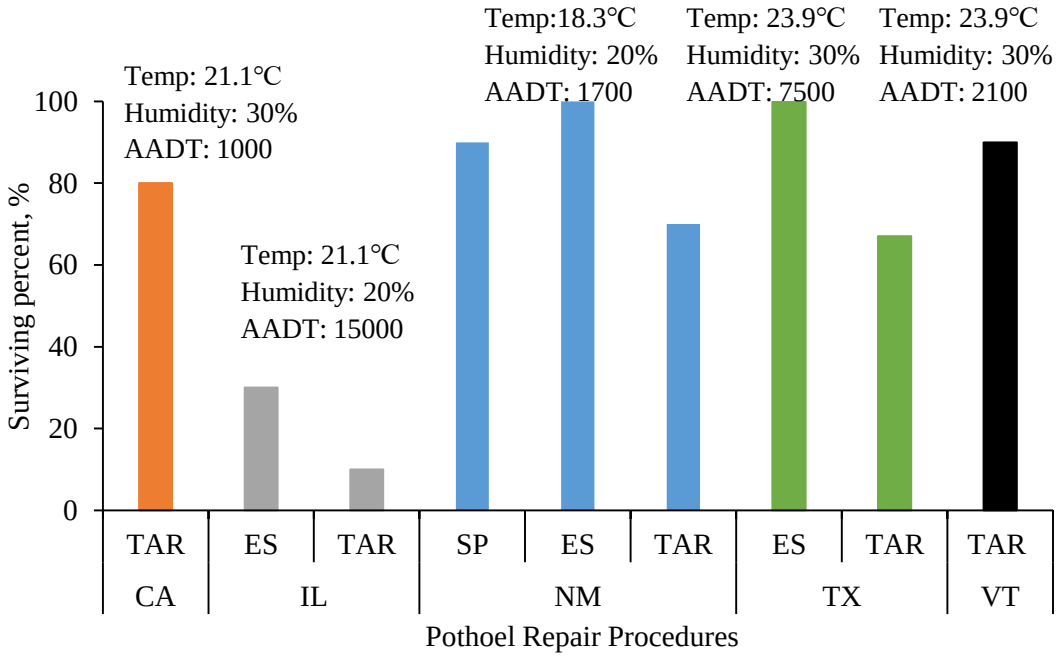

(a)

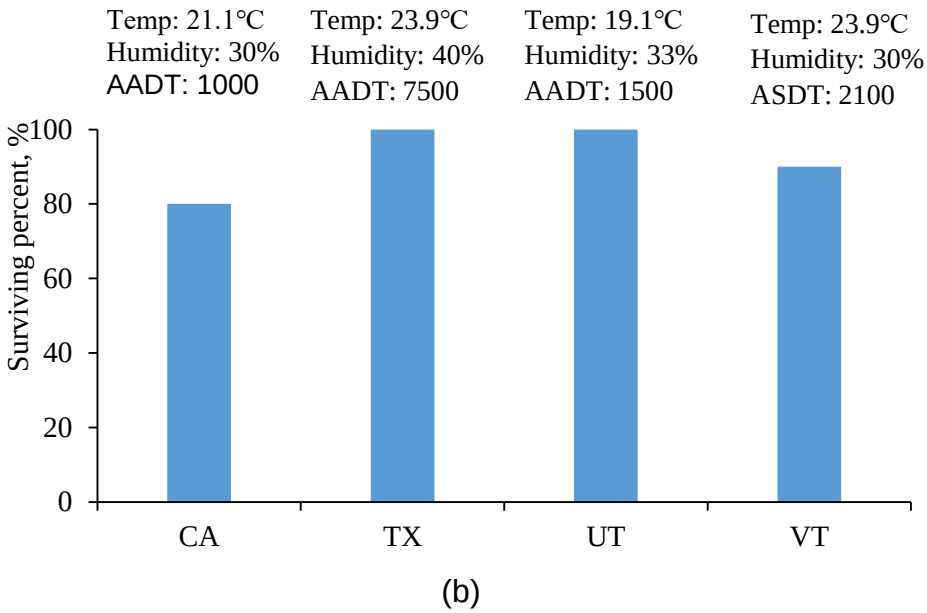

(b)

Figure 9. Surviving rates of pothole repair: (a) different repair procedures with UPM (TAR: Throw and Roll, ES: Edge seal, SP: Semi-permanent), (b) spray injection

Figure 10 shows the surviving rate of patches repaired by throw and roll with different patch materials in CA. Note that different patches were constructed in different segments on the same road. Throw and roll with UPM was used as the control case to compare with other materials under the same environment condition. It was found the patches repaired by throw and roll with different materials had similar surviving rates, although the differences between sites were observed. In general, patches repaired by PennDOT 486, Perma-Patch and HFMS-2 showed comparable surviving rates as UPM, while spray injection and PennDOT 485 showed lower surviving rates. Only the surviving rate of QPR-2000 was higher than that of UPM.

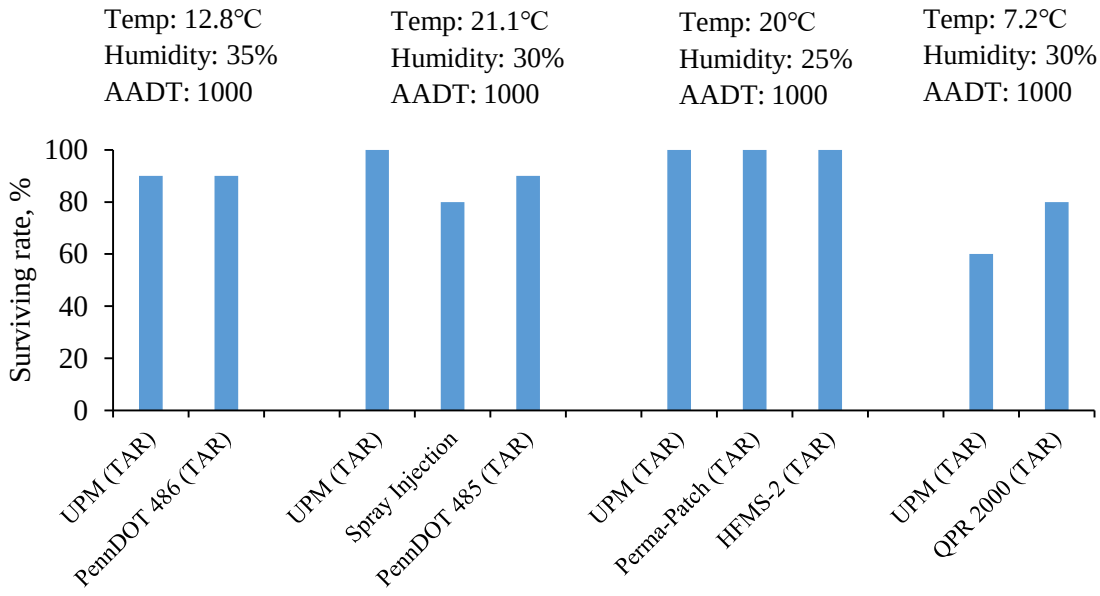

Figure 10. Surviving rates of patches repaired by throw and roll (TAR) with different materials

Field evaluation conducted in Virginia

Prowell and Franklin (1996) carried out field performance evaluation of 13 proprietary cold-mix patching materials repaired by throw and roll method in Virginia [55]. The performance after one year for the test sections repaired in summer 1994 and the performance after 5 months for the test sections repaired in February 1995 were evaluated. The performance rating and survivability formula are given by Equation 1 and 2.

$$\text{Performance rating} = \text{Survivability} \times \frac{[(0.171W)+(0.177R)+(0.156E)+(0.114B)+(0.180D)+(0.204PS)}{4} \times 100 \quad (1)$$

Where: W is workability evaluation rating; R is raveling evaluation rating; E is edge disintegration evaluation rating; B is bleeding evaluation rating; D is dishing evaluation rating; PS is pushing and shoving evaluation rating; and Sur is survivability.

$$\text{Survivability} = \frac{\text{surviving number of patches of the material}}{\text{original number of patches of the material}} \quad (2)$$

The performance ratings after one year for the test sections repaired summer 1994 are presented in Figure 11. As seen, Hei-way performed statistically the same as HMA patches and UPM, which had the highest overall rating among all cold mixes. Though Sylcrete performed worse than HMA, it performed statistically as well as the two best cold-mix products, Hei-way and UPM. For other commonly used proprietary materials like Perma-Patch and QPR-2000, their performance ratings are around the average.

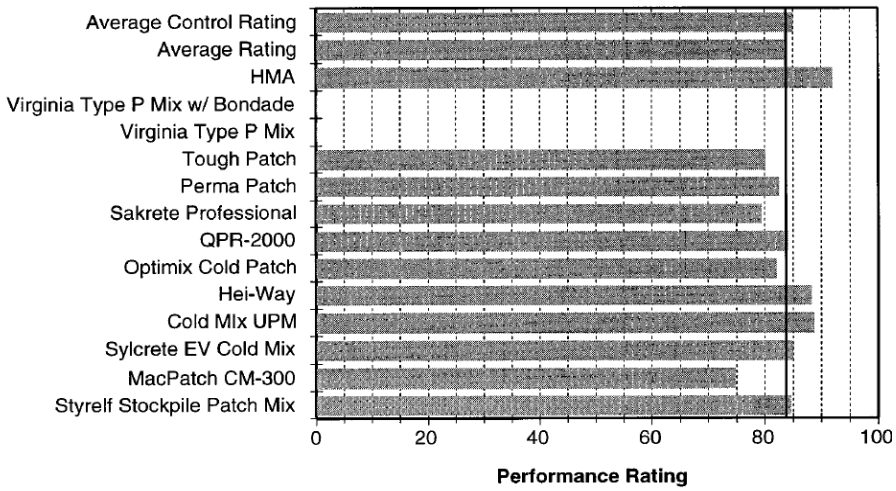

Figure 11. Average performance ratings after 1 year for test sections repaired in summer 1994 [55]

Figure 12 presents the average performance ratings after 5 months for the test sections repaired in February 1995. FiberPave Cold Mix and RePAVE performed significantly worse than the other products. The workability of both products was poor. Fiber-Pave suffers from higher than average dishing and raveling. RePAVE had not cured after 5 months. The material could still be displaced with light pressure. Both Bond-X and VTRC HP (which was produced with Bond-X binder) performed extremely well. All materials placed in the test sections repaired in February 1995 (with the exception of RePAVE) showed significantly less dishing than the sections repaired in summer 1994. This was probably caused by the reduced pothole depth. This observation suggested that potholes deeper than 50 mm should probably be filled in two lifts.

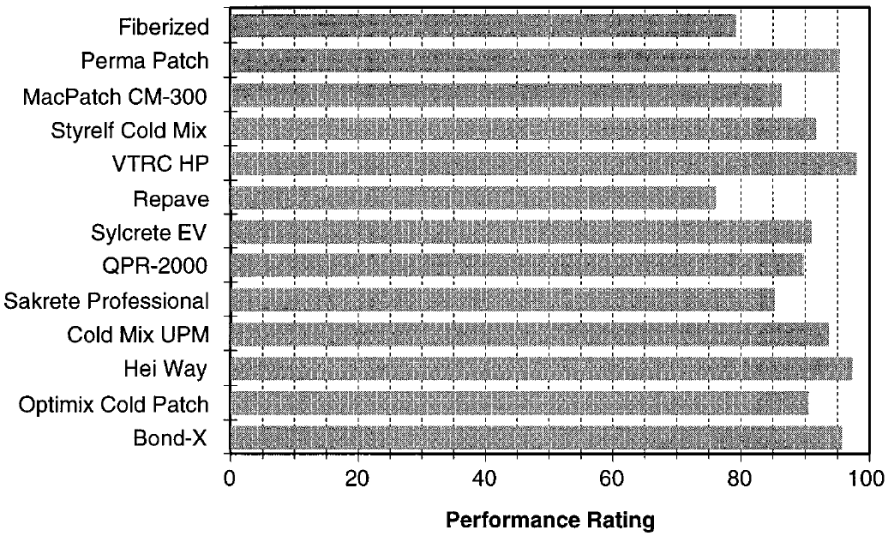

Figure 12. Average performance ratings after 5 months for test sections repaired in February 1995 [55]

Field evaluation from survey questionnaire

In the SHRP H-105 project, Smith et al. (1991) drew some conclusions from the survey questionnaire of pothole repair performances [56]. The effects of construction environment and patch material on field performance are summarized as follows:

- For both hot and cold mix materials, the longest lasting patch is placed using permanent procedures at >0 ℃ in a dry hole.
- The patch life difference between dry and wet conditions is very large, for both hot and cold mix materials.
- For proprietary patching material, the patch life difference at dry and wet conditions is significant, but less than conventional cold mix.
- The patch life difference at cold and warm temperatures is very large, for hot mix material and cold mix material (dry condition only).
- For proprietary patching materials, the patch life difference at cold and warm temperatures is significant, but less than conventional cold mix.

Field Performance of Pothole Repair with Heating Methods

Infrared heating

Infrared heating has been tried in the pilot project conducted by Ohio DOT [4]. As shown in Figure 13, the infrared heating equipment was Tow-Behind Combination Infrared Asphalt Heater/Reclaimer, which consists of a reclaimer and a pavement heater. The reclaimer is a hopper heated by two infrared heaters, which is designed to recycle asphalt material by reheating it to workable temperature without burning it. The reheating process can take between 8 to 16 hours, depending on ambient temperatures and the amount of asphalt that is being heated. The infrared pavement heater is placed over the area to be repaired for 5 to 10 minutes to heat both the pothole and the surrounding area.

Figure 13. Infrared heater/reclaimer [4]

All potholes were created by ODOT by drilling holes in the pavement that are 0.9-m- to 1.2-m-wide, 0.9-m- to 1.5-m-long, and 7.6-cm- to 10.2-cm-deep. The man-made potholes

were used to ensure that the performances of the various pothole patching methods were evaluated under the same conditions. The patching material used for the throw and roll method was the regular cold mix ODOT typically used. The steps to apply infrared heating for pothole repair include: 1) Cleaning; 2) Lighting the infrared heater; 3) Lowering heater over pothole area; 4) Scarifying the damage area; 5) Applying rejuvenator; 6) Adding virgin asphalt; 7) Luting asphalt pavement surface to be smooth; and 8) Compaction. The asphalt mixture was obtained from the asphalt plant at the end of construction season and stored in one large pile under the shed.

Figure 14 shows the time required for infrared heating and other two methods, which were measured by Ohio DOT in the field. Compared to spray injection and throw and roll, applying infrared heating would cost much more time. The patching duration significantly increased when there were some problems in igniting the infrared heater, Additionally, the spray injection equipment had to be cleaned during the patching due to cooling down when it was not in use, which resulted in much longer patching time.

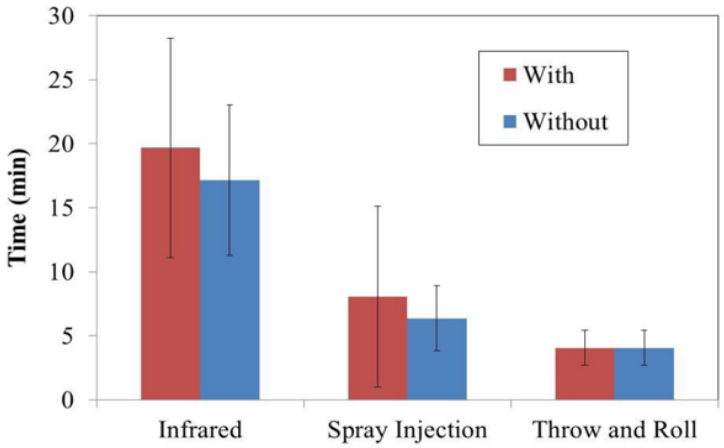

Figure 14. Time required for infrared heating [4]

Another infrared heating system named HeatWurx was operated by MnDOT, which is shown in Figure 15. This unit is designed to heat up in-place asphalt concrete to a temperature of 175℃ to 190℃ in order to perform patching on distressed areas [57]. The unit has a footprint of 1m by 2.4m in which it can heat up the pavement. After the pavement is heated, crews can use rakes and shovels or a rototiller type of attachment to work/disaggregate the softened pavement prior to re-compaction. The unit essentially acts as hot in-place recycler. The larger footprint of the HeatWurx unit appears to make it a better-suited device for situations where larger-scale pavement heating is needed, as opposed to doing pothole-sized repairs. In October, the efficiency of HeatWurx system was measured in field. The pavement reached about 90℃ at depth of 1.2cm after 30 minutes and about 82℃ at depth of 5cm after 60 minutes. After about 2 hours and 4 minutes, surface temperature close to 204℃ was measured (pavement temperature is about 2℃ before heating).

Figure 15. Heatwurx system [5]

Field performance of asphalt patch repaired with infrared heating

The study by ODOT conducted survivability analysis on patches repaired by infrared heating, spray injection, and throw and roll. Survival analysis was also conducted to quantify the longevity and determine the expected life of patches installed using each of three methods. The results are shown in Table 6. The data were collected after 188 weeks of construction. Potholes repaired by infrared heating showed a remarkably higher surviving rate than other methods. Almost all the potholes were still in service after 188 weeks, which can be considered as semi-permanent repair. While most of the potholes constructed by the other two methods failed and need a second repair.

Table 6. Surviving rate in field after 188 weeks of installation [4]

Patching method	Material	Total	Failed	Survived	Surviving rate
Infrared	Cold HMA	15	1	14	93.33
Spray injection	Emulsion and Aggregate	15	13	2	13.33
Throw and Roll	Cold mix	15	11	4	26.67
Total		45	25	20	44.44

MnDOT also monitored the performance of the patch made by different heating methods and materials. The real pothole conditions were surveyed in a certain interval and recorded by photos. The repair was done with HeatWurx on 10/30/2012. The pothole repair process is similar to hot in-place recycling. Temperature measurements indicated that the HeatWurx's surface-downward heating mechanism resulted in steep temperature difference between pavement surface (hot) and the deeper underlying pavement (cooler). Figure 16 shows the field surveyed photos for potholes (date for Pothole 1#: 11/20/2012, Pothole 2#: 11/13/2012). The repair deteriorated rapidly, with the repair de-bonding from the underlying pavement, and also raveling. The premature failures could be partially attributed to temperature difference along pavement depth caused by infrared heating. If the temperature of the surface asphalt becomes too hot, the overheated asphalt binder can be aged quicker. Another factor that probably played a role was the mechanical "tilling" of the heated pavement, which removed not only damaged asphalt pavement in

the pothole but likely incorporated some deeper asphalt material.

(a) Pothole 1 (b) Pothole 2

Figure 16. HeatWurx repaired potholes [5]

Microwave heating

MnDOT adopted microwave equipment to heat the pavement for pothole repair, using a patented microwave system from Microwave Utilities, Inc. (MUI) [5]. The equipment is shown in Figure 17. It is much more effective than the HeatWurx unit for heating asphalt pavement to higher temperatures at significantly greater depth and in much less time. MnDOT tested the efficiency of microwave heating in October. With the microwave set at 50kW, the intact pavement surface was heated from 26℃ to 93℃ in just 7 minutes. At 5cm below the surface, the pavement would reach temperatures over 148℃. Considering that the asphalt and aggregates are nonmagnetic, specific aggregate such as taconite rock or steel slag can be used in patching material in order to enhance the microwave heating effect. Figure 18 shows the microwave heating rates of taconite rock and conventional aggregate studied by Zanko et al. (2004) [58]. Generally, the higher the magnetite content, the higher microwave heating efficiency.

Figure 17. Microwave Utilities [5]

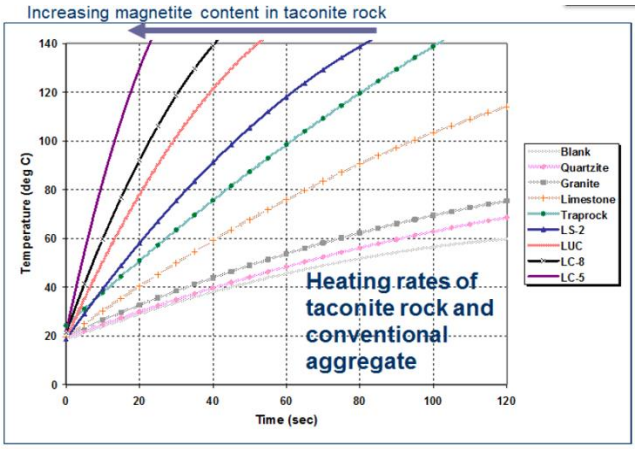

Figure 18. Microwave heating rates of taconite rock and conventional aggregate [58]

Case 1: Microwave heating repair by MnDOT:
Repair time: 10/30/2012 (Hole 1 and hole 2)
Last field survey date: 01/07/2013

Material: As-is RAP from a Lake County OPERA project (no magnetite nor RAS) (Hole 1), RAP + magnetite powder (about 2.5% by weight) (Hole 2)

Construction: The patches were heated for 4 minutes at 50kW power and compacted. This repair attained a temperature of about 80°C to 105°C.

Performance: As shown in Figure 19, the center of the Hole 1 repair (the MUI test patch portion) lost material with time, while the as-is RAP remained relatively intact a week later, but all the material was lost on 7th Jan 2013. Hole 2 repair remained intact until it was also removed by other repairs.

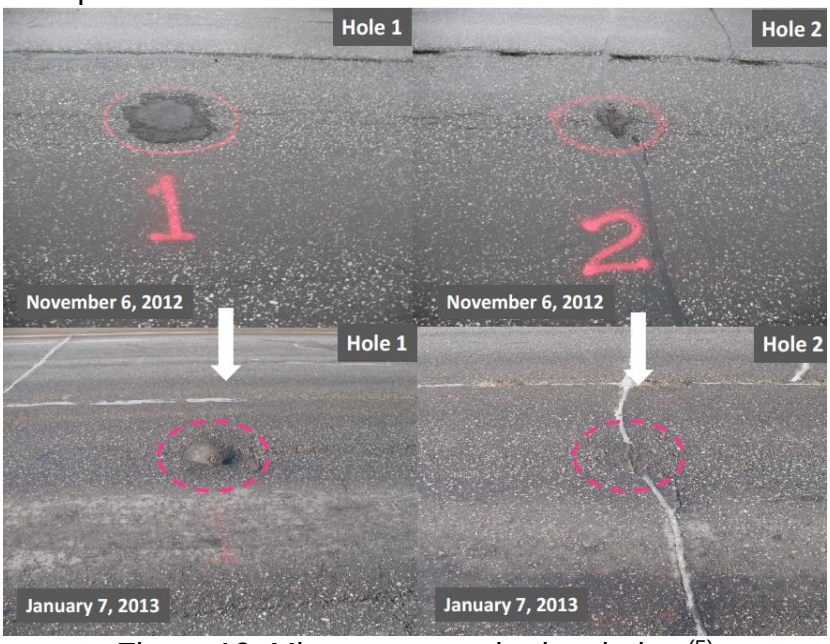

Figure 19. Microwave repaired potholes [5]

Case 2: Microwave heating repair by MnDOT:
Repair time: 10/30/2012
Last field survey data: 07/30/2013

Material: RAP + Recycled Asphalt Shingles (RAS) + magnetite powder (about 2.5% by weight).

Construction: The patch was heated with microwave equipment for 6 minutes at 50kW; shoveled, raked, and combined with the softened adjacent pavement; and compacted. The temperature of the pre-compacted mixture was noted to average 105°C.

Performance: The repair held up well following installation, exhibiting a minor amount of surface loss (raveling) with time. According to the last observation, it generally remained sound repair, as shown in Figure 20. The surrounding pavement, however, continued to deteriorate.

Figure 20. Microwave repaired pothole [5]

Induction heating

Due to the requirement of conductive material, the purpose of induction heating in pothole repair was mainly heating the patching material instead of preheating the old pavement. The U.S. Army Engineer Research and Development Center (ERDC) studied the feasibility of heating the patching material to hot mix temperature for all seasons using induction heating [59]. In order to make inductive heating feasible, the fine aggregates were replaced by steel particles. Firstly, laboratory experiments were conducted to evaluate heating properties of aggregates with different contents and types of steel particles. A 15 kW Ambrell EKOHEAT 15/100C power supply with an auto-tuning frequency range of 50 to 150 kHz was used in conjunction with a four-turn copper induction coil designed, as shown in Figure 21. It was found that there was a large temperature difference between the final surface temperature and internal temperature. The increase of material temperature with heating time is shown in Figure 22. The increase of temperature with the volume replacement was observed for internal temperature but not for surface temperature. The internal temperature could reach 150℃ in fewer than 8 min with 15% volume replacement. For fixed steel content with varying steel types, it was found that the peak temperature of the material was generally lower for the larger size with cube shot steels but higher for the smaller size with grit steels.

Although induction currents nearly raised steel temperature instantly, the bulk mix temperature lagged behind as heat was dispersed into surrounding aggregates and throughout the mix. The larger steel particles dissipated heat more slowly.

(a) (b)

Figure 21. laboratory induction heating setup: (a) EKOHEAT 15/100C power supply; (b) 3.8 L fiber tube in laboratory coil [59]

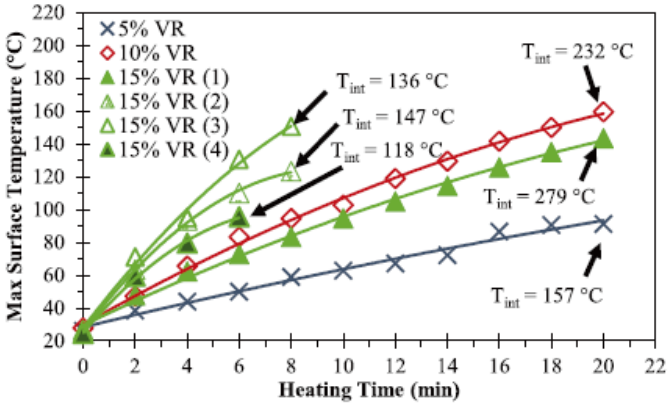

Figure 22. Maximum surface temperature and internal temperature with heating time [59]

Field tests were further conducted to evaluate the performance of the designed inductive hot mix asphalt (iHMA), HMA, and CMA, as shown in Figure 23. The prototype field induction heater (FIH) unit was used. The FIH contained an induction coil for a 19L container, a 35kW diesel generator and a water-cooled heat exchanger to power and cool the unit. It was found that iHMA containing 7.5% cube shot and 7.5% steel grit by volume of total aggregate was successfully heated in 19L containers using the prototype FIH. The mix was capable of achieving 160℃ temperatures in 5 min. In full-scale field rutting tests, the rut depth of iHMA was comparable to or slightly less than that of HMA, while the CMA had much greater rut depth.

Figure 23. Field repair of pothole using induction heating [59]

LIFE CYCLE COST ANALYSIS

Life Cycle Cost Analysis (LCCA) is an indispensable technique that employs well established principles of economic analyses to evaluate long-term performance of competing investment options. The LCCA process is performed by summing up the discounted monetary equivalency of all benefits and costs that are expected to be incurred in each option. Most of the LCCA input parameters are inherently uncertain, such as the discount rate that should be employed to convert costs occurring at different points in time to a common time frame, the analysis period over which the options are to be evaluated, and the type and timing of future rehabilitation activities that will take place in each of the life cycle options. In order to conduct LCCA in a reliable and trustworthy manner, a thorough understanding of the theoretical engineering and economics background must be acquired.

Currently, there are different pothole repair procedures that could be used for pothole repair, and each of them has different material, equipment or labor requirements. The cost of each component in pothole repair could be collected by literature review or survey, while due to the uncertainty of the lifespan, the life cycle cost analysis of each procedure could have a high variance. Given that the throw and roll is the simplest and most widely used procedure, using throw and roll as a base case and comparing the life-cycle cost of other procedures as a function of repair life with the base case could be a more reliable way to analyze the cost effectiveness. Subsequently, the relationship between the lifespan of each procedure and the total cost difference can be established, which could be used to determine under what lifespan one repair procedure can cost the same as throw and roll. Hence, the decision maker could select the most cost-effective procedure in practice.

Additionally, for procedures with heating, when there is no technical problem, the productivity of the procedure mainly depends on heating time, which could differ a lot from different areas and seasons. The variation of heating time would in turn impact the total cost. Therefore, in life cycle cost analysis, the sensitivity of heating time on total cost should be figured out in order to improve the cost effectiveness. In this chapter, the life-cycle cost of different repair methods as a function of repair life would be compared in different analysis periods; the sensitivity analysis of the heating time will also be conducted.

Cost Inputs of LCCA

Material cost

The cost most commonly associated with pothole patching is the cost of materials. This is usually one of the least significant contributors to the overall cost of patching operation. However, the material used for patching does impact the cost of the overall operation when there are differences in performance. More expensive materials that are placed with less effort and last longer can reduce the cost of the initial patching effort, as well as the amount of repatching needed. This reduces the labor and equipment costs for the overall operation.

The cost of all kinds of patching materials was collected from NJDOT and existing reports, which are listed in Table 7. The shipping cost is not included. It should be noted that both bulk and bags of cold mix were adopted in life cycle cost analysis for throw and roll and semi-permanent procedures. The loose HMA was adopted for infrared and microwave heating. Moreover, although the material for microwave heating might need extra additives like magnetic power, given that they are not indispensable and are recycled materials in some places, the price of them was not included.

Table 7. Material Cost [4]

Patching Materials	Material Cost / ton
Bulk cold mix	$110.9
Bags of cold patch	$232
HMA	$84
Spray injection material	$203

Labor cost

The crew number and wage for the repair and traffic control were determined based on the information collected from different studies [See references 1,4,8 and 57]. The number of workers in the repair differs from one patching method to another, but each crew has one supervisor/manager.

For the throw-and-roll technique, the labor cost can be as little as two workers who do the actual patching, plus traffic control. One of the two workers shovels the material from the truck into the pothole, and the other drives the truck over the section to compact the patch. In some instances, the driver of the vehicle is able to shovel material when patching large areas. This generally improves the productivity of the overall operation. The semi-permanent patching operation has proven to be the most efficient when four workers are used, along with the appropriate traffic control. Two workers clear out debris and square-up the edges, while the other two follow behind, place material and compact the patches. This procedure can be accomplished using more or fewer workers, but the experience of many agencies has found four workers to be optimum. For spray injection, the single-unit spray-injection device requires one single operator. Two operators are recommended when using the trailer-unit equipment (one to operate the vehicle and one to place the material).

Basically, the infrared heating method needs at least two workers, operating the heating machine and then placing and compacting the patch. Based on the practice from ODOT, four workers are usually involved in infrared heating, which may have better efficiency and could solve the potential lighting problem quickly. For microwave heating, normally two or three workers are needed based on the field testing conducted by MnDOT. One operates the heating machine and two place and compact the patch, which may lead to an effective repair. The daily wage is assumed to be $190 per day per labor and $323 per day per supervisor, according to the wage level in Ohio [4]. Table 8 shows the labor needed and cost that was computed for each patching method.

Table 8. Summary of Labor Cost for Different Pothole Repair Methods [1,4,5]

Patching method	Number of workers and supervisor	Number of traffic control crews	Labor for traffic control ($/day)	Labor for pothole repair ($/day)	Total
Throw and Roll	2+1	2	$380	$703	$1083
Semi-permanent	4+1	2	$380	$1083	$1463
Spray injection	2+1	2	$380	$703	$1083
Infrared Heating	4+1	2	$380	$1083	$1463
Microwave heating	3+1	2	$380	$893	$1273

Equipment cost

Depending on the type of patching operation performed, different pieces of equipment are needed. Trucks, compressors, jackhammers, compaction devices and heating machines may be used, and each has costs associated with it. Table 9 provides a summary of the devices used for each patching method and their corresponding costs, which were collected from different reports and studies. The cost of DuraPatcher and Minutema equipment per day includes the daily equivalent cost, maintenance cost and operating cost, based on the information of existing study [4]. The total cost of Microwave Utilities was collected from other research [58].

Table 9. Equipment Cost [1,4,5]

Equipment	Cost ($/day)				
	Throw and roll	Semi-permanent	Spray injection	Infrared heating	Microwave heating
Material Truck	$25	$25	-	$25	$25
Traffic control sign	$25	$25	$25	$25	$25
DODGE 4W Truck	$14	-	-	-	
Vibratory roller	-	$150	$150	$150	$150
Edge-straightening device	-	$5	-	-	-
Air compressor	-	$10	-	-	-
DuraPatcher			$327		
Infrared heating Minutema				$163	-
Microwave Utilities					$450
Total	**$64**	**$215**	**$502**	**$363**	**$650**

Productivity

Each pothole-patching crew has different values for the average productivity achieved. One way of estimating average productivity is to divide the total amount of cold mix placed during a season by the total days spent patching. The value should be expressed in terms of tons per day of material placed. The productivity of pothole repair methods will affect the repair efficiency, and the higher the productivity, the lower the total cost. By combining the field performance information of the patching methods, the productivity can be computed using the following equation 3 [(4)]:

$$P = (V/T) \times (\gamma) \times (1/2{,}000 \text{ ton/lb}) \times (60 \text{ min/hr}) \times (4 \text{ hr/day}) \quad (3)$$

Where: P is productivity of the patching crew, tons per day; γ is patch density, 125 lb/ft^3 assumed here; V is total volume of the potholes being patched using given method, ft^3; and T is total time required to patch the potholes using given method, minutes.

It is assumed that the entire crew will work for 4 hours per day. This assumption was made as the actual percentage of a day spent patching versus setting up traffic control, taking breaks, or traveling between pothole locations could not be taken into account [(54)]. According to the pothole repair performances in SHRP-353 program, the repair time using different pothole repair methods obtained from various field sites can be summarized in Table 10. The time required for patch mainly depends on repair procedure and pothole size. Generally, the time required for each procedure would increase as the pothole size increases. Therefore, the repair time for comparison is normalized as minutes per one cubic feet pothole. It is noted that there was no patch area data for microwave heating method, the average patch area was assumed to be similar with others (1.2 ft^3). For infrared heating method, although the patch area was not provided in existing studies, its productivity had been calculated directly elsewhere [(4)], thus, the repair time needed for infrared heating was back calculated. The productivity of each repair method was shown in Table 11.

Table 10. Summary of repair time using different pothole repair methods at various field sites (minutes per one cubic feet pothole) (See references 3,4,5 and 54)

Procedure	Components	Field sites								Range	Average
		CA	IL	NM	OR	TX	UT	VT	ON		
Throw and roll	Total	1.8	3.6	2.9	3	1.5	1.6	1.8	5.6	1.5-5.6	2.7
Semi-permanent	Total	3.9	9.8	4.9	-	4.9	6.1	4.2	8.4	3.9-9.8	6.0
Spray injection	Placement	1.4	2.2	2.3	-	1.1	2.4	1.8	-	1.1-2.4	2.2
Infrared heating	Total	OH									18
Microwave heating	Total	MN									7

Table 11. Productivity

Procedure	Productivity (Tons/Day)
Throw and roll	5.56
Edge-seal	5
Semi-permanent	2.5
Spray injection	6.8
Infrared	0.89
Microwave	2.1

Repair life

The longevity and survival rate are important factors in evaluating the cost-effectiveness as it determines the number of repatching that will occur in analysis period. However, in most cases the life expectancy cannot be observed exactly and can only be estimated. SHRP-353 program conducted a comprehensive study of field performance on potholes repaired by different patching materials and methods. However, the specific life of pothole repair is not known and only the surviving rate was provided. Note that the construction temperature of the potholes repaired in CA, IL, NM, TX, UT and VR were all above 15℃. To better estimate the surviving life of potholes constructed in winter conditions and compare the effectiveness of preheating method with normal procedures, the data of OR, ON and MN were used.

Nazzal et al. (2014) and Zanko (2016) studied field performance of potholes repaired by infrared and microwave heating methods [4,5]. In this chapter, the average life for most repairs was recorded. For life span of pothole repaired by microwave heating, the data was limited, and the potholes almost survived in the last observation. Thus, the average time between the construction and last observation was used. The estimated average life of each procedure is summarized in Table 12.

Table 12. Average Surviving Life for Material-Procedure Combination (Weeks) [4,5,54]

States	Mean	Throw and roll	Semi-permanent	Spray-injection	Infrared heating	Microwave heating
ON	Estimate	26.33	34.43	23.50	-	-
	Std. Error	1.39	2.92	5.96	-	-
OH	Estimate	14.50	-	9.30	Max>188	-
	Std. Error	2.47	-	1.99	-	-
MN	Estimate	-	-	-	-	Max>130
TOTAL	Mean	20	34	16	Max>188	Max>130

Total cost calculation

In the economic evaluation of projects, there are several formats of economic indicators for the analysis results. The most common are Net Present Value (NPV), Cost-Benefit Ratio (B/C), Equivalent Uniform Annual Costs (EUAC), and Internal Rate of Return (IRR). Since the life cycle cost analysis aims at evaluating project alternatives that result in equal categorical benefits but entail unequal costs, the Net Present Value (NPV) is considered the appropriate (and the prevalent) indicator for comparing the differential economic worth of projects. The calculation of the NPV is shown in Equation 4 [60].

$$NPV=\text{Initial Cost} + Pwf * (\text{rehabilitation Costs}) - Pwf * (\text{Salvage}) \quad (4)$$

Where: Pwf_t is present worth factor of costs incurring at year t, which can be calculated according to Equation 5.

$$Pwf_t = \frac{1}{(1+d)^t} \quad (5)$$

Where: d is discount rate.

Analysis and Findings

Case study

According to the survey response from NJDOT, the spray injection equipment often breaks down during its usage, and the semi-permanent procedure is not a common-used method, thus, the life cycle cost analysis would be based on two heating methods. To compare the cost-effectiveness of the heating methods, the throw and roll procedure is used as the basic case, and 2- and 5-years analysis periods will be analyzed. According to the survey response, the bulk or bags of CMA are usually used in pothole repair and the price of them is respectively $110 and $232. Moreover, the average life of the pothole repaired by throw and roll was about 20 weeks based on the filed observation in SHRP-353 program, while the life estimated by NJDOT was about 12 weeks. Therefore, the base case was divided into 4 different scenarios where two material prices and two lifespans were used.

<u>Scenario 1 ($110 material cost and 12 weeks lifespan)</u>

Figure 24 shows the total cost difference between heating methods and throw and roll procedure with $110 material cost and 12 weeks lifespan. If the value of total cost difference is zero, it means adopting the heating method would cost the same as throw and roll. The correspopnding lifespan is a breakeven point. While if the value is negative, using the heating method would cost more, and vice versus. For microwave heating method in both 2 and 5 years analysis periods, in order to be more cost effective than throw and roll, the lifespan of the potholes should be over about 42 weeks. While the required lifespan for infrared heating is around 91 weeks because it has a higher labor cost and lower productivity than microwave heating. Also, the lifespan of both heating methods in 5 years analysis period has a higher sensitivity to the total cost.

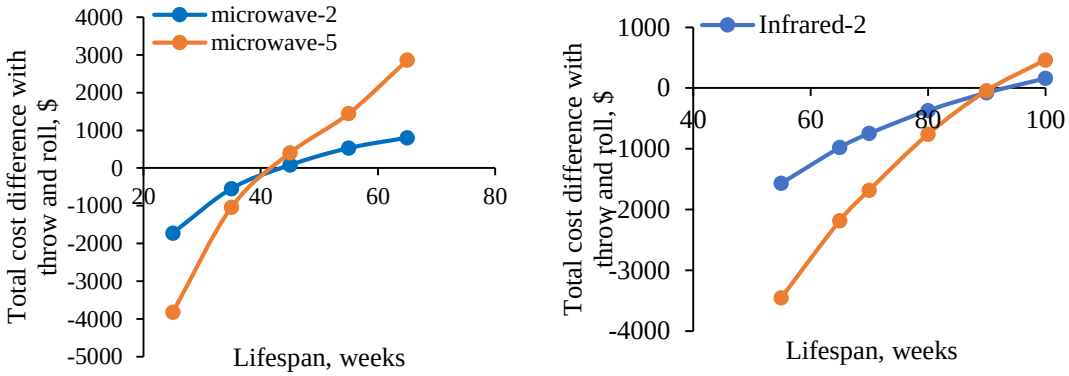

(a) (b)

Figure 24. Relationship between total cost difference and lifespan of heating methods in scenario 1, (a) Microwave, (b) Infrared

Assuming that there are no technical problems with heating machines, the repair time of both microwave and infrared heating methods would mainly depend on the environment temperature, which would differ a lot from different areas and seasons Hence, the heating time would in turn impact the productivity and the total cost. Once total cost changes with productivity, the breakeven point of the lifespan would also change. The ratio of this lifespan to the average life of the base case was used as a life ratio here. Figure 25 shows the relationship between the heating time and life ratio. For microwave heating, every 30 seconds saved in heating time could lead to about 2.5 weeks decrease in breakeven lifespan. For infrared heating, as 30 seconds saved in heating time, the average reduction in breakeven lifespan would be about 3 weeks.

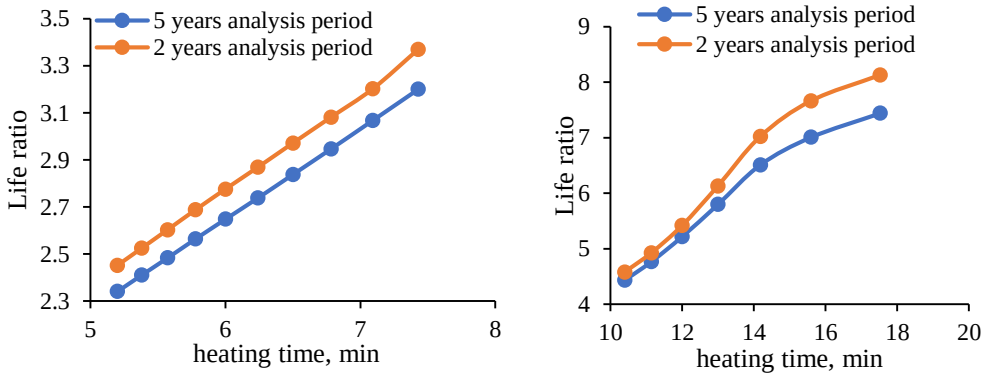

(a) (b)

Figure 25. Relationship between heating time and life ratio in scenario 1, (a) Microwave, (b) Infrared

<u>Scenario 2 ($110 material cost and 20 weeks lifespan)</u>

Assuming the cost of CMA is $110, and the lifespan of throw and roll is 20 weeks, the total cost difference between heating methods and throw and roll procedure is shown in Figure 26. In both 2 and 5 years analysis periods, the breakeven point of lifespan of microwave heating methods is 55 weeks. While for infrared heating, in 2 years analysis period, the initial cost of is higher than the total cost of base case, thus, no breakeven lifespan could be found. In 5 years analysis period, the breakeven point of lifesapan for

infrared heating is aroung 150 weeks.

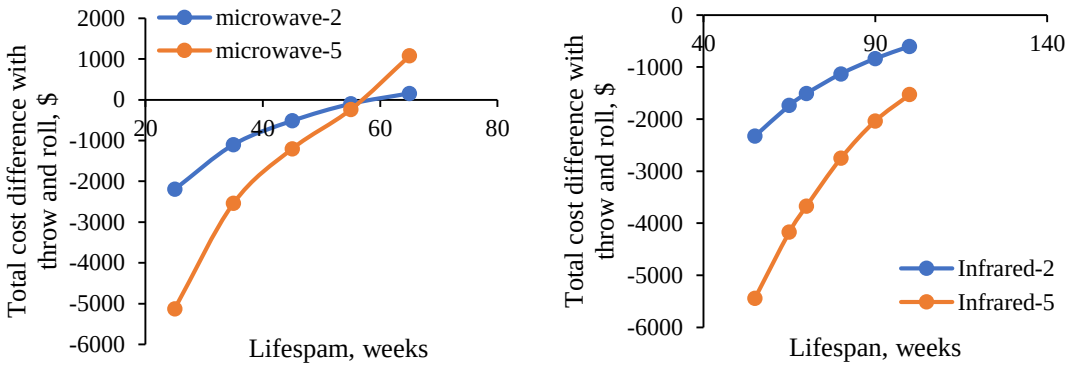

(a) (b)

Figure 26. Relationship between total cost difference and lifespan of heating methods in scenario 2, (a) Microwave, (b) Infrared

Figure 27 is the relationship between the heating time and life ratio for scenario 2. Compared to scenario 1, every 30 seconds saved in microwave heating time could lead to 3.5 weeks decrease in breakeven lifespan. For infrared heating, every 30 seconds saved in heating time could lead to about 0.9 week reduction in the breakeven lifespan.

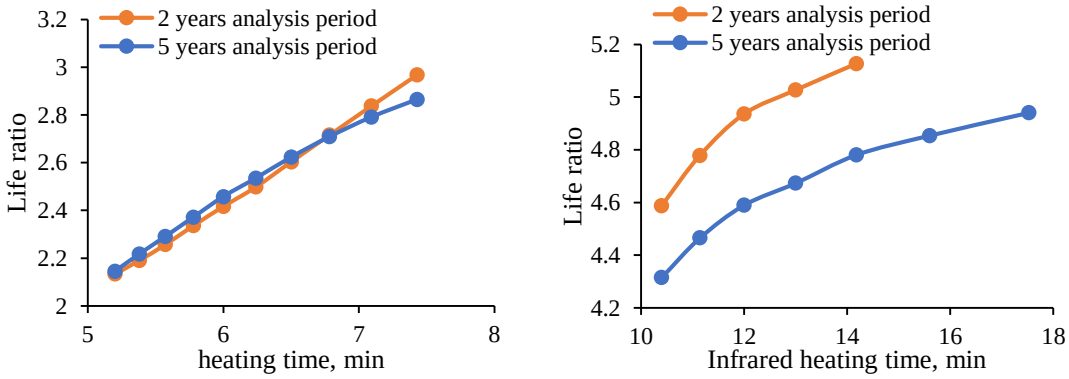

(a) (b)

Figure 27. Relationship between heating time and life ratio in scenario 2, (a) Microwave, (b) Infrared

Scenario 3 ($232 material cost and 12 weeks lifespan)

When using bags of CMA, the price of the material in base case increased to $232 according to the response from NJDOT, the relationship between the breakeven point of lifespan and the total cost difference is shown in Figure 5. For both 2 and 5 years analysis periods, the approximate breakeven point of lifespan of microwave and infrared heating methods are respectively about 40 and 65 weeks.

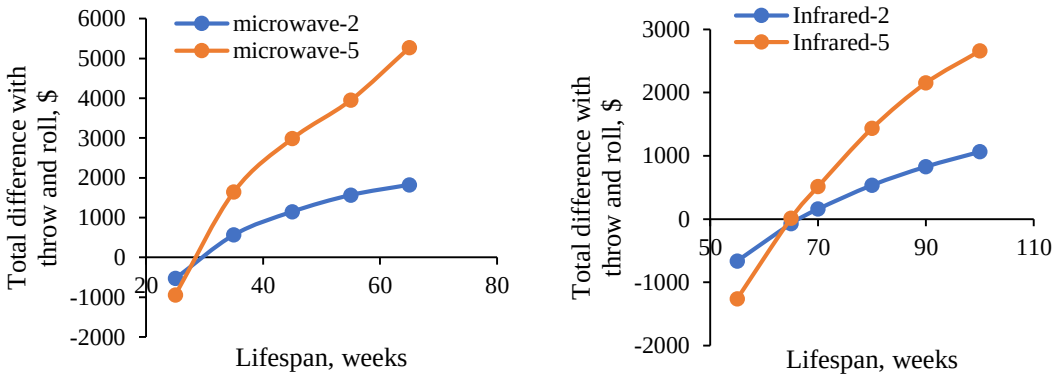

(a) (b)

Figure 5. Relationship between total cost difference and lifespan of heating methods in scenario 3, (a) Microwave, (b) Infrared

Figure 28 shows the variation of life ratio with heating time, every 30 seconds saved in microwave heating time could lead to 1.8 weeks decrease in breakeven lifespan, and every 30 seconds saved in infrared heating would lead to 1.9 weeks decrease in lifespan.

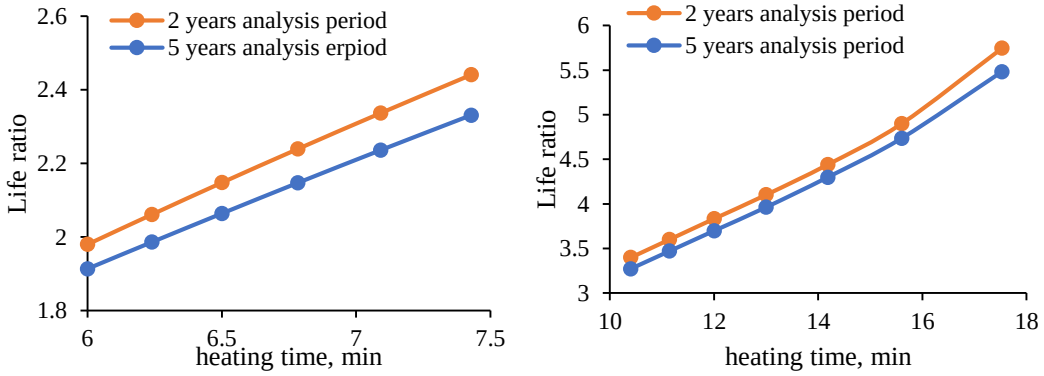

(a) (b)

Figure 28. Relationship between heating time and life ratio in scenario 3, (a) Microwave, (b) Infrared

Scenario 4 ($232 material cost and 20 weeks lifespan)

As shown in Figure 29, when the lifespan of base case increased to 20 weeks, the approximate breakeven point of lifespan of heating methods for both 2 and 5 years analysis periods are respectively about 45 and 99 weeks. Compared to previous scenarios, the increase in material cost would lower the sensitivity of base case lifespan to the breakeven lifespan of heating methods. And as the base case lifespan increased, the sensitivity of material cost to the breakeven lifespan of heating methods would increase accordingly.

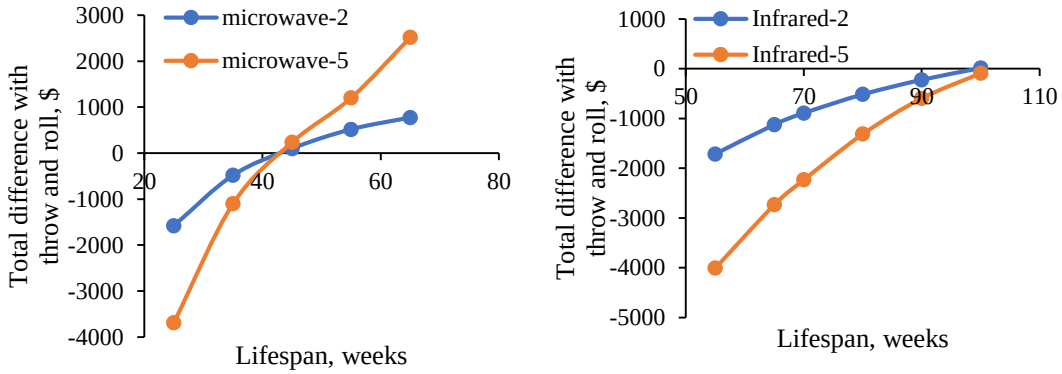

(a) (b)

Figure 29. Relationship between total cost difference and lifespan of heating methods in scenario 4, (a) Microwave, (b) Infrared

Figure 30 shows the variation of life ratio with heating time, every 30 seconds saved in microwave heating time could lead to 2.5 weeks decrease in breakeven lifespan, and every 30 seconds saved in infrared heating would lead to 3 weeks decrease in lifespan. This reduction is close to that in scenario 1, which means for microwave and infrared heating, the actions of the increase in base case material cost and the increase in lifespan offset each other. Overall, as the total cost of base case increase, the heating time per unit saved would lead to a lower decrease in breakeven lifespan, and vice versus.

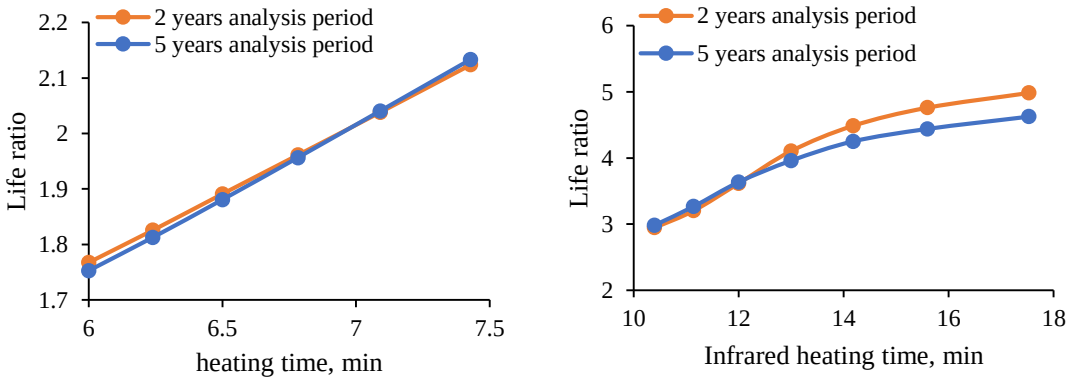

(a) (b)

Figure 30. Relationship between heating time and life ratio in scenario 4, (a) Microwave, (b) Infrared

Contribution to total cost

In life cycle cost analysis, the cost components are mainly material, labor and equipment costs. The analysis period and the lifespan of each procedure only impacts the number of rehabilitation events. Given that the cost of each rehabilitation is the same, the contribution of each component to the total cost equals to the contribution to the cost in each rehabilitation. On the other hand, the productivity determines how many days should be spent on each rehabilitation. Thus, in order to improve the cost effectiveness of repair procedure, the sensitivity of the productivity to each component contribution should be figured out. Figure 31 shows the relationship between the proportion of each cost

component and productivity. As seen, for both infrared and microwave heating methods, the labor cost accounts for the largest proportion of total cost, which is over 50%, and the material cost has the least contribution to the total cost. As productivity increased, for both heating methods, the proportion of labor and equipment cost decreased while that of material cost increased. However, in a reasonable variation of productivity, the labor cost still accounted for the largest proportion.

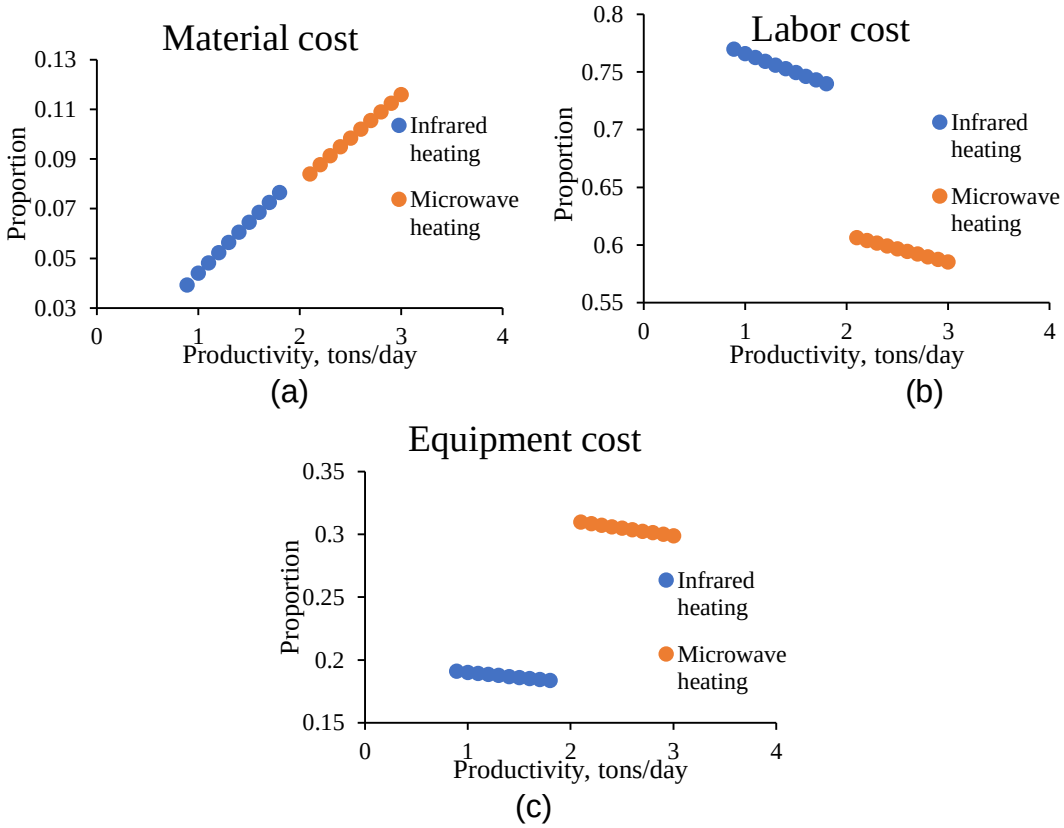

Figure 31. The relationship between cost proportion and productivity, (a) Material cost, (b) Labor cost, (c) Equipment cost

Summary

This chapter conducted life cycle cost analysis of different pothole repair methods. The information of each input like material cost, equipment cost, labor cost, lifespan and so on was collected. To compare the cost effectiveness of heating methods, the throw and roll procedure was used as a base case. Due to the uncertainty of the input information, two different material costs and two different lifespans were adopted according to the survey response from NJDOT and literature review. The relationship between the lifespan of two heating methods and the total cost difference with throw and roll were plotted and the breakeven lifespan of two heating methods were determined in different scenarios, the sensitivity of heating time to breakeven life was analyzed as well. The results are summarized in Table 13. In the whole life cycle of the patch repaired by heating methods, labor cost was found to be the majority regardless of the productivity and material cost only accounted for a small proportion.

Table 13. Breakeven lifespan and variations under different scenarios

Heating method	**Breakeven lifespan, weeks**		**Reduction in breakeven lifespan per 30s saved in heating, weeks**	
	Microwave	Infrared	Microwave	Infrared
Base case: $110 and 12 weeks	42	91	2.5	3
Base case: $110 and 20 weeks	55	150*	3.5	0.9
Base case: $232 and 12 weeks	40	65	1.8	1.9
Base case: $232 and 20 weeks	45	99	2.5	3

1. * means the breakeven lifespan in 5 year analysis period

FIELD EXPERIMENTS ON ASPHALT POTHOLE REPAIR USING PREHEATING

Test Section Construction

Test section site and construction plan

To investigate the field performance of asphalt patches, a field test section was built in the southeast site of asphalt laboratory at Rutgers University, as shown in Figure 32. The test section is 15-m-long, 3.65-m-wide and 15-cm-thick. The use of this area for construction had been approved by the university facility.

Figure 32. Location of test section

The test section was constructed in two lifts using the same materials. The first lift was 8.9-cm-thick and the second was 6.4-cm-thick. All the potholes were made, and thermocouples were installed in the top lift.

The procedure of creating artificial potholes and installing thermocouples is as follows:

1) Mark the location of pothole at the side after paving the first lift.
2) Spray WD-40 lubricant to the wood blocks and put them on the first lift. Two screws were preliminarily installed on each wood block for easy removal after compaction, as shown in Figure 33.

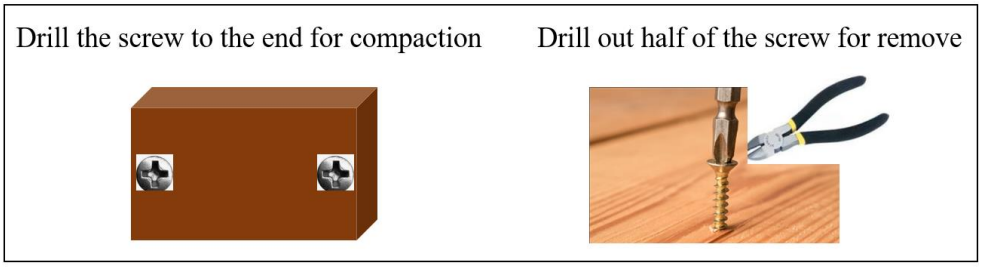

Figure 33. Instruction for removing the wood block

3) Paving the surface lift.
4) Insert thermocouples from the sides at two different depths for temperature measurement.
5) Compact the surface lift after inserting thermocouples.
6) After compaction, remove the wood blocks.

Construction process

Figure 34 shows the process of first lift construction. As seen, the uneven soil surface of the test section was covered with gravel and weeds initially. Before construction, the gravel and weeds were removed, and the ground was leveled. When the temperature was around 28℃ in the morning, HMA with 9.5mm nominal maximum aggregate size (NMAS) was paved on the flat soil ground. Roller compactor was used to compact the first lift to 8.9-cm-thick, and vibrator was adopted to compact the surrounding materials. After that, the longitudinal sides of the first lift were marked to determine the positions for placing the wood blocks. Two adjacent wood blocks were separated from center to center by 0.3m. In total, 52 wood blocks sprayed with lubricant were placed on the first lift, and each wood block was 30.5-cm-long, 12.7-cm-wide and 6.35-cm-thick.

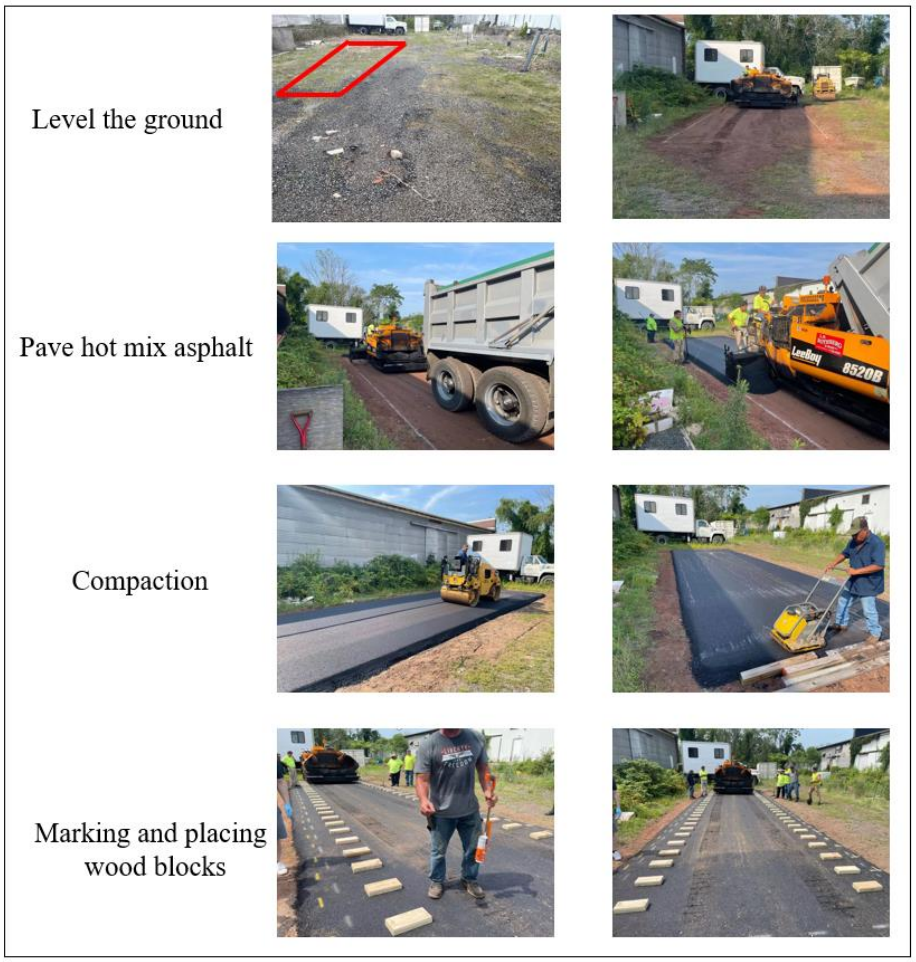

Figure 34. First layer construction

Figure 35 shows the construction of the second lift. It was conducted at noon when the temperature was about 35℃. The materials were paved directly over the wood blocks. After paving, two thermocouples were inserted into two different depths beside each wood block immediately, and a total of 16 thermocouples were installed. Given that the wood blocks were embedded in the second lift, to achieve a better compaction quality, the loose materials over each wood block were removed manually. Subsequently, the second lift was compacted using roller compactor and the vibrator. To ensure that the wood blocks can be removed without damaging the surrounding hot materials, they were lifted using pliers about 15 minutes after compaction. Figure 36(a) shows the artificial pothole after construction, which was 30.5-cm-long, 12.7-cm-wide and 6.35-cm-thick. The shape of the pothole was regular, and the edges were straight in general. Figure 36(b) shows the pothole condition after tornado “Ida” in August 2021. It can be found that raveling occurred at the edges of the potholes, which could be attributed to the scouring effect caused by water.

Figure 35. Second layer construction

(a) (b)

Figure 36. Artificial pothole (a) After construction, (b) After tornado “Ida”

Heating Trial Tests

Microwave heating test

To monitor the temperature distribution, the field heating test was conducted using microwave unit with a horn, as shown in Figure 37. The embedded thermocouples were used to measure the internal temperatures of the pavement, and the thermal camera was used to measure the pavement surface temperature. The power of the microwave unit is 1450W with 65% efficiency, and the frequency is 2.45GHz. A 5500W generator was used to support it. It should be noted that because the microwave port is rectangular, its orientation impacts the electromagnetic wave path, which will further affect the temperature distribution.

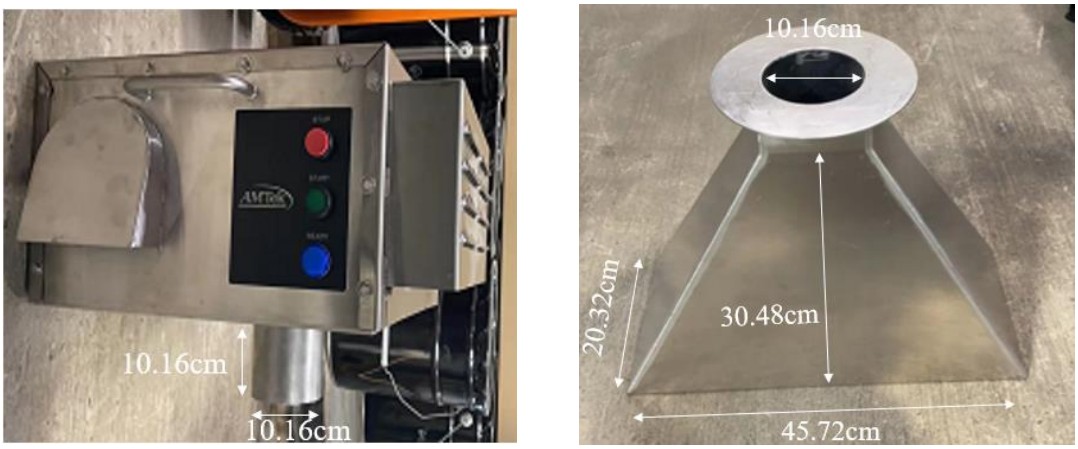

(a) (b)

(c)

Figure 37. Microwave heating apparatus, (a) Microwave unit, (b) Horn, (c) Port

Heating test 1

Figure 38 shows the first heating test. In this case, the longer edge of the microwave port is parallel to the longer edge of the pothole. Before testing, the surface temperature was 8.6 ℃, and the temperatures detected by sensors at 2cm and 5cm depths were 12.4℃ and 12℃, respectively. It can be found in Figure 39 that most of the pothole was heated after heating for 8 minutes, while the maximum surface temperature was only about 27℃. Figure 40 shows the temperature detected by thermal sensors. As seen, the difference in temperature at different depths was less than 2℃. The temperature increasing rate at a lower part of the pavement was similar to that at the surface area. It indicates that microwave does can heat the internal material of the pavement; however, the overall increasing rate was low.

Figure 38. The first heating test

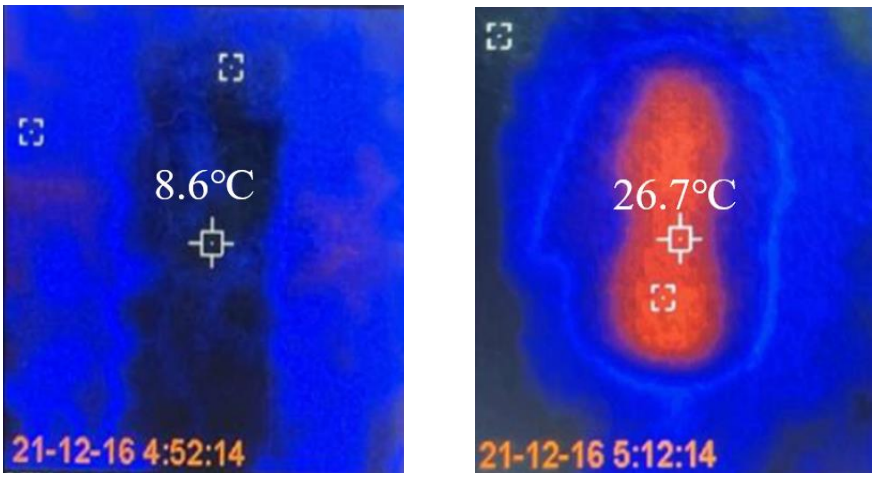

(a) (b)

Figure 39. Temperature distribution, (a) Before heating, (b) After heating

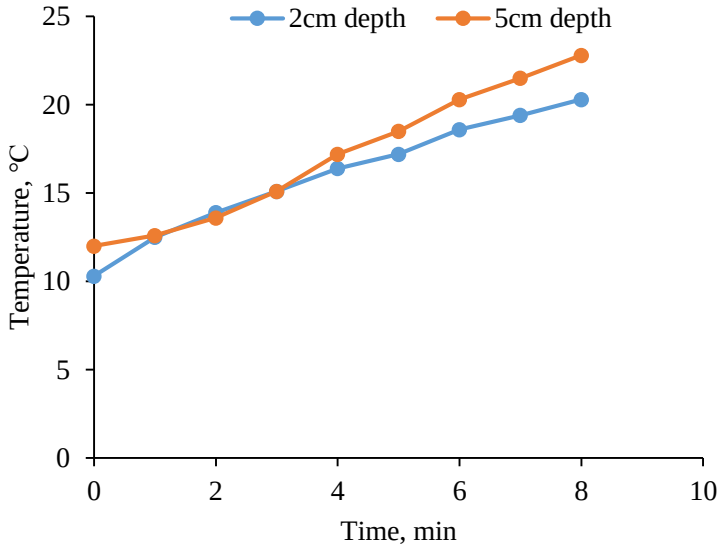

Figure 40. Temperatures detected by thermocouples

Heating test 2

Figure 41 shows the second test. In this case, the longer edge of the microwave port is parallel to the shorter edge of the pothole. Before testing, the surface temperature was 6 ℃ and the temperatures detected by sensors at 2cm and 5cm depths were 9.5 ℃ and 10.2℃, respectively. After heating for 8 minutes, the temperature distribution pattern was totally different from that in the first test. The maximum temperature was located near the shorter edge of the pothole and was around 42 ℃. Figure 42 shows the surface temperature distribution before and after heating. As can be seen, the temperature was symmetrically but quite unevenly distributed over the pothole area. The temperatures at the shorter edges of the pothole were remarkably higher than those at other areas. Moreover, the center of the pothole was heated slightly, and the longer edges of the potholes were almost not heated. Figure 43 shows the temperatures detected by internal sensors. The general temperature increasing rates was lower than those in test 1, and

the internal temperatures only increased by around 5℃ after heating for 8 minutes, indicating a low heating efficiency under the current power.

Figure 41. The second heating test

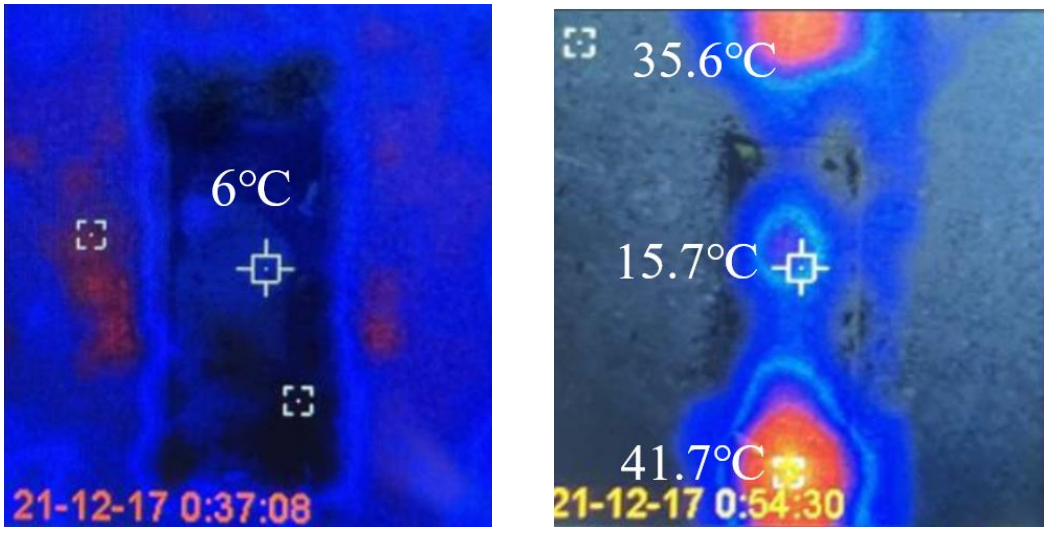

Figure 42. Temperature distribution, (a) Before heating, (b) After heating

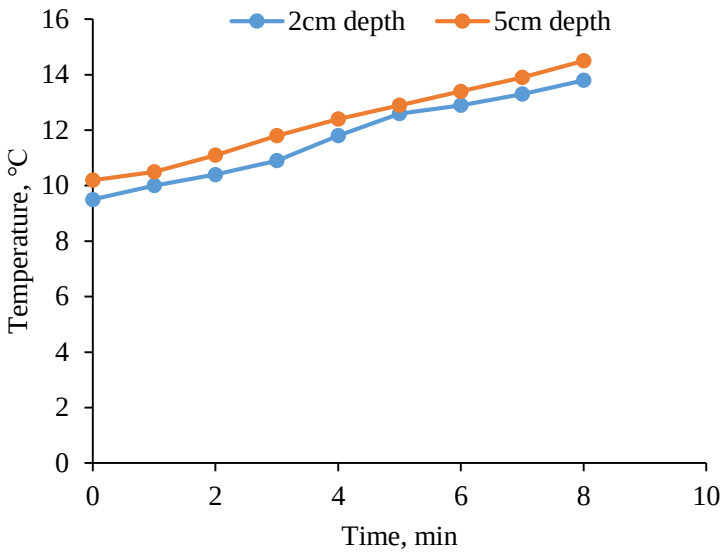

Figure 43. Temperatures detected by thermocouples

Infrared heating test

Since the acquired microwave unit did not show a satisfactory heating performance, a portable infrared heater was further adopted to investigate its heating efficiency in field, as shown in Figure 44. The infrared heater can heat a 0.7-m-long and 0.5-m-wide area, and its power is 4300W.


Figure 44. Portable infrared heater

Figure 45 shows the infrared heating test. The initial surface temperature of the pavement was 10.1 ℃, and the temperatures detected by sensors at 2cm and 5cm depths were 14.2℃ and 18.1℃, respectively. **Error! Reference source not found.** shows the surface t emperature distribution and the temperature detected by thermocouples. As seen, the highest surface temperature was located at the edges of the pothole after 5 minutes heating, and the temperature was evenly distributed over the other areas. The maximum temperature at edges was around 165℃ while the temperature measured at shallow

surface area was only 33℃. This is because the asphalt mixture has a low thermal conductivity, and the lower part of the pavement was heated by thermal conduction only. However, compared with microwave heating, which can only heat the pavement surface to around 45 ℃ after 8 minutes, the infrared heating shows a great potential for preheating.

Figure 45. Infrared heating test

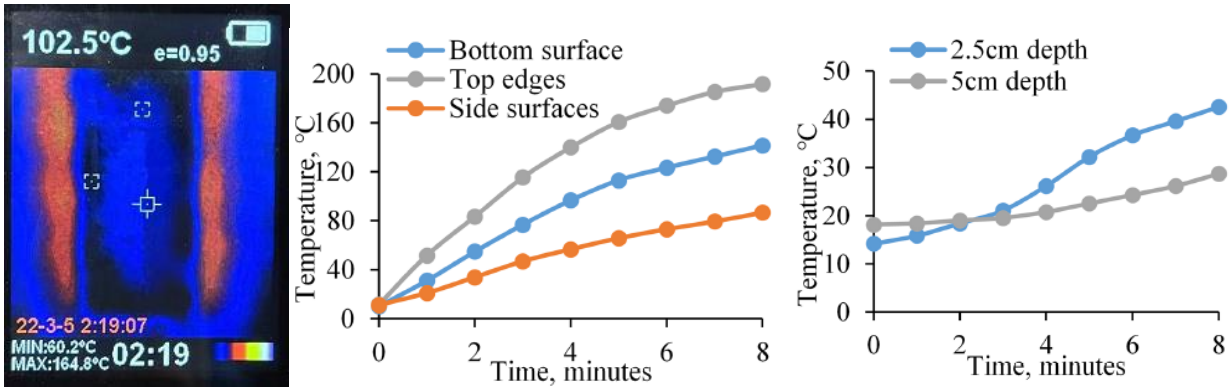

(a) (b) (c)

Figure 46. Temperature measurements: (a) surface temperature distribution, (b) surface temperature with heating time, and (c) internal

Pothole Repair with Preheating

Repair process

Given the infrared heating exhibited better efficiency and performance in trial tests, it was adopted to repair potholes in the test section. Specifically, six potholes were repaired, among which two were repaired without preheating, two were repaired after infrared preheating for 5 minutes, and two were repaired after preheating for 8 minutes. Debris was removed before repair. HMA with 9.5 mm NMAS was used as patching material. The gradation of the material is shown in Figure 47, and other general information is shown in Table 14.

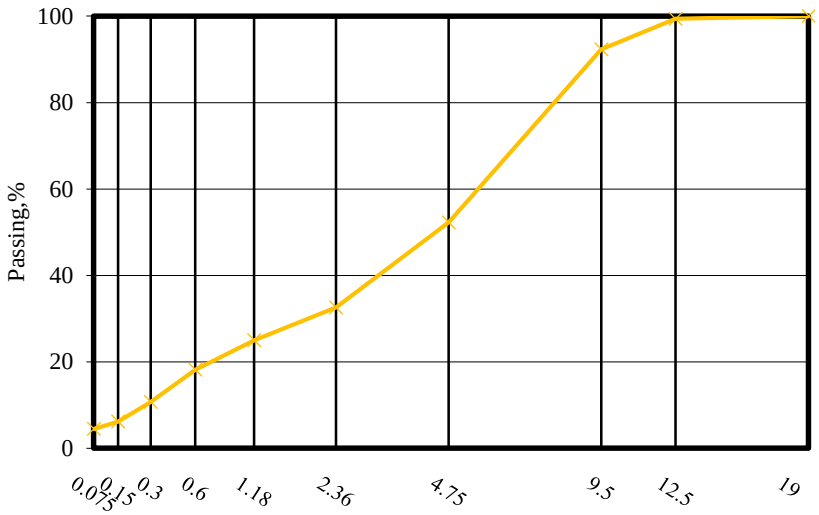

Figure 47. Gradation of asphalt mixtures

Table 14. General information of the paving material

Mix type	Asphalt content, %	Maximum specific gravity of mixture, G_{mm}	Bulk specific gravity of aggregate, G_{sb}	Bulk specific gravity of specimen, G_{mb}
9.5-mm HMA	5.29	2.508	2.719	2.21

Figure 48 shows the repair process, and the environment temperature was around 10.1℃. As can be seen, the edges of the pothole became loose after preheating, indicating a good heating effect. The HMA which was kept under 145℃ was filled in the pothole immediately after preheating. In an effort to ensure good patch quality, the vibratory plate compactor was used to compact each patching for 10s.

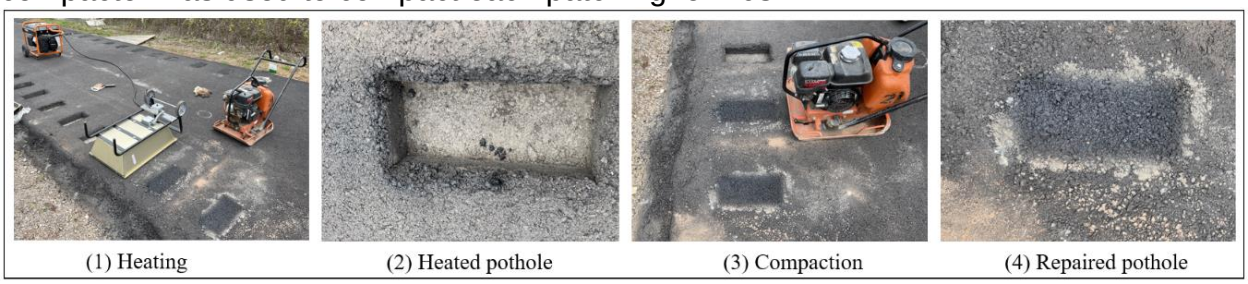

Figure 48. Pothole repair with infrared heating method

Field coring and test plan

To further evaluate the effect of preheating on performance enhancement of the asphalt patch, field cores were taken from repaired potholes, and mechanical tests were then conducted. Full-depth field cores were taken from the potholes 2 weeks after the repair. Figure 49(a) shows the field coring process. The diameter and height of the core were 101.6mm and 152.4mm, respectively. For potholes repaired without preheating, the

interface bonding strength was not high enough to withstand the torsion of the drilling machine, which lead to the patch material being separated from the old pavement before testing. Nevertheless, when preheating was applied in pothole repair, all the cores survived and were intact after drilling.

Figure 49(b) shows the mechanical testing plan. Firstly, interface shear strength test was conducted to measure the interface bonding strength between the patch material and the existing pavement. Secondly, interface tensile strength test was performed on the sample composed of both patch material and the existing pavement. Thirdly, the cylindrical patch material which was detached from the field core by interface shearing will be used for IDT test.

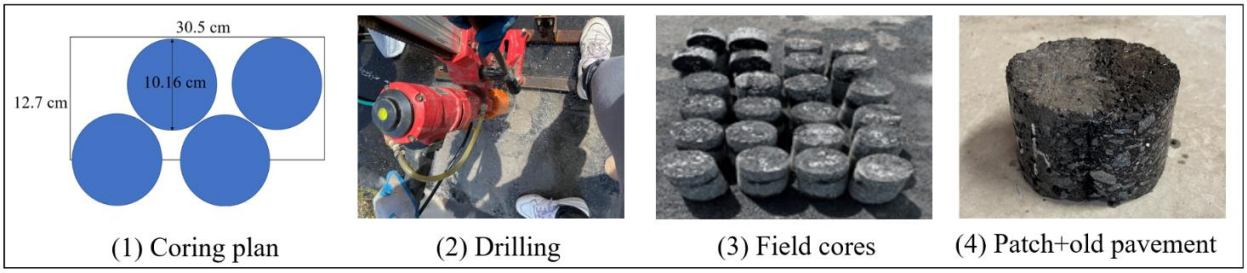

(a)

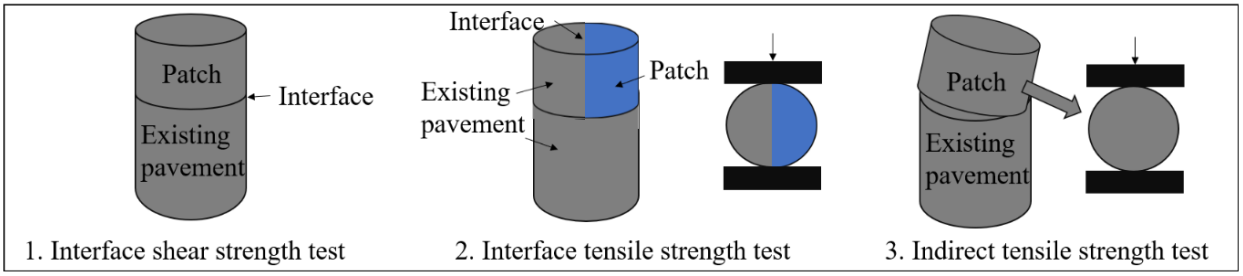

(b)

Figure 49. Preparation for mechanical testing, (a) Field coring, (b) Test plan

Interface shear and tensile strength of field cores

The interface shear strength test was performed using the modified Marshall stability-testing device at room temperature. A stationary response frame and a moveable shearing frame are two major components of the device, as shown in Figure 50(a). The cylindrical field core was placed inside the shearing and reaction frames, and the shearing frame was subjected to vertical force during the test. The test was conducted at a constant rate of 50.8mm/min until shear failure at the interface occurred. The interface tensile strength test was conducted using the IDT test setup in accordance with AASHTO T 322 [61] at 25°C, as shown in Figure 50(b). The dimensions of cylindrical field core tested were 101.6-mm diameter by 63.5-mm high. A constant displacement rate of 50.8-mm/min is applied on the top and bottom of the cylinder specimen perpendicular to the radial direction until failure. The tensile strength and strain at the peak were calculated automatically by the test program at the end. Both tests were performed on quadruplicate specimens.

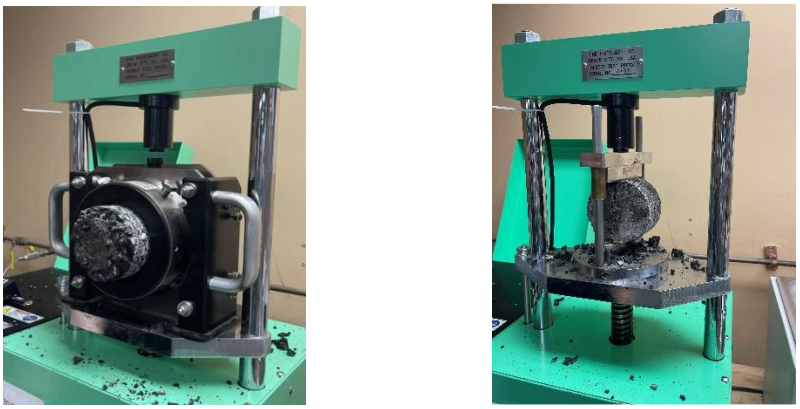

(a) (b)

Figure 50. Interface bonding strength tests, (a) Interface shear strength test, (b) Interface tensile strength test

The testing result of interface shear strength is shown in Figure 51(a). The data show that the shear strength varies within a wide range from 0 to 1200kPa, which highly depends on the heating time. If the pothole is repaired without preheating, the patch material was separated from the old pavement during coring, and no interface shear strength was measured. As the preheating time increased from 5 to 8 minutes, the interface shear strength increased over two times.

Figure 51(b) shows the tensile strength of the interface between the patch material and old pavement. As seen, without being heated, the interface tensile strength was around 500kPa, while it increased by almost two times after 8 minutes of heating. It demonstrates that the preheating has a significant effect on the interface bonding condition between the patch material and the existing pavement.

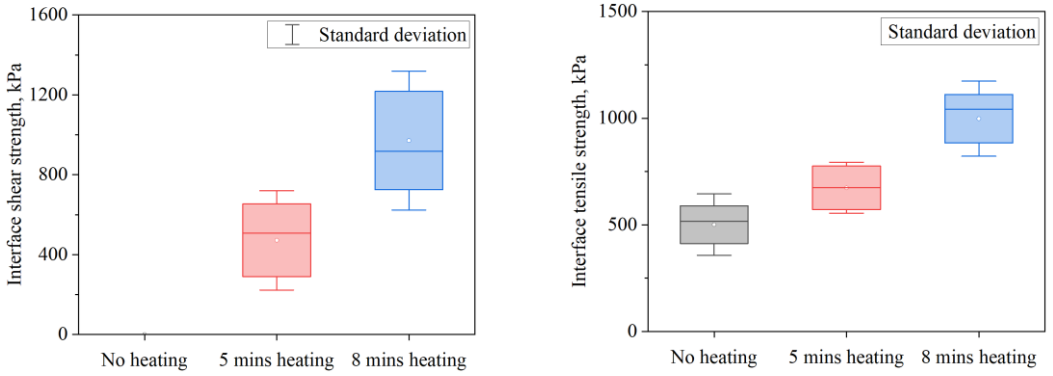

(a) (b)

Figure 51. Interface strength test results, (a) Interface shear strength, (b) Interface tensile strength

IDT strength of field cores

After interface shear strength test, the cylindrical patch material detached from the old

pavement was used for IDT strength test. The test procedure was the same as interface tensile strength test, and quadruplicate tests were conducted.

Figure 52(a) shows the air voids of the pure patch material which was separated from the full-depth field core after interface shearing, and Figure 52(b) shows the corresponding IDT strength. As can be seen, the air voids of the specimen taken from the pothole without preheating was over 8%, which may lead to the generation of pore water pressure under traffic loading because of the possible water penetration on rainy days. When preheating is applied, the air voids decreased with the increase in heating time, and satisfactory air voids of 5% can be achieved after heating for 8 minutes. From mechanical response perspective, the IDT strength of the patch material increased when the old pavement was heated for a longer time, probably because of the better compaction quality.

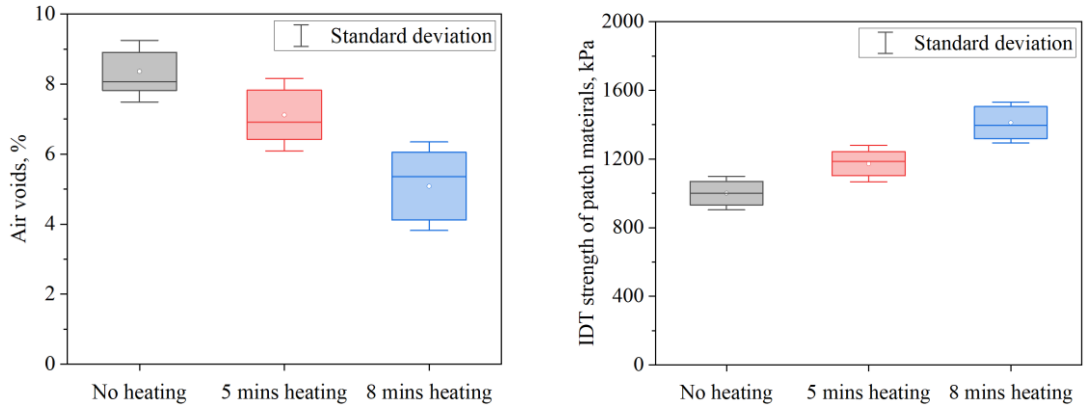

Figure 52. Laboratory test results of pure match material, (a) Air voids, (b) IDT strength

LABORATORY AND FIELD INVESTIGATION ON PATCHING MATERIALS

Laboratory Experiments on CMA

General information on different CMA

The cold mix used for laboratory experiments includes the bulk and different commercial materials. Different commercial materials were described as CMA-A, CMA-B and CMA-C. The bulk cold mix was stored in field, as shown in Figure 53. Commercial cold mix materials were stored in buckets under room temperatures. The general information is shown in
Table 15. During pothole repair, the bulk cold mix needs to be heated to 60℃ to obtain the workability, while the CMA-B and CMA-C mixtures can be directly placed in the pothole and then compacted. When using CMA-A, a certain amount of water needs to be added before compaction, and the weight ratio of water to mixture is around 0.167. To compare the performance of different CMA materials, IDT and interface shear strength tests were conducted, and Marshall specimens were made for each test, as shown in Figure 54.

Figure 53. Bulk cold mix

Table 15. General information of cold mix

CMA	Maximum aggregate size, in	Aggregate % passing No. 200	Asphalt content, %	Reclaimed asphalt pavement, %	Air voids, %
Bulk cold mix	0.187	N/A	1-5	10-20	20.7
A	0.187	2-10	5-8	0	9.7
B	0.187	2-5	3.75	0	11.7
C	0.5	2-5	1-10	0	9.0

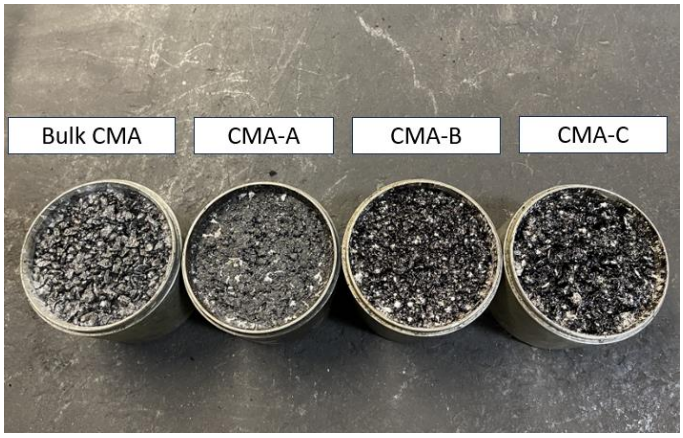

Figure 54. Specimens made of different cold mix

IDT strength of CMA

The IDT strengths of various cold mix after different curing times were tested. The standard Marshall specimens were first made under room temperature, and then different groups of specimens were cured under 0℃ for 30 minutes and 24 hours, respectively. After that, the IDT test was conducted immediately to simulate the condition in cold weather. The IDT test results are shown in Figure 55. As seen, the bulk cold mix has the highest strength 30 minutes after repair, it also has higher strength than CMA-B and CMA-C 24 hours after repair. As curing time increased, the strength of commercial cold mix increased gradually. Among them, CMA-A demonstrates the highest strength regardless of the curing time. Adding water during repair also makes CMA-A have an advantage that there is no need to remove the existing water in pothole when the pavement is wet. Once the commercial cold mix materials are fully cured, their final strengths are all higher than bulk cold mix. Nevertheless, in real condition the pothole repaired by commercial cold mix may not be able to survive that long to form the ultimate strength.

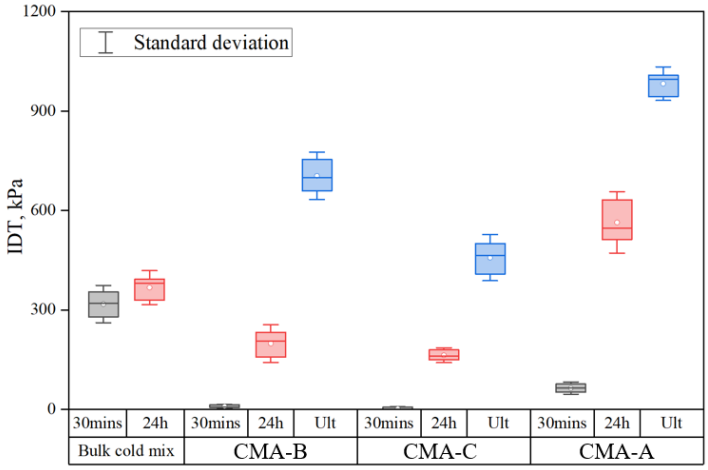

Figure 55. IDT test results

Interface shear strength of CMA

The interface shear test was conducted to analyze the temperature effect on the strength of interface between patch material and the existing pavement. Four different cold mix materials were used, and the interface strength was measured after different curing times. The sample used for test was composite Marshall specimen, which was made based on the following procedure:

1. Heat HMA to 140℃ in the oven, and then use the Marshall compactor to compact the material into 3.2-cm-thick specimen. As shown in Figure 56.
2. After compacting 50 times, use the demolding machine to lift the specimen, and do the compaction on the other side (50 times).
3. Keep the 3.2-cm-thick specimen in the mold for 24 hours.
4. After 24 hours, keep the mold with the specimen under 0℃, 20℃, 50℃ and 80℃ for 3 hours. Heat the bulk cold mix to 60℃ and keep commercial cold mix under room temperature.
5. Add loose cold mix to the 3.2-cm-thick specimen and do the compaction (50 times one side). The total thickness of the Marshall specimens is around 6.35cm. It should be noted that the water needs to be added before compacting CMA-A.
6. Cure cold mix specimens under 0℃ for 30 minutes and 24 hours before test. Keep another group of cold mix specimens under 110℃ for 25 hours to be fully cured. After that, they were kept under 0℃ for 6 hours before test. The appearance of the specimen which is ready for test is shown in Figure 57.

Figure 56. 3.8-cm-thick Marshall specimen

Figure 57. Composite Marshall specimen made with HMA and cold mix

Figure 58 shows the interface shear test results. The horizontal axis is the conditioning

temperature of HMA, and the results under 0℃ could indicate the strength of interface under current practice where the existing pavement is not heated in cold weather. As seen from Figure 58(a), with the increase in HMA temperature, the interface shear strength 30 minutes after compaction first increased and then decreased for bulk cold mix, CMA-B and CMA-C. This may be because when heating the specimen to a relatively high temperature, the specimens did not fully cool down 30 minutes after compaction, and the asphalt binder might be more fluid than that cooled from a lower temperature. Thus, the interface shear strength was lower under a higher temperature.

Figure 58(b) shows the interface shear strength 24 hours after compaction. The strength increased with the conditioning temperature of HMA, indicating that preheating the existing pavement can effectively improve the bonding condition. It should be noted that the test results of CMA-B were not recorded because its cohesive strength was not high enough so that the cold mix damaged first before interface debonding, as shown in Figure 59. However, the ultimate interface shear strength of CMA-B shown in Figure 58(c) is the highest among all cold mix materials and is much larger than that of bulk cold mix.

Overall, the bulk cold mix showed a higher interface shear strength at early stage after repair, and the strength of commercial cold mix will grow with time. The CMA-A shows a higher interface strength than that of CMA-B regardless of the curing time, and the CMA-B shows comparable interface shear strength with bulk cold mix even after being fully cured.

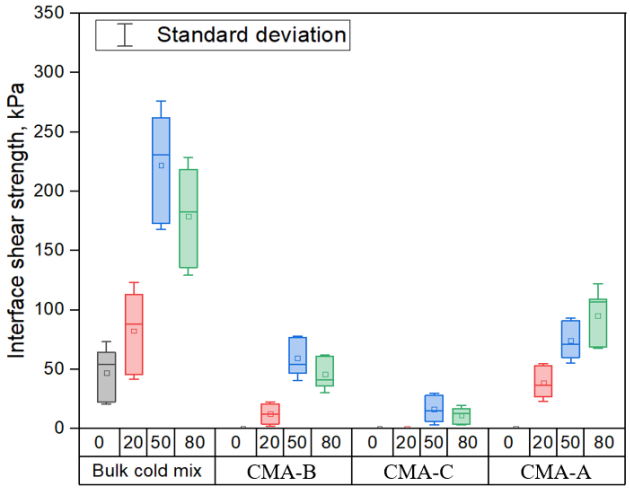

(a)

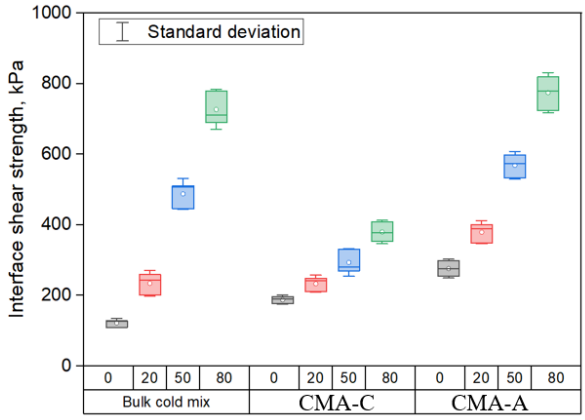

(b)

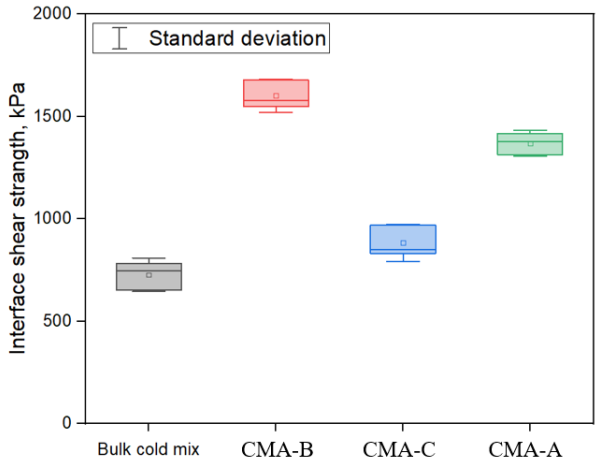

(c)

Figure 58. Interface shear test results, (a) 30 minutes curing, (b) 24 hours curing, (c) Complete curing

Figure 59. Damage form of CMA-B during interface shear test

Laboratory Experiments on Recycled Asphalt Pavement (RAP)

Material and specimen preparation

In this section, the patching material was made by mixing HMA with different contents of RAP under 145℃. The HMA was collected from the asphalt mix plant, and asphalt biner of PG64-22 was used in the mixture. Both HMA and RAP had a NMAS of 9.5-mm. Figure 60 shows the appearance of RAP. It should be noted that the RAP was directly mixed with HMA without adding additional asphalt binder. This patching material can reduce the usage of virgin binder, which can achieve additional environmental benefits as the binder production is the main factor for life cycle environmental burdens [62]. The gradations of HMA and RAP materials are shown in Figure 61.

Figure 60. Appearance of RAP materials

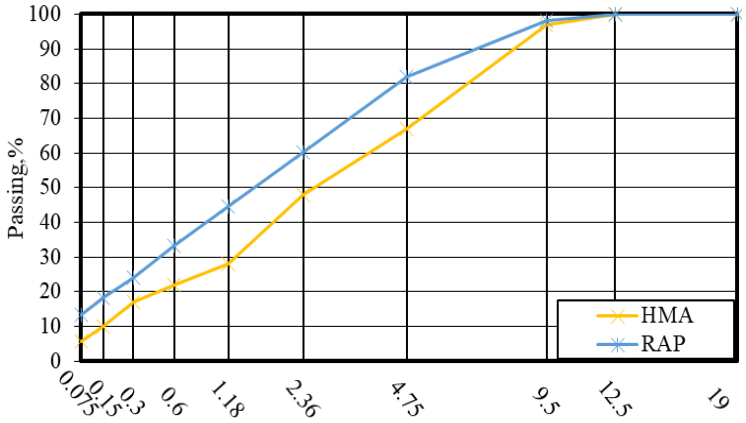

Figure 61. Gradations of HMA and RAP

Based on field observation of over 1000 asphalt patches, edge disintegration (debonding) and raveling were found to be the primary failure modes [54]. Rutting was also reported as another problem of pothole repair according to the survey responses from local agencies [63], and it happened more frequently when the compaction was poor [64]. Therefore, for laboratory experiments in this chapter, the IDT test was conducted to evaluate the rutting resistance of the patching material, the interface shear strength test was performed to evaluate the interface bonding condition, and the Cantabro test was used to assess the abrasion resistance.

Marshall specimens were made for IDT and Cantabro tests using HMA with different RAP contents (0%, 15%, 30% and 50% by weight). For interface shear strength test, the composite Marshall specimens were prepared in two steps. Firstly, the Marshall specimens were compacted as the first layer (representing existing pavement) using HMA without RAP and then conditioned under 20℃ and 80℃, respectively. Then, the second layer was added using HMA with different RAP contents to represent the patch material. The dimensions of all the specimens were 101.6 mm in diameter and 63.5-mm in height. Table 16 shows the volumetric parameters of different asphalt mixtures.

Table 16. Volumetric parameters of asphalt mixtures

Materials	G_{mm}	G_{mb}	Air voids, %
HMA	2.696	2.468	8.5
HMA + 15% raw RAP	2.664	2.421	9.1
HMA + 30% raw RAP	2.635	2.365	9.2
HMA + 50% raw RAP	2.589	2.335	10.0

Environmental conditioning of specimens

As water is widely accepted as the main cause for pothole repair failure, the specimens used for laboratory tests were conditioned by freezing-thaw (FT) and dynamic pore water pressure. The FT cycles were applied using the freezer and water bath, and the dynamic pore water pressure was applied using the moisture induced stress tester (MIST). Specimens under dry condition were also used for comparison.

The FT conditioning was conducted following the AASHTO T-283 standard [65]. The specimens were first saturated by using the vacuum under a pressure of 98.3-98.7 kPa for 15 minutes. Then, the surfaces of specimens were dried with soft cloth and covered with plastic wrap. After that, the specimens were placed in the freezer at -18°C for 24 hours and then thawed at 60°C for 24 hours. Finally, the specimens were placed in a water bath at 25°C for 2 hours.

The MIST conditioning is intended to simulate the stress caused by passing vehicle tires in a wet pavement. The MIST device (shown in Figure 62) can operate at higher-than-normal temperatures and create pore pressure to achieve accelerated failure of asphalt mixture. The conditioning procedure was conducted in accordance with ASTM D7870 standard [66]. To simulate the moisture-induced stress on real roads, the standard pressure magnitude is 278 kPa, the number of cycles is 3500, and the environment temperature is 60℃.

(a)

(b)

Figure 62. MIST device, (a) External view, (b) Internal view

IDT strength of HMA with RAP

Figure 63(a) shows the IDT test results on lab specimens. The data indicate that the IDT strength increased with RAP content under dry condition, which is consistent with findings in many other studies [67,68]. This is because RAP material was much harder as it was coated with highly aged binder, as compared with HMA. The addition of 50% RAP can lead to around 20% increase in IDT strength. After FT conditioning, all the mixtures demonstrate reduction of IDT strength. However, the HMA containing RAP still shows higher IDT strength than the HMA made with virgin aggregate. The maximum strength increase after FT was around 15% when 50% RAP was added. Different from previous scenarios, the addition of RAP material led to reduced IDT strength after MIST conditioning, and the reduction became more remarkable as the RAP content increased. The maximum reduction could be up to 37% when 50% of RAP was added.

Figure 63(b) shows the results of tensile strength ratio (TSR), which is the average IDT strength of FT or MIST conditioned specimens divided by that of specimens in dry conditions. It can be found that the TSR of specimens under both conditions decreased with RAP content, indicating the patching material with more RAP was less resistant to moisture damage. When the RAP content was below 50%, the TSR values of MIST conditioned specimens were higher than those of the specimens conditioned by FT. It means that the patching material was more resistant to pore water pressure than freezing thaw in general. A similar trend was also found by Shu et al. (2012) [69]. However, the TSR values of MIST conditioned specimens decreased more remarkably as RAP content increased, demonstrating the resistance to pore water pressure was more sensitive to RAP content. Given that the minimum TSR of 70% is specified for FT conditioned specimens by AASHTO T283 standard [65], and the TSR of 80% for MIST conditioned specimens is recommended from previous researchers [70], adding 30% or less of RAP to the patching materials can lead to satisfactory performance.

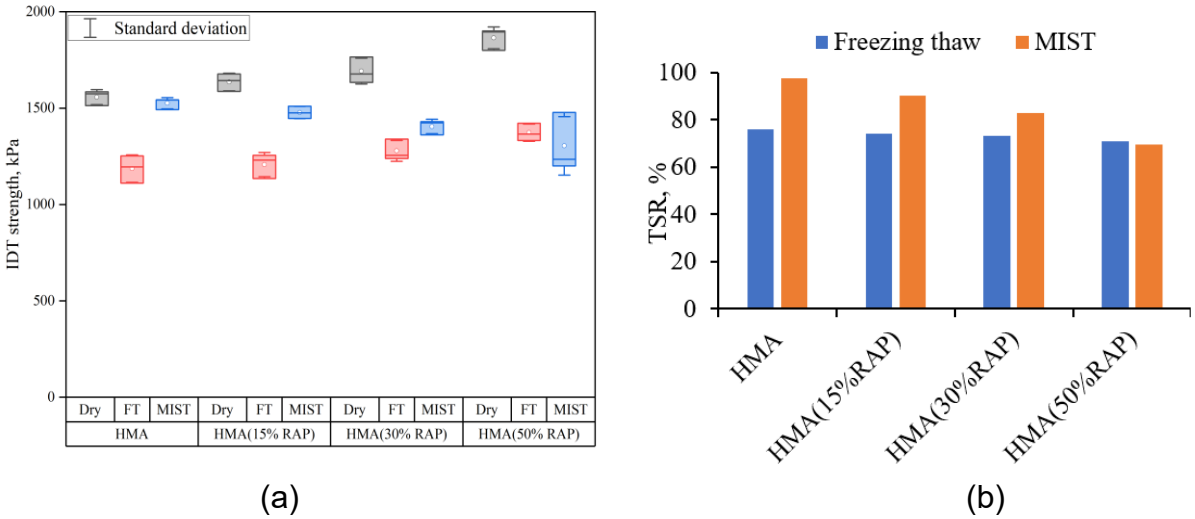

(a) (b)

Figure 63. IDT test results of HMA with different RAP contents at dry and after environmental conditioning: (a) IDT strength, (b) TSR value

Interface shear strength of HMA with RAP

Figure 64(a) shows the interface shear strength after different conditioning environments. The interfaces of the specimens were all bonded at 20℃. As observed, the interface shear strength did not necessarily increase or decrease as the RAP content varied. The possible reason is that as the materials arbitrarily distributed during the mixing process, the actual RAP content located at the interface was random. Considering that the standard deviation of interface shear strength is small, especially for the HMA with 50% RAP, the addition of RAP may not have significant impact on interface bonding regardless of environmental conditioning. On the other hand, compared with the interface shear strength of specimens under dry condition, the strength decreased remarkably after FT and MIST conditioning, and the maximum reduction caused by FT was up to 60%. This phenomenon demonstrates that moisture has a significant impact on interface bonding.

Figure 64(b) shows the shear strength of the interfaces which were compacted at 80℃ after preheating. Similarly, the addition of RAP did not have significant impact. As the increase in the temperature during compaction, the shear strength under all conditions increased distinctly. It means that preheating the material surface before compaction can help enhance the bonding condition.

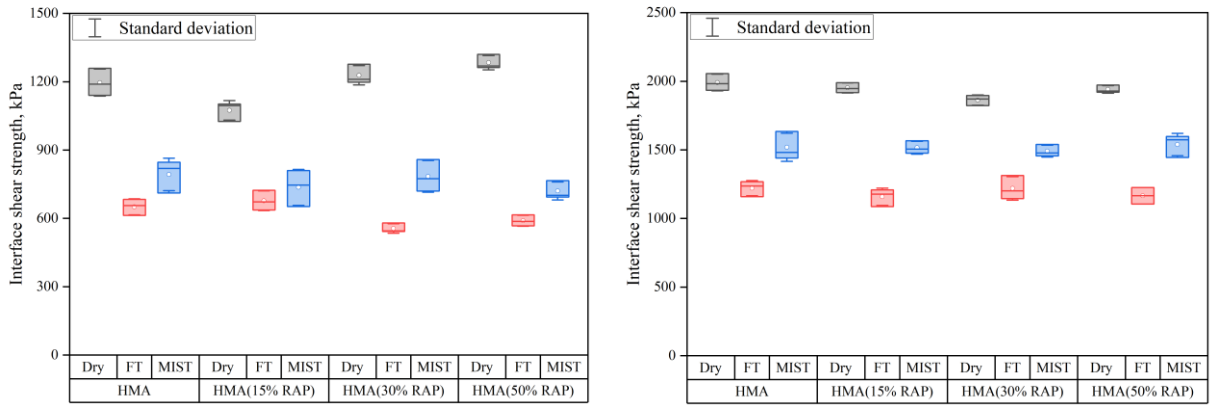

(a) (b)

Figure 64. Interface shear strength of HMA with different RAP contents at dry and after environmental conditioning (a) at 20℃, (b) with preheating at 80℃

Figure 65(a) and (b) show the interface shear strength ratio (ISSR) of FT and MIST conditioned specimens, respectively. The ISSR was calculated similarly as TSR. For all the mixtures, the ISSR of the interface formed at 80℃ after preheating is higher than that of the interface formed at 20℃. It means that preheating can improve not only the bonding condition, but also the moisture damage resistance. Compared to FT conditioned specimens, the ISSR of MIST conditioned ones was higher in all cases, indicating the interface shear strength was more resistance to pore water pressure than FT.

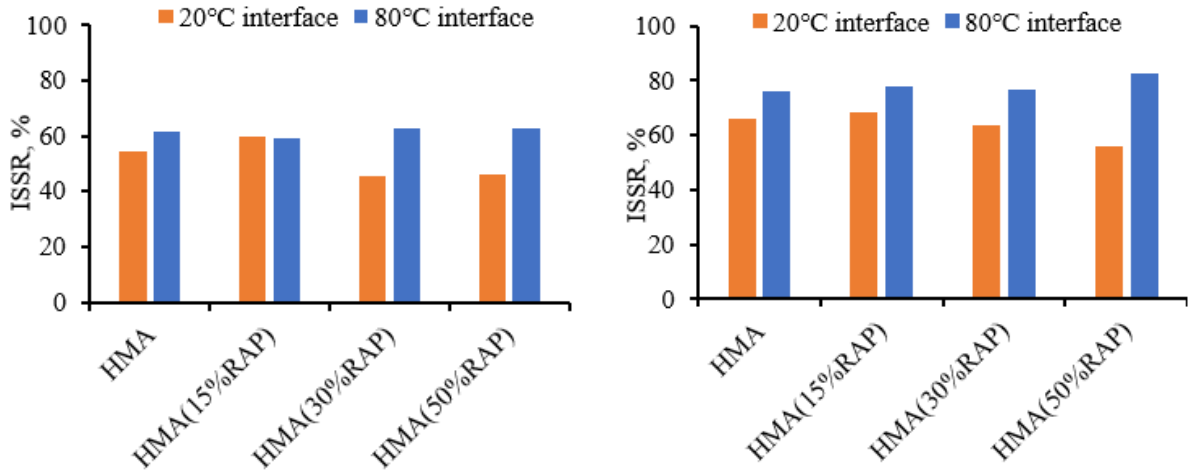

(a) (b)

Figure 65. ISSR results HMA with different RAP contents after: (a) FT, (b) MIST conditions

Mass loss of HMA with RAP

The Cantabro abrasion test was performed using the Los Angeles abrasion machine according to AASHTO TP 108-14 [71]. The machine operates at a speed of 30-33 rpm for

300 revolutions at 25℃. The specimen is weighed before and after the test. The percentage of mass loss is the indicator for adhesive strength between asphalt binder and aggregate. The mass loss can be calculated based on Equation 6.

$$Mass\ loss=\frac{m_1-m_2}{m_1}\times 100 \quad (6)$$

Where, m_1 is the weight before test, and m_2 is the weight after test.

The mass loss results of patching materials with different RAP contents after Cantabro test were shown in Figure 66. It can be observed that as the RAP content increased, the mass loss increased accordingly, regardless of the conditioning environments. Yang et al. (2022) also found that with the addition of RAP, the mass loss under dry and MIST conditions increased [72]. This is understandable because the higher proportion of aged binder content can lead to decreased molecular diffusion. As a result, the adhesion between the binder and aggregate will reduce [73]. Nonetheless, even with this reduced adhesion, the mass losses of all mixtures remained under 15% in dry conditions. It was reported that the mass loss of different dense graded asphalt mixtures without RAP were also below 15% after Cantabro test [74]. This indicates that the HMA with RAP can withstand wear and tear to a comparable extent with the HMA made with virgin aggregate in dry condition.

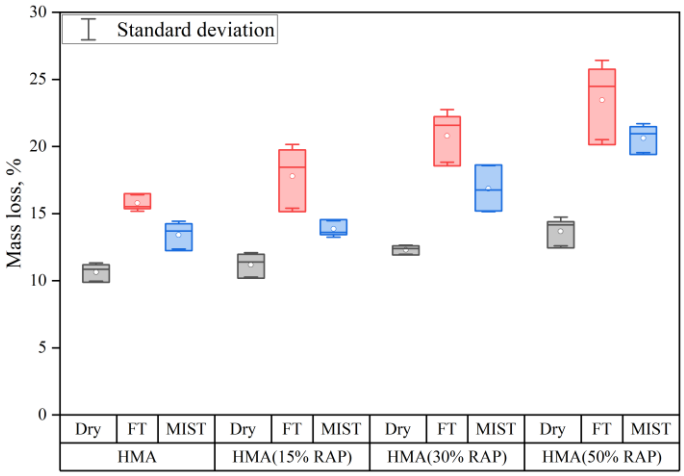

Figure 66. Mass loss of HMA with different RAP contents

Figure 67 shows the mass loss ratio (MLR) of FT and MIST conditioned specimens. MLR was calculated similarly as TSR and ISSR. The MLR increased with RAP content under both conditions. This indicates that the RAP material has adverse effect on the resistance to water-induced abrasion loss. Also, the MSR of FT conditioned specimens was larger than that of MIST conditioned ones. It demonstrates that the patching material is more resistant to FT than pore water pressure from mass loss perspective, which is different from the observations on IDT and interface shear strength.

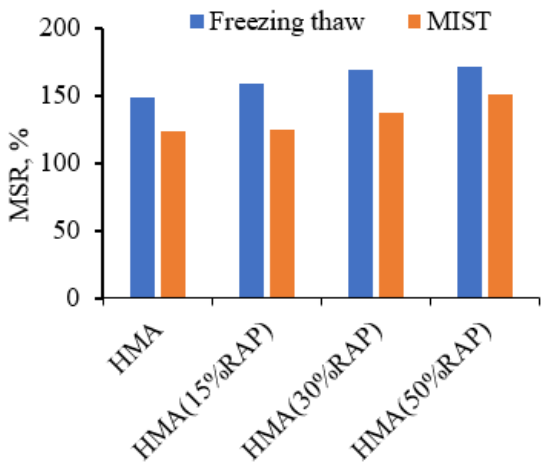

Figure 67. MSR results HMA with different RAP contents

Field Experiments on Pothole Repair using RAP

Material selection and pothole repair procedure

According to the testing results on lab specimens, it can be known that the introduction of RAP into HMA will impact performances of patch material. The results indicate that for HMA containing 30% RAP, the FT conditioned TSR value meets the minimum requirement of 70% from AASHTO T283 [65], and the MIST conditioned TSR value meets the recommendation of 80% proposed by LaCroix et al. (2016) [70]. Moreover, the interface bonding condition and abrasion resistance of the HMA with 30% RAP were close to that of the HMA made with virgin aggregate. Therefore, it was determined to add 30% RAP into HMA as the patching materials for field experiments of pothole repair.

A total of 16 artificial potholes in the test section were repaired using different materials and methods. Four potholes were repaired using HMA without heating, four using HMA with 30% RAP without heating, four using HMA with 5-minute pre-heating, and four using HMA with 30% RAP and 5-minute pre-heating. The preheating was achieved by using the 4300W portable infrared heater.

Figure 68 shows the repair process of potholes in the test section. The potholes were repaired on a sunny and windless day in February 2023. The air temperature of 5.3℃. No tack coat was used prior to heating based on the current practice in New Jersey. The patching materials were kept in the conventional oven at 145℃ before repair. When preheating was not applied, the potholes were directly filled with patching material and then compacted by vibratory plate compactor for 10 seconds. When 5-mins preheating was applied, the infrared thermometer detected the increase of temperature to approximately 100℃ and 160℃ at the bottom surface and longitudinal edge of the pothole, respectively. Figure 10 illustrates that the edges of the old pavement became loose after 5 minutes' preheating, indicating the effectiveness of heating process. The patching materials were then placed in the heated pothole and compacted for 10 seconds.

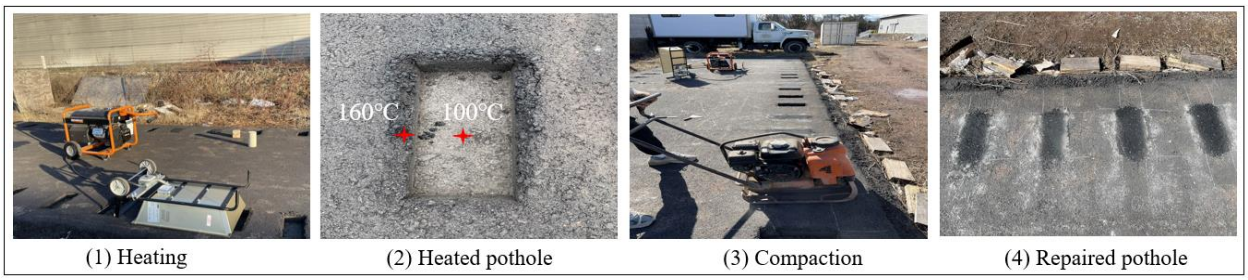

Figure 68. Field pothole repair process

Field coring and test plan

To evaluate mechanical strength of patching material with RAP and the effect of preheating, full-depth field cores with a diameter of 101.6mm were taken for laboratory analysis, as illustrated in Figure 69. The field coring was conducted three months after repair. Two cores were taken within the asphalt patch and two were taken at the interface between patching and surrounding pavement. There are a total of 64 field cores taken from the test section. However, some of the field cores were damaged because of the torsion from the drilling machine. For the cores taken within the asphalt patch, the patching materials themselves were intact while almost all of them were detached from the surface of the existing pavement, regardless of the addition of RAP or the application of preheating. When the potholes were repaired by the HMA with 30% RAP without heating, 7 out of 8 field cores were damaged on the vertical interface between asphalt patch and the surrounding pavement. Table 17 lists the survival conditions of field cores.

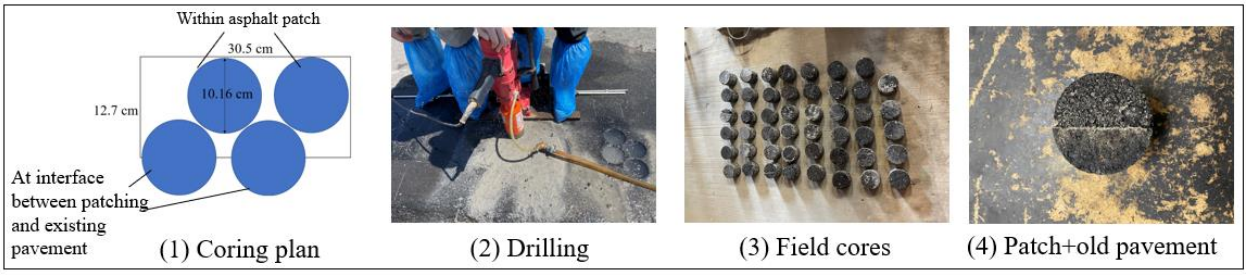

Figure 69. Field coring process

Table 17. Survival condition of field cores

Material	Heating time, mins	Field cores within asphalt patch		Field cores at vertical interface between patching and surrounding pavement
		Horizontal Interface	Patching material	
HMA	0	0 out of 8	8 out of 8	8 out of 8
HMA	5	1 out of 8	8 out of 8	8 out of 8
HMA+30%RAP	0	0 out of 8	8 out of 8	1 out of 8
HMA+30%RAP	5	1 out of 8	8 out of 8	8 out of 8

Based on surviving condition of field cores, the laboratory test plan is described as follows:

1) Interface tensile strength test was conducted on the vertical interface between the patching material and the existing pavement.
2) IDT and Cantabro tests were performed on cylindrical patching materials that were detached from the existing pavement.

Results from lab-made specimens indicate that the FT conditioning had a more remarkable impact on IDT and interface bonding strength than MIST, while MIST could cause more severe abrasion damage. As such, the plan of specimen conditioning is determined for laboratory analysis, as shown in Table 18. For IDT strength on each mixture, two field cores were tested under dry condition, and two were tested after FT conditioning. For interface tensile strength test, four field cores were tested under dry condition, and four were tested after FT conditioning. For Cantabro test, two field cores were tested under dry condition, and two were tested after MIST conditioning.

Table 18. Laboratory test plan on field cores

Material	**Heating time, mins**	**IDT test**		**Interface tensile strength test**		**Cantabro test**	
		Dry	Freezing thaw	Dry	Freezing thaw	Dry	MIST
HMA	0	2	2	4	4	2	2
HMA	5	2	2	4	4	2	2
HMA+30%RAP	0	2	2	1	0	2	2
HMA+30%RAP	5	2	2	4	4	2	2

Field Performance Evaluation

Air voids of field cores

Figure 70 shows the air voids of the patching materials repaired with different materials and methods. The data from the field repair at 10.1℃ in the previous chapter was compared. It can be found that in both cases, the air voids of asphalt patches with preheating were lower than those without preheating. This could be attributed to the fact that preheating the existing pavement retards the temperature drop of patching materials and thereby improves the compaction quality. Nevertheless, the air voids here were slightly higher due to lower temperature (i.e., 5.3℃). It indicates that the environmental temperature can affect the pothole repair quality. Considering the initial air voids of newly constructed pavements usually range from 5% to 6%, the air voids of all the asphalt patches are relatively higher, which may result in water infiltration and lead to moisture damage in wet weather. To further reduce the air voids and improve the repair quality, prolonging the preheating time or using a heater with higher power can be adopted [(75)].

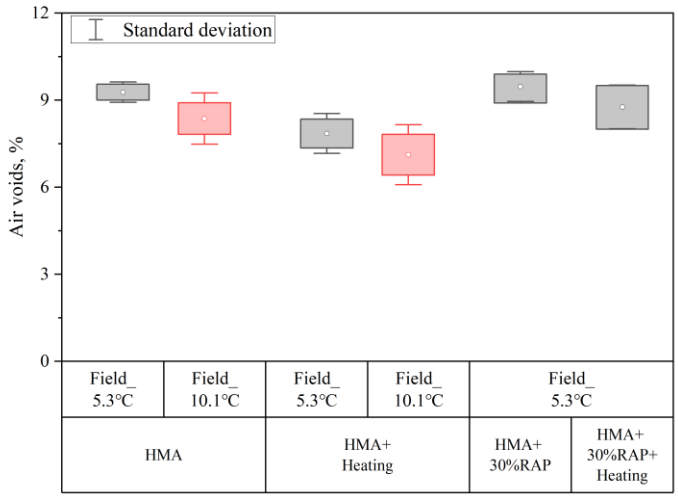

Figure 70. Air voids of field cores

IDT strength of field cores

Figure 71 demonstrates IDT strength of field cores repaired with different materials and methods. The results from the repair at 10.1℃ in the previous chapter are also included for comparison. It was observed that the IDT strength of potholes repaired at 5.3℃, as depicted by the black boxes, showed small variation. This is attributed to the limited number of cores used for tests. Those data suggest that when preheating was not applied, the addition of RAP can lead to an increase in IDT strength of asphalt patch under dry condition and the comparable IDT strength after FT. It means that the addition of RAP can potentially improve rutting resistance of patching materials. When preheating was applied, the IDT strength increased under both conditions, which verified the positive effect of preheating on performance enhancement of patching materials. As the ambient temperature decreased from 10.1℃ to 5.3℃ during repair, the IDT strength in dry condition decreased by up to 44%. The reasons can be twofold. One is that the lower ambient temperature led to lower compaction temperature, resulting in poor compaction quality. The other is that the asphalt patches here suffered from more severe environmental action because the field cores were taken three months after repair, whereas the cores were taken only after two weeks in the authors' previous study. These results indicate that the environmental factors have significant impacts on the performance of asphalt patches. Christensen et al. (2000) conducted IDT tests on gyratory specimens which were designed using the mix designs of different in-service pavements [(76)]. The IDT strength was then correlated with the rut depth of corresponding pavements. It was concluded that the IDT strength over 440kPa could indicate excellent rut resistance performance. Based on the findings from Christensen et al. (2000) [(76)], the patching materials can have satisfactory rutting resistance. Although the strength may gradually decline under repeated environmental actions, the HMA with 30% RAP still has comparable or better performance as compared to pure HMA.

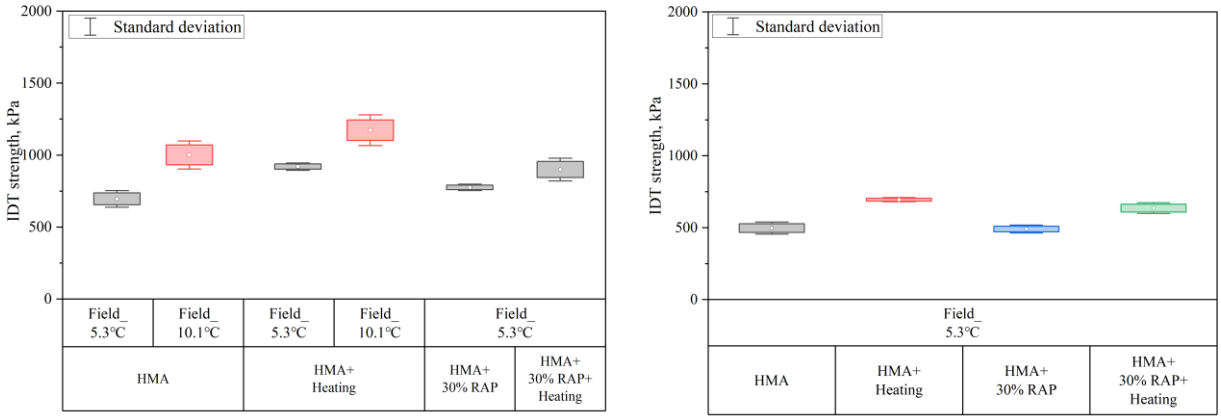

Figure 71. IDT strength results: (a) Dry, (b) FT

Figure 72 shows the TSR results of field cores repaired with different materials and methods. Although the HMA containing 30% RAP has the lowest TSR, it increases after preheating and becomes comparable with that of pure HMA. This means that applying preheating when using the HMA with 30% RAP can lead to satisfactory moisture resistance.

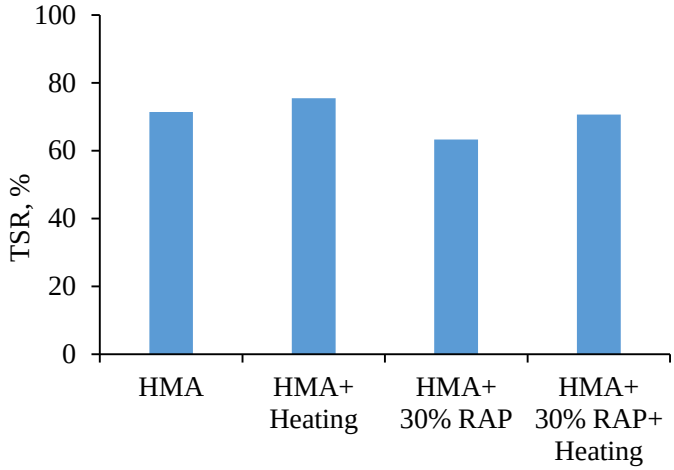

Figure 72. TSR results of field cores

Interface shear strength of field cores

Figure 73(a) shows the interface tensile strength of field cores. It was observed that the results were over 300kPa in all scenarios. Based on the numerical study conducted by Fang et al. (2021) [77], the tensile stress around the loading area at shallow surface of asphalt pavement was less than 100kPa under standard traffic loading. Even with cracks below the asphalt layer, the maximum tensile stress was still less than 300kPa [78]. Compared to the results in this chapter, it can be known that using HMA as patching material can have good bonding with the existing pavement in dry condition, regardless of the application of preheating. However, with the addition of RAP or FT action, the patching materials that were not preheated experienced damage at the interface,

indicating that adding RAP and experiencing FT can cause interface debonding. When preheating was performed, field cores remained intact and exhibited the interface tensile strength of over 300kPa. It suggests that preheating can remarkably enhance interface bonding condition under both dry and wet conditions, yielding a better interface performance of the HMA with 30% RAP as compared to pure HMA without preheating.

Figure 73(b) shows the interface tensile strength ratio (ITSR) results of field cores repaired with different materials and methods. The ITSR of the HMA with 30% RAP was even higher than that of the HMA without RAP when preheating was performed, demonstrating that the combination of RAP and preheating can help patching materials resist moisture damage at the interface.

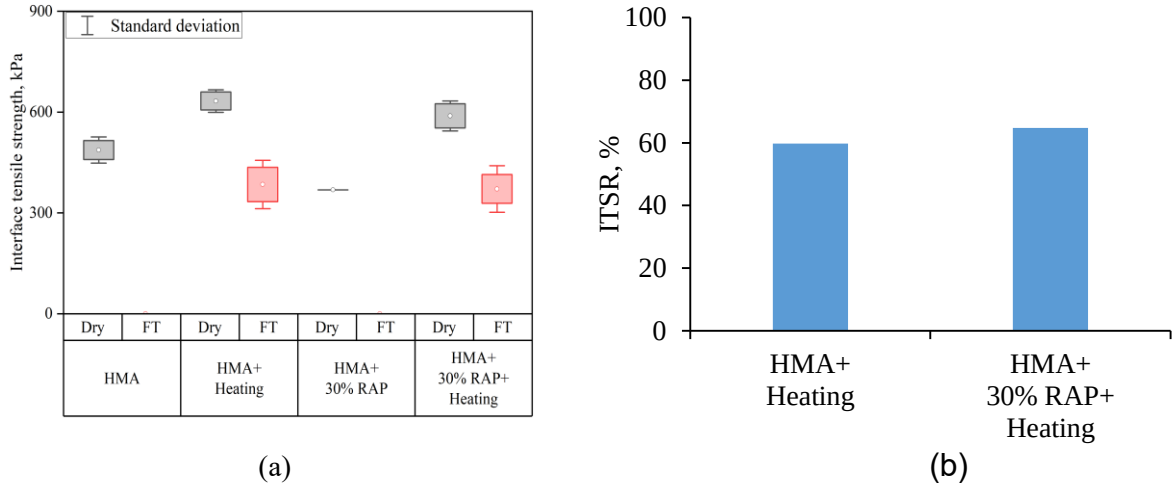

(a) (b)

Figure 73. Interface tensile strength test results of field cores: (a) Interface tensile strength, (b) ITSR value

Mass loss of field cores

Figure 74 shows Cantabro test results of field cores repaired with different materials and methods. As shown in Figure 74(a), the mass loss of patching materials was over 20% in all scenarios. Nevertheless, it is noteworthy that the mass loss results in most cases had a small variation due to the limited number of field cores. When 30% RAP was added to the HMA, the patching material experienced up to 40% weight reduction after MIST conditioning, which indicates great potential to raveling. However, when preheating was performed, the mass loss decreased remarkably and became comparable with that of pure HMA without preheating. Similar trends can be found for the MSL as shown in Figure 74(b). Overall, although the addition of RAP can lead to high mass loss and increase its sensitivity to moisture, the application of preheating can mitigate its negative impact and lead to comparable abrasion resistance with pure HMA.

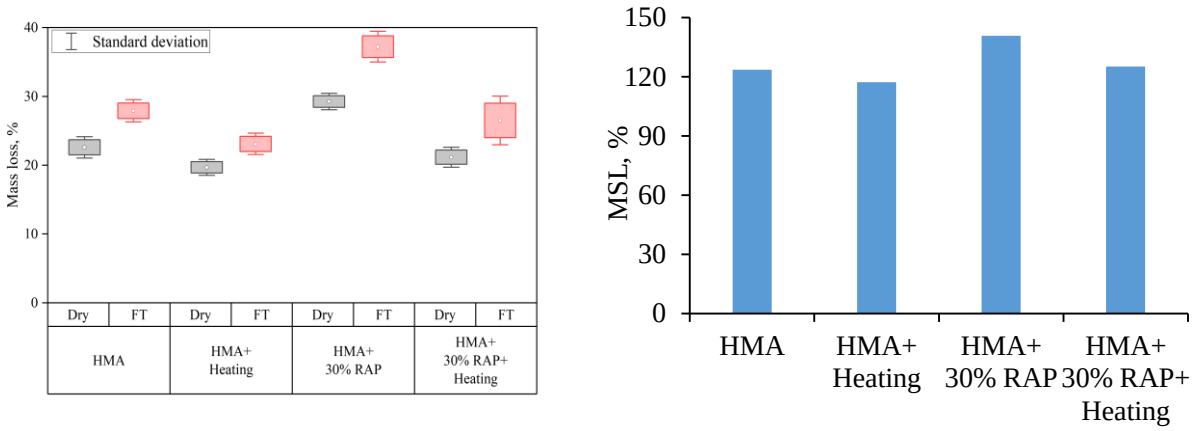

(a) (b)

Figure 74. Cantabro test results of field cores: (a) Mass loss, (b) MLR value

DEVELOPMENT OF NUMERICAL MODEL FOR TEMPERATURE PREDICTION

Thermal Property and Microwave Oven Heating Tests

General information of asphalt mixtures

Five different asphalt mixtures were used for thermal property and microwave oven heating tests. Gyratory specimens were made for testing. The diameter was 152mm, and the height was 114mm. The general information is listed in Table 19, and the gradation information is shown in Figure 75.

Table 19. General information of the materials

Mixture type	Region	RAP content, %	Aggregate type	Air void, %	Asphalt content, %	G_{mm}, g/cm^3	G_{sb}, g/cm^3	G_{mb}, g/cm^3
12.5 HMA	Tilcon Mt. Hope	30	Gneiss	6 (8)	5.32 (5.32)	2.543 (2.522)	2.804 (2.804)	2.39 (2.32)
12.5 SMA	Trap Rock Industry	0	Trap rock	8.7	5.84	2.727	2.958	2.48
9.5 HMA	South State	0	Recycled concrete aggregate	11.4	5.29	2.508	2.719	2.21
4.75 HMA (HPTO)	Stone Industries	0	Trap rock	6.1	7.04	2.491	2.792	2.34

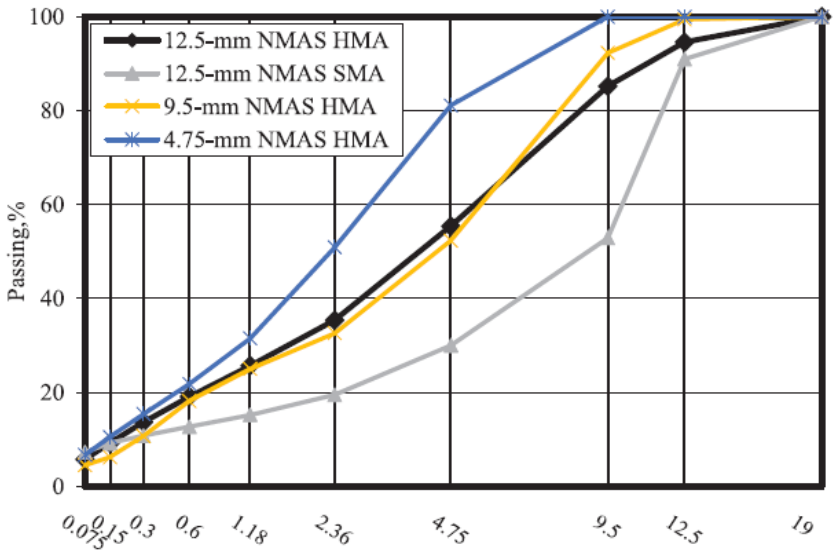

Figure 75. Gradation information of asphalt mixtures

Thermal property test

Thermal property tests were conducted to obtain thermal conductivity and specific heat capacity of different asphalt mixtures, which were necessary for analyzing both microwave and infrared heating characteristics. In this chapter, the transient plane source (TPS) method was used to test the thermal parameters of asphalt mixtures. Hot Disk

develops and provides equipment for measuring and testing thermal property, which is an easy, fast and non-destructive way that could be used to test the thermal properties of the asphalt mixtures. The test setup is shown in Figure 76(a). It utilizes a plane sensor sandwiched between two halves of sample to simultaneously determine thermal conductivity, thermal diffusivity, and specific heat capacity from a single measurement, which has been widely used by other studies [79,80]. This flexible method merely requires one or two pieces of the sample to test, each with no more than one flat surface where the sensor can be inserted into the specimen.

To conduct the thermal property test, 114-mm high specimens were cut into three pieces, and each piece was 38mm high. The sensor was placed on the surface between two pieces during the test, as shown in Figure 76(b). Three different locations were tested for each mixture design in order to mitigate the effect of material anisotropy. The probe depth was 20mm, the electric current during the test was 220mA, the test time was 20s, and the specimens were tested under 20℃, 50℃ and 75℃.

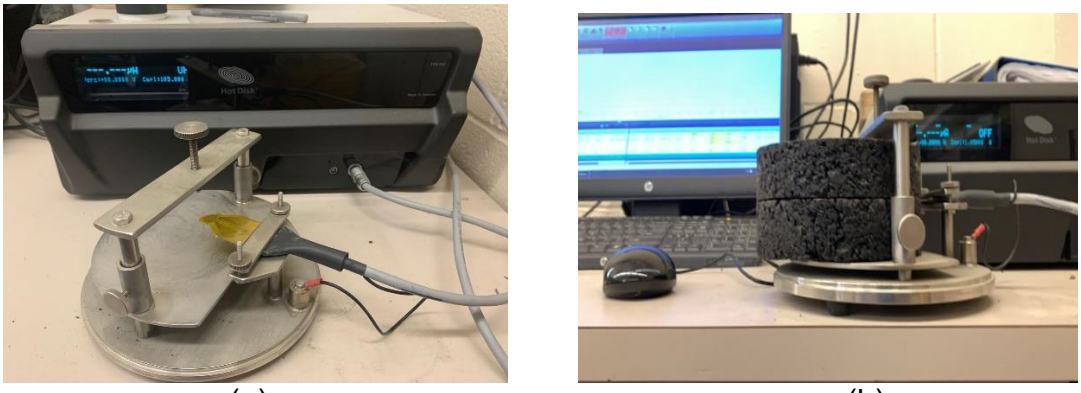

(a) (b)

Figure 76. Laboratory thermal property test: (a) Test setup; (b) Test process

The measured thermal conductivity and specific heat capacity are shown in Figure 77. It was found that as temperature increased, the thermal conductivities of different mixtures decreased but the specific heat capacity increased. It means during the thermal conduction process the heat transfer rate of asphalt mixture is not constant and differs at different temperatures. Compared with the results in other studies, the variations in thermal parameters were in reasonable ranges and showed similar trends that could follow a power function [81,82,83]. In order to consider the impact of temperature variation for further analysis, regression fitting was made on thermal conductivity and specific heat capacity of asphalt mixtures, and the results are shown in Table 20.

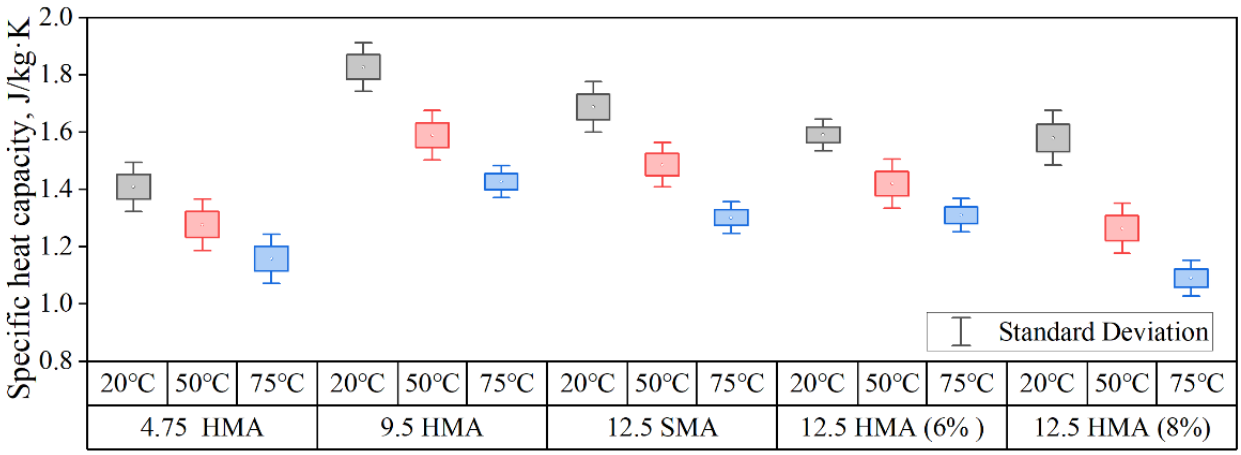

(a)

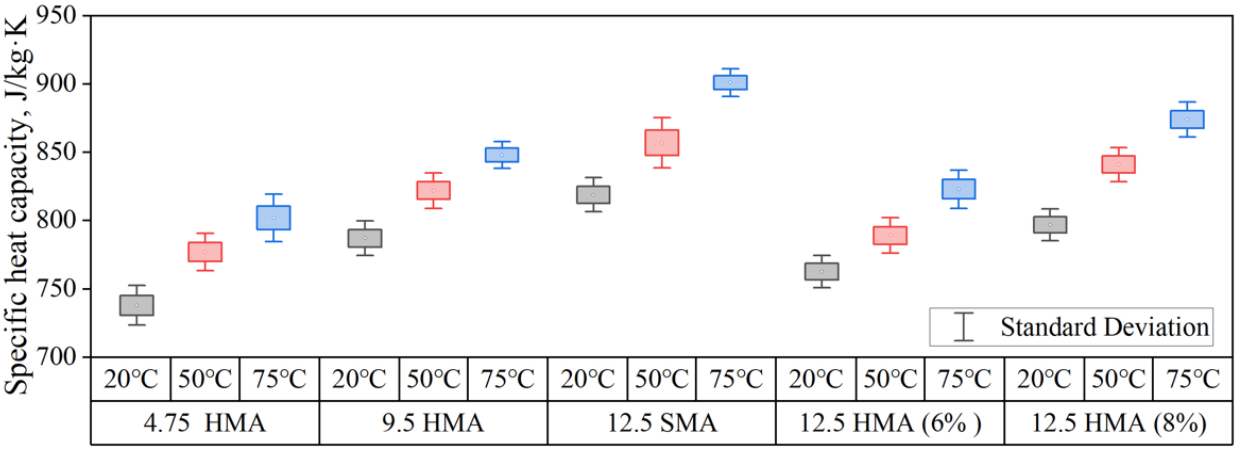

(b)

Figure 77. Thermal parameters of different mixtures: (a) Thermal conductivity, (b) Specific heat capacity

Table 20. Power curve fitting parameters for thermal properties

Mix type	Thermal conductivity = a×Temperature^b			Specific heat capacity = c×Temperature^d		
	a	b	R^2	c	d	R^2
4.75-mm NMAS HMA	2.17	-0.14	0.96	612.58	0.06	0.99
9.5-mm NMAS HMA	3.16	-0.18	0.98	666.48	0.06	0.98
12.5-mm NMAS SMA	3.19	-0.20	0.96	664.70	0.07	0.94
12.5 -mm NMAS HMA, 30%RAP, 6% AV	2.45	-0.14	0.99	627.30	0.06	0.95
12.5 -mm NMAS HMA, 30%RAP, 8% AV	3.62	-0.28	0.99	649.05	0.07	0.98

Microwave oven heating test

As microwave heating is a multi-physics phenomenon that involves heat transfer and electromagnetic radiation, electromagnetic properties of materials are important in the microwave heating process in addition to thermal properties. In this chapter, microwave oven heating tests were conducted to measure the temperature increase after different heating times, which was further used with numerical models to back-calculate the electromagnetic parameters of asphalt mixtures. Specimens with two different heights (38mm and 114mm) were used for tests. Figure 78 shows the specimens in the microwave chamber, and Figure 79 shows the temperature measurement setup. Holes with a depth of 1 cm and diameter of 5mm were drilled at the center of the upper, bottom, and edge surfaces of each specimen for temperature measurements. After testing, the holes in 114mm high specimens were further drilled to a depth of 3 cm for a second round of tests. The temperatures were measured after 30 s, 60 s, 90 s, 120 s, 150 s, and 180 s of heating, and each heating event was conducted after the specimens cooled down to room temperature. The average temperature measured from different locations was used to represent the heating effect.

Figure 78. Microwave and specimens

Figure 79. Temperature measurement

The temperature measurement results are shown in Figure 80. It can be found that after the same heating time, the temperatures of larger specimens are much lower than those of smaller ones. Although the larger specimen usually absorbs more microwave power than the smaller specimen, the greater mass will take a longer time to heat as more time is needed for thermal conduction to cause the temperature gradient to reach equilibrium

[83,84]. Thus, the overall temperature of the object with greater mass will be lower [85]. On the other hand, different asphalt mixtures demonstrated various heat transfer rates, which means the mixture design will have an impact on the heating efficiency of microwave. However, the relationship between heating time and temperature was found to be approximately linear for all the asphalt mixtures, and this trend was also found in other studies [86,87]. The possible reason is that although the thermal property of asphalt mixtures varies with temperature, the electromagnetic property is relative stable [88], so the temperature change caused by electromagnetic heating is much more remarkable than that of thermal conduction. Figure 81 shows the heat transfer rate of 4.75-mm NMAS HMA specimens heated from different initial temperatures. As can be seen, the impact of initial temperature on heat transfer rates is minor, which also verifies that the heat transfer rates of asphalt mixtures are almost constant in microwave heating.

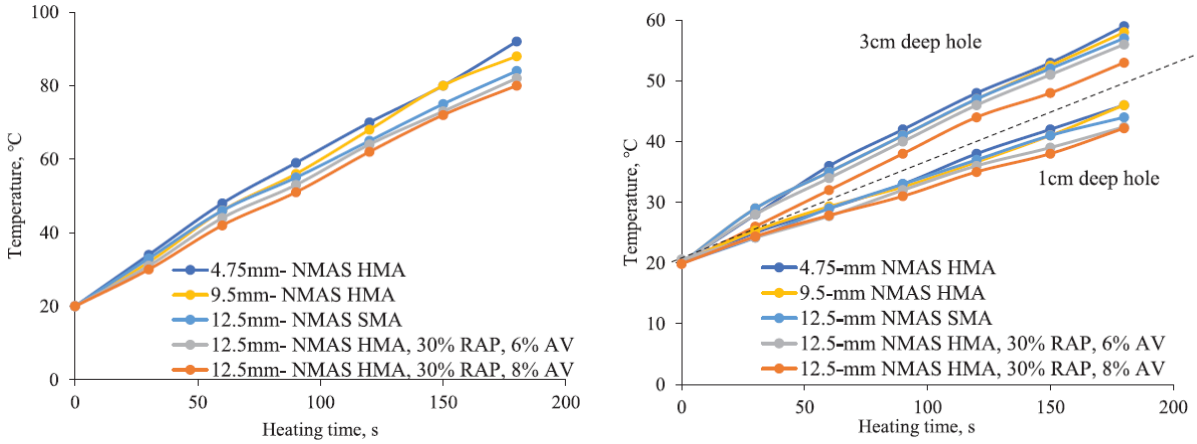

(a) (b)

Figure 80. Temperature curve of compacted materials, (a) Temperature of 38mm high specimen, (b) Temperature of 114mm high specimen

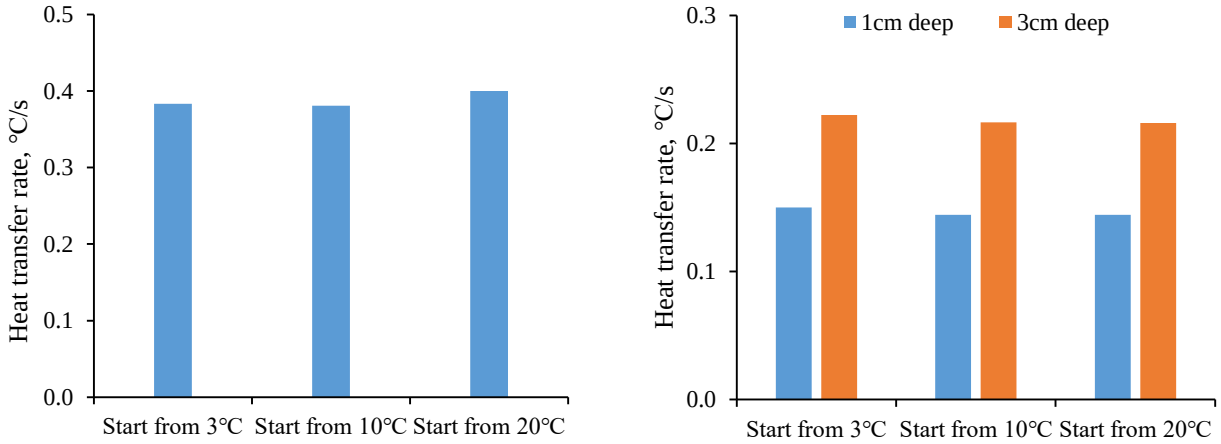

(a) (b)

Figure 81. Heat transfer rate of 4.75-mm NMAS HMA specimens under different initial temperatures: (a) 38mm high, (b) 144mm high

Development and Calibration of Microwave Oven Heating Model

Model development

COMSOL Multiphysics software was used to simulate microwave and infrared heating processes and calibrate electromagnetic parameters of asphalt mixtures. The distributed heat source of asphalt mixture is calculated based on the static electromagnetic analysis in the frequency domain, and then the transient heating simulation is carried out to analyze the redistribution of heat in the asphalt mixture. As the radiated electromagnetic field exists at every point inside the asphalt mixture to generate heating power, the asphalt mixture will be continuously heated, and heat conduction will occur inside it as well. During the heating process, the asphalt mixtures also have convection with the surrounding air and self-radiation to the ambient environment.

A closed microwave oven with cylinder specimen inside was created in the model, as shown in Figure 82(a). The dimension of the model was the same as that of microwave oven used in the laboratory. The inner surfaces of the oven except the port were set as impedance boundaries, and the surfaces of the specimen were set to have convection with the air and self-radiation to the environment. The power of microwave was 700W, the convection heat flux was 5 W/(m^2/K), and the surface emissivity was 0.9 [89,90]. Figure 82(b) shows the meshed microwave oven, specimen and glass plate. Quad meshes were applied to the microwave oven, and fine free tetrahedral meshes were applied to the specimen and glass plate. The total computational elements for microwave heating model for the 38mm and 114mm high specimens were 75,221 and 98,921, respectively. Given that the objects in the microwave oven usually rotate during the heating process, a moving mesh of the specimen with revolution speed of 0.1/s was set based on the real condition.

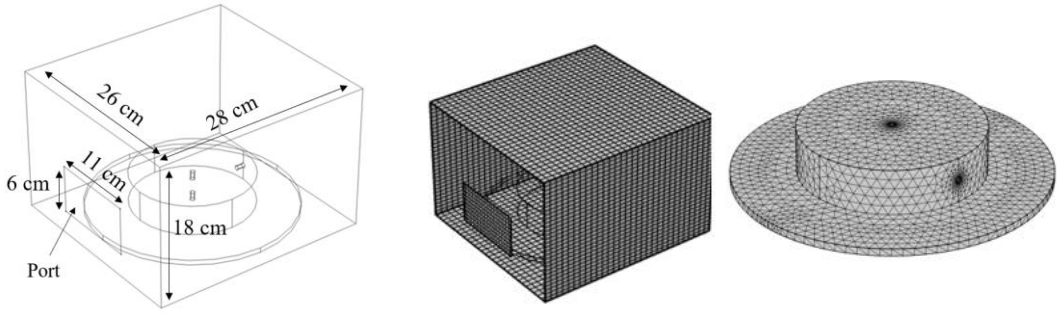

(a) (b)

Figure 82. Model development: (a) Model geometry, (b) Meshing condition

Calibration of electromagnetic parameters

In microwave heating, the parameters like relative permittivity, relative permeability and electrical conductivity are used to represent the electromagnetic properties of the material. The relative permittivity includes dielectric constant and loss factor, which determines the amount of storable energy in the material and how much of that energy can dissipate in the form of heat. The relative permeability is the measure of magnetization obtained by the material in response to an applied magnetic field, which was assumed as 1.0 for different materials as the asphalt mixtures are almost nonmagnetic material. Sensitivity analysis was first conducted to investigate the impact

of electrical conductivity and relative permittivity on heating efficiency. The typical range for electric conductivity of asphalt mixtures was from 3.8×10^{-7} to 8×10^{-10} S/m [21,91,92], for dielectric constant was from 4 to 12 [See references 93,94,95 and 96], and for loss factor was from 0 to 0.6 [92,93,94]. The results show that both dielectric constant and loss factor were found to be sensitive to the temperature, while the electrical conductivity was not. Therefore, based on the findings in other studies, the value of 4.5×10^{-9} S/m was used as the electrical conductivity parameter of asphalt mixtures in this chapter. Subsequently, the dielectric constant and loss factor are parameters that need to be calibrated.

Currently, the complex refractive index model, Rayleigh model, and Bottcher model are three widely used empirical models for predicting the dielectric constant of asphalt mixtures. Leng et al. (2011) concluded that all three models provided reasonably accurate predictions [96], and the modified Bottcher model performed the best [97]. Thus, this model was used here to estimate the dielectric constant of different asphalt mixtures from the empirical point of view. Equation 7 shows the modified Bottcher model.

$$G_{mb} = \frac{(\varepsilon_{AC}-\varepsilon_b)/(3\varepsilon_{AC})-(1-\varepsilon_b)/(1+2\varepsilon_{AC})}{(\varepsilon_s-\varepsilon_b)/(\varepsilon_s+2\varepsilon_{AC})(1-P_b)/G_{sb}-(1-\varepsilon_b)/(1+2\varepsilon_{AC})(1/G_{mm})} \quad (7)$$

Where: G_{mb} is the bulk specific gravity of asphalt mixture; G_{mm} is the maximum specific gravity of asphalt mixture; G_{sb} is the bulk specific gravity of aggregate; P_b is the binder content; ε_{AC} is the dielectric constant of asphalt mixture; ε_b is the dielectric constant of binder; and ε_s is the dielectric constant of aggregate.

Considering that the dielectric constant values of asphalt binder and aggregate may vary, their typical ranges were used to estimate the dielectric constant of asphalt mixtures in this chapter, which were 3-5 for binder and 6-15 for aggregate, respectively [96,97]. The calculated ranges of dielectric constant values are shown in Table 21. As seen, the different asphalt mixtures showed similar dielectric constant ranges, which are all reasonable compared to the reported values from measurements [95,96]. However, due to the uncertainty of dielectric constant values of binder and aggregate, the empirical model only provides a general range of dielectric constant instead of specific values. Also, the loss factor could not be obtained from the empirical model while it is critical for analyzing the generated heat from microwave radiation. Thus, the calibrations of dielectric constant and loss factor using numerical modelling were further conducted.

Table 21. Dielectric constant real part of materials

Mix type	4.75 HMA	9.5HMA	12.5 SMA	12.5 HMA (6%)	12.5 HMA (8%)
Dielectric constant	5.05-11.8	4.83-11.31	5.01-11.8	5.15-12.20	4.98-11.70

In order to calibrate both dielectric constant and loss factor in numerical model, the laboratory test data shown in Figure 80 were used. The calibration results are shown in Figure 83, and the material parameters are summarized in Table 22. It can be found that the measured temperatures match well with the predicted ones for different asphalt mixtures. Compared with dielectric constant values obtained from empirical model and other literature, the results shown in Table 22 are in a reasonable range [See references

[92,93,94,95 and 96], indicating satisfactory calibration results. Therefore, the calibrated electromagnetic parameter for each asphalt mixture was used in further analysis.

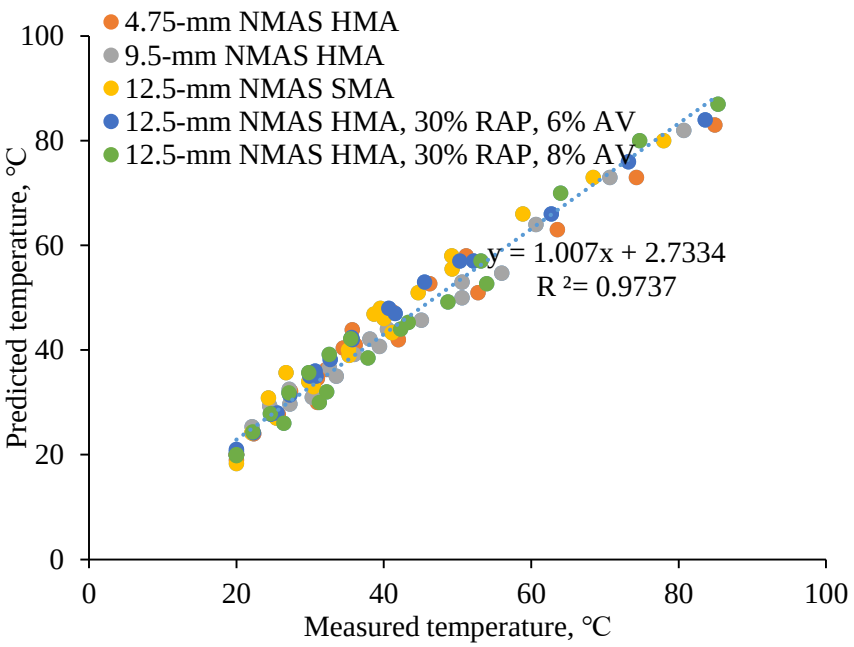

Figure 83. Temperature calibration result

Table 22. Calibrated Parameters

Mix type	Density, kg/m^3	Thermal conductivity, W/mK	Specific heat capacity, J/(kg·K)	Electrical conductivity, S/m	Dielectric permittivity	Relative permeability
4.75-mm NMAS HMA	2491	$2.17\times T^{-0.14}$	$612.58\times T^{0.06}$	4.5×10^{-9}	7.10-0.5j	1
9.5-mm NMAS HMA	2508	$3.16\times T^{-0.18}$	$666.48\times T^{0.06}$	4.5×10^{-9}	7.15-0.6j	1
12.5-mm NMAS SMA	2727	$3.19\times T^{-0.20}$	$664.70\times T^{0.07}$	4.5×10^{-9}	7.00-0.5j	1
12.5-mm NMAS HMA (6%)	2543	$2.45\times T^{-0.14}$	$627.30\times T^{0.06}$	4.5×10^{-9}	6.95-0.5j	1
12.5-mm NMAS HMA (8%)	2522	$3.62\times T^{-0.28}$	$649.05\times T^{0.07}$	4.5×10^{-9}	6.75-0.4j	1

Development and Validation of Field Heating Models

Microwave heating model and validation

Based on the actual sizes of the microwave, horn and pothole, the previously developed

numerical model was modified to simulate the field condition. The geometries of models which simulate test 1 (shown in Figure 39(b)) and 2 (shown in Figure 42(b)) is shown in Figure 84(a) and (b), all the geometric parameters were the same with the real condition except that the pavement area was reduced to 3m × 3m. The material was 9.5mm NMAS HMA. The initial temperature was set as 6℃ for the whole pavement in modelling.

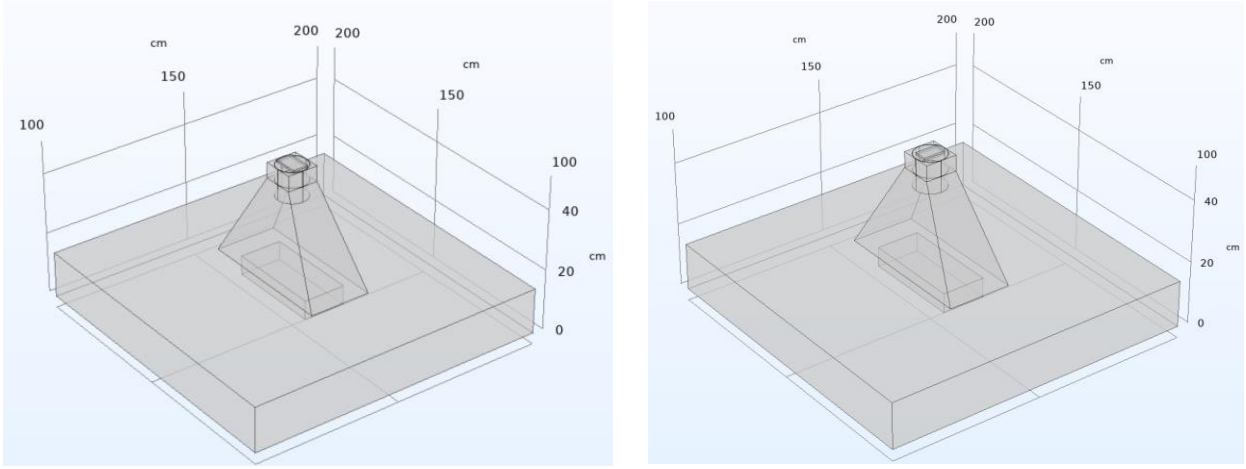

Figure 84. Model geometry, (a) Test 1, (b) Test 2

Figure 85(a) and (b) show the predicted surface temperature distributions for test 1 and 2. It can be found that the predicted surface temperature pattern shown in Figure 85(a) is similar to the test result shown in Figure 39(b). A small difference can be found in temperature pattern while the maximum temperatures were both close to 27℃. On the other hand, the predicted surface temperature for test 2 is shown in Figure 85(b). The maximum temperature was located at the shorter edge of the pothole and close to 40 ℃, and the bottom of the pothole was slightly heated. These characteristics were quite similar to field measurement shown in Figure 42(b).

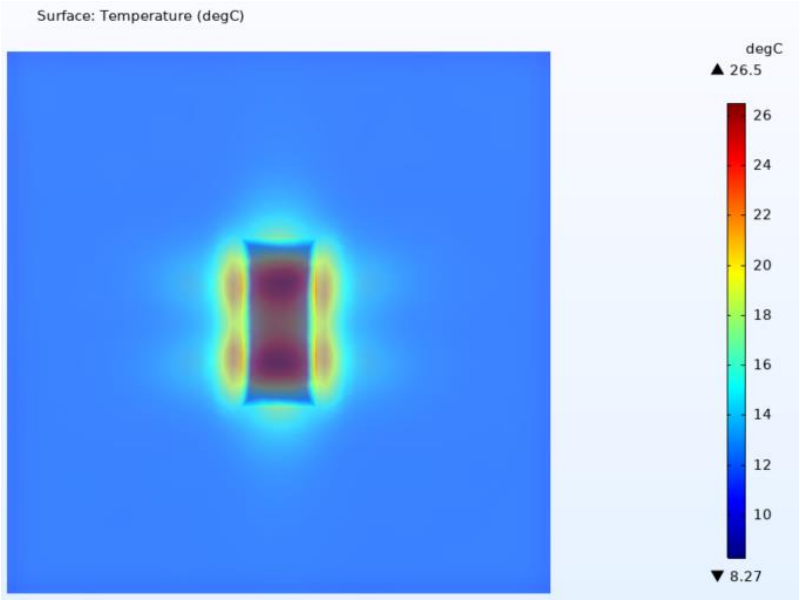

(a)

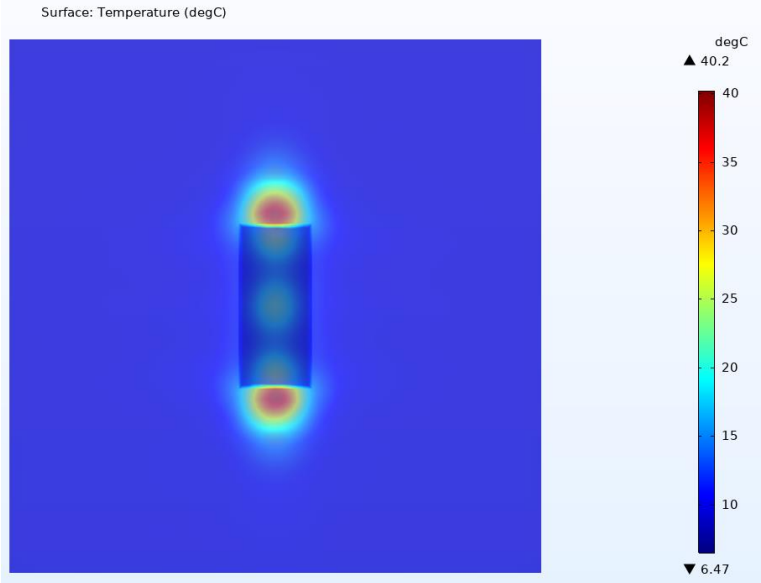

(b)

Figure 85. Predicted surface temperature distribution, (a) Test 1, (b) Test 2

Figure 86(a) and (b) show the comparison between measured temperatures detected by sensors and predicted ones for test 1 and 2, respectively. As seen, both measured and predicted temperatures increase in an approximately linear trend. There are some fluctuations in measured temperatures as compared to predicted ones, while the difference between them is minor. The discrepancies are reasonable because the edge materials of the pothole were loose during construction, and raveling distress can be found from the pothole appearances after experiencing natural weather events. Overall, from both temperature distribution and the magnitude perspectives, the predicted results from the numerical model showed a good consistency with the field measurement.

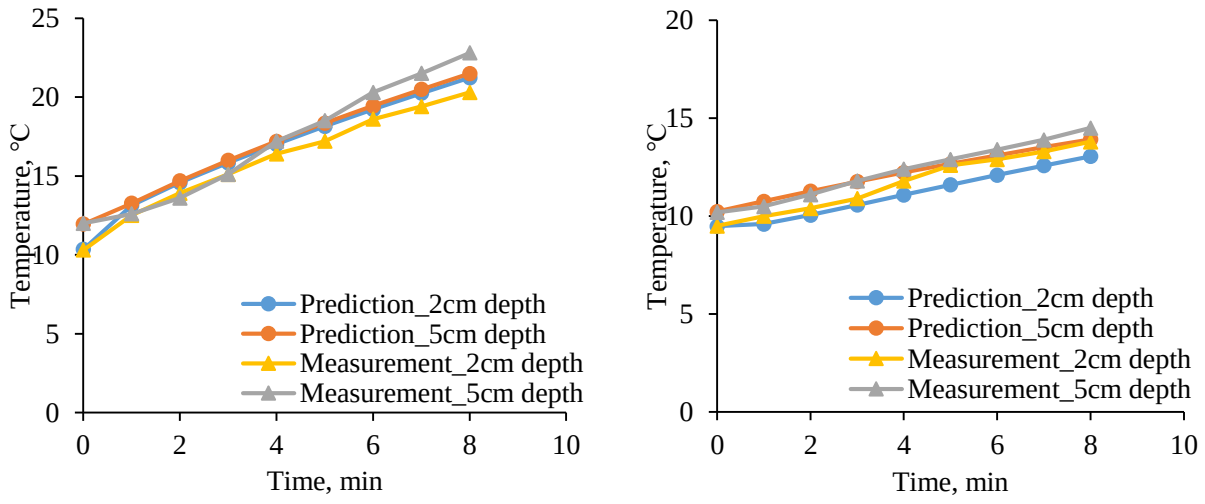

Figure 86. Temperature comparisons, (a) Test 1, (b) Test 2

Infrared heating model and validation

Figure 87(a) shows the geometry of infrared heating model. The asphalt pavement model was 1000-mm-long, 1000-mm-wide, and 150-mm-thick. The dimensions of the infrared heater were the same as the actual one used in the field test. The heating plate was surrounded by a hexahedral shield, which had an opening at the bottom to enable heat radiation. The size of the heating plates was 508mm × 280 mm × 10mm. The dimension of the opening at the bottom was 760mm × 460mm. The height of the heating plate was 150mm. Figure 87 (b) shows the meshing condition of the infrared heating model. Free tetrahedral meshes were applied to the model and there were 77,595 tetrahedron elements in total for the whole model. 9.5mm NMAS HMA was selected as the pavement material, and the material property parameters are shown in Table 22. In terms of the boundary conditions, surface-to-surface radiation was applied between the heating plate and the pavement surface. The asphalt mixtures also had convection with the air and self-radiation to the ambience. The power of the infrared heater was 4300W and its loss rate was 30%. The convection heat flux was set as 5 W/(m^2/K), and the surface emissivity was 0.9 in the modeling [98].

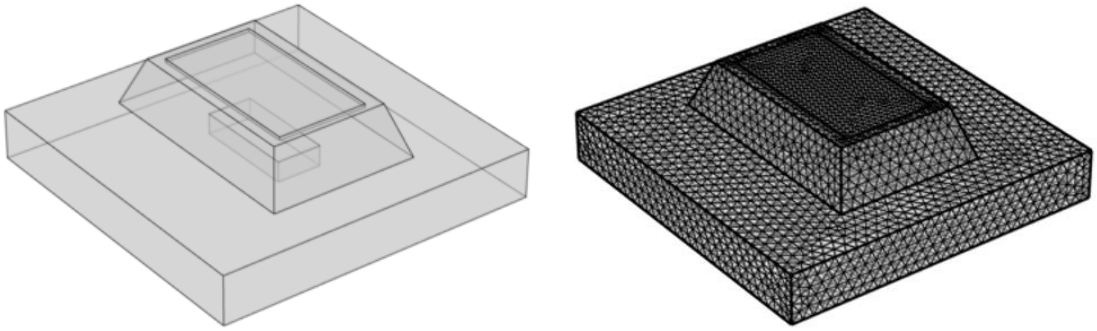

(a) (b)

Figure 87. Model development, (a) Model geometry, (b) Meshing condition

The data of the infrared heating test shown in **Error! Reference source not found.** was u sed for validation. In the modeling, the initial surface temperature of the pavement was set as 10.1℃ and the temperatures at 25-mm and 50-mm depths beside the pothole were 14.2℃ and 18.1℃, respectively. The pavement was assumed to be completely dry. Figure 88 shows comparisons of pavement temperature from field measurements and model predictions. It can be found that the general trend of predicted temperatures has good consistency with that of measured ones. The predicted surface and top edge temperatures were much higher than the internal ones, which is similar to the measured results. Although some deviations can be found in temperature predictions at different locations, the mean absolute error (MAE) was about 1 ℃ for internal temperatures and was less than 8 ℃ for top edge and surface temperatures. The errors can be attributed to raveling distress that occurred on the surface of the pothole after long-time exposure to the natural environment, the anisotropy of the pavement materials, and other environmental factors. Overall, the numerical model developed in this chapter can successfully capture the increasing trend of pavement temperatures due to infrared heating, which provides reliable results for future analysis. Additionally, this numerical

model is also applicable to predict the temperature of other HMAs after changing the corresponding thermal parameters. The thermal parameters of various asphalt mixtures under high temperatures can be found elsewhere (*21*).

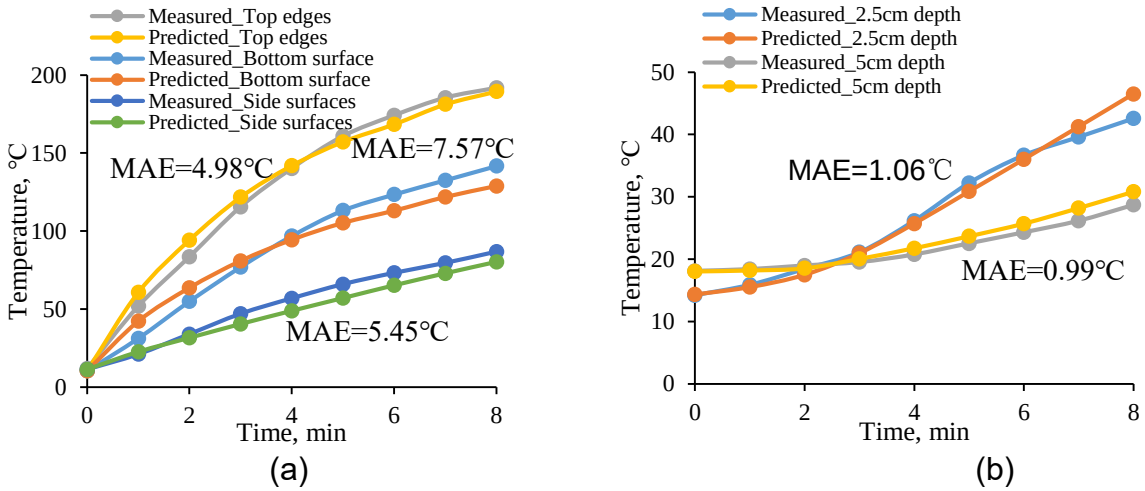

Figure 88. Validation results, (a) Surface temperatures, (b) Internal temperatures

Infrared heating time prediction and energy consumption

As the infrared heating was adopted for pothole repair, the infrared heating model was further modified to predict the required heating time under different heating powers and field conditions. Based on the field heating and laboratory testing results, 8 minutes of heating can result in satisfactory air voids and improved interface strength of asphalt patch. Therefore, the temperatures of five measurement points after 8-minutes heating as shown in **Error! Reference source not found.**(b) and (c), were set as the minimum t arget temperatures of pre-heating. The upper limit of the temperature was 200℃. On the other hand, considering that the average volume of the pothole was around 0.028m^3 based on a large scale of field observations [54], the required heating time of potholes with two different sizes was analyzed here. A big-shallow pothole with the size of 900mm × 600mm × 50mm and a small-deep pothole with the size of 640mm × 420mm × 100mm were selected. The area of the heating plate was assumed to be 1.2 times that of the pothole. The environment temperature in modeling was set as 0℃ and 20℃ to simulate cold and mild weather conditions. The initial temperature profile at different pavement depths was determined using the models developed using field measurement [99,100]. The pavement size, thermal properties of asphalt mixture, and power loss rate of infrared heater were assumed to be the same as the ones used in the validation model. Figure 89 shows an example of temperature increasing trends of big-shallow pothole under 32kW heating power at 0℃ environment. As seen, the top edges and bottom surface have high temperature increasing rates, while the internal temperature increased slowly due to low thermal conductivity. To meet the temperature requirement shown in Figure 88, approximately 2.3-minutes pre-heating are needed.

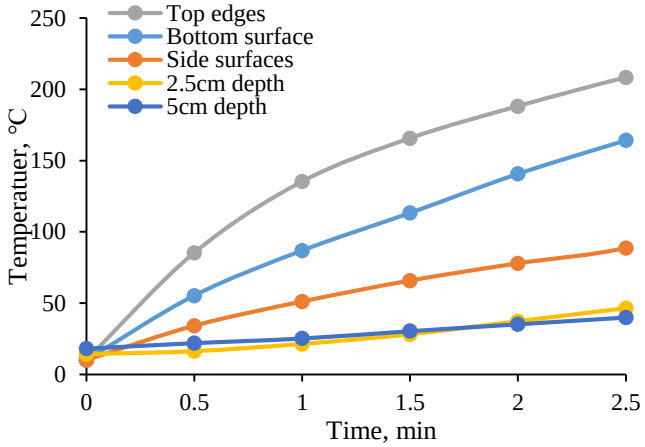

Figure 89. Temperature increasing trends

Assuming that the ideal pre-heating time in practical pothole repair will not exceed 3 minutes, the required heating time under different heater powers are calculated, as shown in Figure 90. As can be seen, the power within certain ranges can be selected and is recommended to reach the targeted temperatures. For big-shallow potholes, the recommended power ranges for pre-heating under 0℃ and 20℃ were 28kW-34kW and 26kW-42kW, respectively. For small-deep potholes, the recommended power ranges for pre-heating under 0℃ and 20℃ were 18kW-24kW and 16kW-26kW, respectively. Above the proposed ranges, the pavement surface will be overheated before the internal materials reach the target temperatures, because the temperature increasing speed of pavement surface is faster than that of internal materials. Below those ranges, longer heating time (more than 3 minutes) is needed. Within those ranges, the required heating time decreases with the increase of power.

When the environment temperature increases from 0℃ to 20℃, less heating time is needed under the same power because of higher initial temperatures of the pavement, while the difference is less than 1 minute. A higher environmental temperature also led to a wider range of power that can be selected. On the other hand, compared with the pothole with a smaller area but greater depth, the pothole with a larger area but smaller depth requires higher heating power to reach the targeted temperature because it has a larger surface area to absorb the heat. When the maximum power within the recommended range is adopted, the minimum heating time for potholes repaired is around 2 and 1.1 minutes, respectively, as the ambient environment is 0℃ and 20℃.

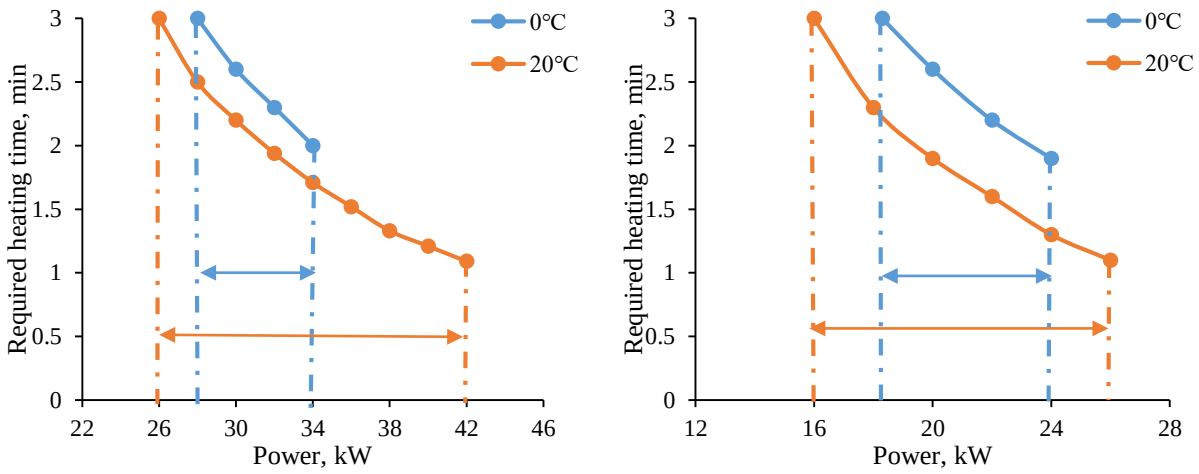

Figure 90. Required heating time under different powers, (a) Big-shallow pothole, (b) Small-deep pothole

Based on the required heating time under different powers, the energy consumption was calculated, as shown in Figure 91. As can be seen, total energy consumption decreases with the increase of power regardless of pothole sizes or ambient temperatures. It means that the higher the power of infrared heating used in pothole repair, the lower the total energy consumed. It should be noted that the selection of infrared heater power should be in the recommended range so that the targeted temperature can be reached.

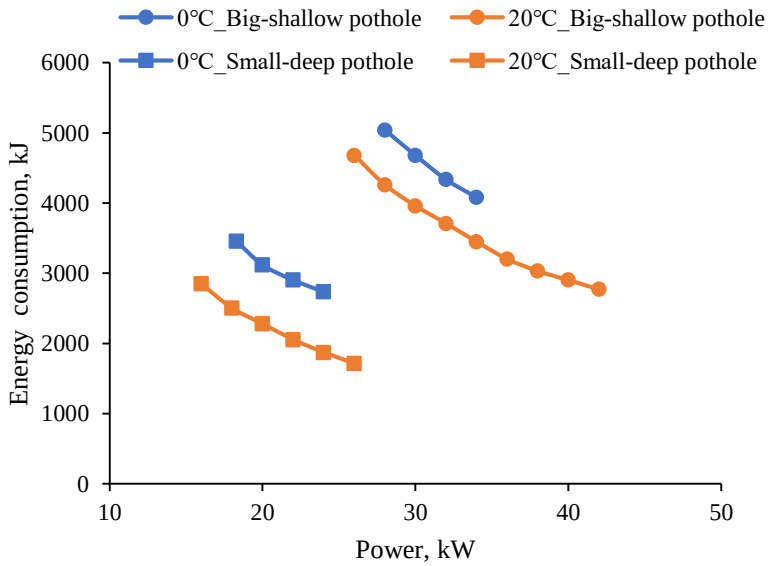

Figure 91. Energy consumption using different infrared heater powers

CONCLUSIONS

Applying Preheating to Pothole Repair

The following conclusions can be concluded from the analysis of preheating effect on the performance enhancement of asphalt pothole repair.

- By conducting field experiments, the microwave heating performance was found to significantly depend on the electromagnetic wave path, which is closely related to the orientation and shape of the port. Although it can heat both the surface and internal materials of the pavement, the heating efficiency of the microwave unit acquired in this study is low and the temperature increasing rate is unsatisfactory.

- The infrared heater was found to be capable of heating the top edges and bottom surface of the pothole to high temperatures in a short time, and the pre-heating method was successfully applied to the pothole repair.

- Based on laboratory test results, pre-heating using infrared heater was found to significantly enhance the performance of asphalt patch. It can increase not only the interface shear and tensile strength between the patching material and the surrounding pavement but also the cohesive strength of the patching material itself.

Performance of Cold Mix Asphalt as Patching Material

The following conclusions can be concluded from the laboratory experiments on different CMA patching materials.

- The bulk cold mix has the highest IDT strength 30 minutes after repair, it also has higher strength than some commercial CMA 24 hours after repair. As curing time increased, the IDT strength of commercial cold mix increased gradually. Once the commercial cold mix materials are fully cured, their final strengths are all higher than bulk cold mix.
-
- The bulk cold mix had a higher interface shear strength at an early stage after repair, and the strength of commercial cold mix will grow with time. The ultimate interface shear strength of all commercial cold mix materials is much larger than that of bulk cold mix.

Applying RAP to Pothole Repair

The following conclusions can be concluded from the laboratory and field experiments on adding RAP to HMA patching materials.

- The test results of lab specimens revealed that as RAP content increased, the IDT strength of patching material increased under dry and FT conditions while decreased under MIST condition. Regardless of conditioning environment, the mass loss of patching material increased with RAP content. Furthermore, RAP did not show significant impact on the interface shear strength.

- The abrasion loss, IDT strength, and interface shear strength of patching material were less resistant to moisture as RAP content increased. Specifically, the dynamic pore water pressure led to a more remarkable reduction in IDT and interface shear strength as compared to FT, while the impact of FT was more significant for abrasion loss.

- With application of preheating, the overall performance of HMA containing 30% RAP is satisfactory as compared to the traditional HMA. This means by incorporating preheating, it is feasible to use RAP material for asphalt pavement pothole repair.

Numerical Simulation for Temperature Prediction

The following conclusions can be concluded from the numerical analysis on temperature prediction using different heating models.

- The thermal properties of different asphalt mixtures were found to vary with temperature. The heat transfer rate was approximately linear under microwave heating, while it gradually decreased as time increased under infrared radiation.

- The developed microwave and infrared heating models were validated against field temperature measurements. The infrared heating model was further used to predict the required heating time under different field conditions with the measured thermal properties of 9.5mm HMA as model inputs.

- Increasing the power of infrared heater can improve the productivity of pothole repair with the pre-heating method. Within the recommended power range, the required heating time and the corresponding energy consumption decrease with the increase in power.

Recommendation for Future Research

The study limitations are that the artificial potholes investigated in the test section were of rectangular shape and may not represent realistic traffic and aging conditions in the field. Further study of pothole repair is recommended to be conducted on in-service pavements to verify the findings. The longevity of the potholes repaired with and without heating is recommended to be monitored to evaluate the benefit of using pre-heating and RAP on the life-cycle cost of pothole repair.

REFERENCES

1. Wilson, T. P., and Romine, A. R. (2001). *Materials and Procedures for Repair of Potholes in Asphalt-surfaced Pavements--Manual of Practice*, No. FHWA-RD-99-168.
2. Miller, J. S., and Bellinger, W. Y. (2014). *Distress identification manual for the long-term pavement performance program,* FHWA-HRT-13-092.
3. McDaniel, R.S., J. Olek, A. Behnood, B. Magee, and R. Pollock. (2014). Pavement Patching Practices, NCHRP Synthesis 463.
4. Nazzal, M. D., Kim, S. S., and Abbas, A. R. (2014). *Evaluation of winter pothole patching methods*, FHWA/OH-2014/2, Ohio. Dept. of Transportation.
5. Zanko, L. M., Hopstock, D. M., & DeRocher, W. (2016). Evaluate and develop innovative pavement repair and patching: Taconite-based repair options. Minnesota. Dept. of Transportation. Research Services & Library.
6. Wilson, T.P. (1998). Long-Term Monitoring of Pavement Maintenance Materials Test Sites, Final Report FHWA-RD-98-073, Federal Highway Administration, Mclean, Virginia.
7. Evans, L. D., Mojab, C. G., Patel, A. J., Romine, A. R., Smith, K. L., and Wilson, T. P. (1993). Innovation Materials Development and Testing, Volume I: Project Overview, No. SHRP-H-352.
8. Maupin, G.W., and Payne, C. (2003). Evaluation of Spray Injection Patching, Virginia Transportation Research Council, Charlottesville, VA.
9. Goh, S. W., You, Z., and Van Dam, T. J. (2007). Laboratory evaluation and pavement design for warm mix asphalt. In *Proceedings of the 2007 Mid-Continent transportation research symposium,* 1-11.
10. Scherocman, J. A. (2010). Compacting Stiff HMA Mixes. *Pavement Maintenance Reconstruction*, 25(3).
11. Jordan, P. G., & Thomas, M. E. (1976). *Prediction of cooling curves for hot-mix paving materials by a computer program,* TRRL Lab Rpt LR 729.
12. Daines, M. E. (1985). Cooling time of bituminous layers and time available for their compaction. Transport and road research laboratory report, 4.
13. Luoma, J. A., Allen, B., Voller, V. R., Newcomb, D. E. (1995). Modeling of heat transfer during asphalt paving. *Numerical Methods in Thermal Problems*, 6 (2), 1125-1135.
14. Timm, D. H., et al. (2001). Calcool: A multi-layer Asphalt Pavement Cooling Tool for Temperature Prediction During Construction. *International Journal of Pavement Engineering,* 2(3): 169 - 185.
15. Vasenev, A., Bijleveld, F., Hartmann, T., and Dorée, A. G. (2012). A real-time system for prediction cooling within the asphalt layer to support rolling operations. In *Euroasphalt and Eurobitume Congress*.
16. Maher, A., Gucunski, N., Yanko, W., and Petsi, F. (2001). Evaluation of Pothole Patch materials, Report FHWA 2001-02, Rutgers University, NJ.
17. Cho, Y., Kabassi, K., and Pyeon, J.H. (2011). Effectiveness Study on Temporary Pavement Marking Removals Methods. Report SPR-P1 (11) M305, Nebraska Department of Roads, Lincoln, NE.
18. Freeman, T. J., and J. A. Epps. (2012). HeatWurx Patching at Two Locations in San Antonio. No. FHWA/TX-12/5-9043-01-1. Texas Transportation Institute.

19. Byzyka, J., Rahman, M., and Chamberlain, D.A. (2018). An innovative asphalt patch repair pre–heating method using dynamic heating. *Construction and Building Materials*, 188: 178-197.
20. Daniel, J. S. (2006). Use of an infrared joint heater to improve longitudinal joint performance in hot mix asphalt pavements. *Journal of performance of constructed facilities*, 20(2), 167-175.
21. Huang, B., Chen, X., & Shu, X. (2009). Effects of electrically conductive additives on laboratory-measured properties of asphalt mixtures. *Journal of Materials in Civil Engineering*, *21*(10), 612-617.
22. Liu, W., Miao, P., and Wang, S. (2017). Increasing Microwave Heating Efficiency of Asphalt-Coated Aggregates Mixed with Modified Steel Slag Particles, *Journal of Materials in Civil Engineering*, 04017171.
23. Clyne, T.R., Johnson, E.N., and Worel, B.J. (2010). Use of taconite aggregates in pavement applications. MN/RC-2010-24, Minnesota Department of Transportation, Saint Paul, MN, USA.
24. Nieftagodien, R. (2013). *Suitability of microwave application to heat reclaimed asphalt and crushed aggregates as an energy efficient method in the production of half warm mix*, Doctoral dissertation, Stellenbosch University.
25. Jenkins, K. J. (2000). *Mix design considerations for cold and half-warm bituminous mixes with emphasis of foamed bitumen* (Doctoral dissertation, Stellenbosch: Stellenbosch University).
26. Liu, M., Han, S., Pan, J., and Ren, W. (2018). Study on cohesion performance of waterborne epoxy resin emulsified asphalt as interlayer materials. *Construction and Building Materials*, 177, 72-82.
27. Liu Q.T., Garcia, A., Schlangen, E., and Van de Ven, M. (2011). Induction Healing of Asphalt Mastic and Porous Asphalt Concrete. *Construction and Building Materials*, 25, 3746–3752.
28. Garcia, A. (2012). Self-healing of open cracks in asphalt mastic. *Fuel*, 93(1), 264-272.
29. Ekman, A., Miettinen, A., Turpeinen, T., Backfolk, K., & Timonen, J. (2012). The number of contacts in random fibre networks. *Nordic Pulp & Paper Research Journal*, 27(2), 270-276.
30. Ajam, H., Lastra-Gonzalez, P., Gomez-Meijide, B., Airey, G., and Garcia, A. (2017). Self-Healing of Dense Asphalt Concrete by Two Different Approaches: Electromagnetic Induction and Infrared Radiation, *Journal of Testing and Evaluation*, 45(6), 1933–1940.
31. Garcia, A., Norambuena-Contreras, J., Partl, M.N. (2013). Experimental evaluation of dense asphalt concrete properties for induction heating purposes, *Construction and Building Materials,* 48, 48–54.
32. Dinh, B.H., Park, D.W., and Le, T.H.M. (2018). Effect of Rejuvenators on The Crack Healing Performance of Recycled Asphalt Pavement by Induction Heating, *Construction and Building Materials*, 164, 246-254.
33. Wan, J., Wu, S., Xiao, Y., Chen, Z., and Zhang, D. (2018). Study on the effective composition of steel slag for asphalt mixture induction heating purpose. *Construction and Building Materials*, 178, 542-550.
34. Obaidi, H., Gomez-Meijide, B. and Garcia, A. (2017). A fast pothole repair method

using asphalt tiles and induction heating. *Construction and Building Materials,* 131, 592-599.
35. Garcia, A., Norambuena-Contreras, J., Partl, M.N. (2014). A parametric study on the influence of steel wool fibers in dense asphalt concrete, *Materials and Structures,* 47, 1559–1571.
36. Serfass, J. P., Poirier, J. E., Henrat, J. P. and Carbonneau, X. (2004). Influence of curing on cold mix mechanical performance. *Materials and Structures*, 37(5), 365-368.
37. Gandi, A., Cardenas, A., Sow, D., Carter, A., & Perraton, D. (2019). Study of the impact of the compaction and curing temperature on the behavior of cold bituminous recycled materials. *Journal of Traffic and Transportation Engineering (English Edition)*, *6*(4), 349-358.
38. Yuan, W. et al. (2012). DCPD resin catalyzed with Grubbs catalysts for reinforcing pothole patch materials. In *Nondestructive Characterization for Composite Materials, Aerospace Engineering, Civil Infrastructure, and Homeland Security,* 8347. International Society for Optics and Photonics.
39. Chavez-Valencia, L. E., Alonso, E., Manzano, A., Pérez, J., Contreras, M. E., and Signoret, C. (2007). Improving the compressive strengths of cold-mix asphalt using asphalt emulsion modified by polyvinyl acetate. *Construction and Building Materials*, 21(3), 583-589.
40. Abd El-Rahman, A.M.M., El-Shafie, M., Abo-Shanab, Z.L. and El-Kholy, S.A. (2017). Modifying asphalt emulsion with different types of polymers for surface treatment applications. *Petroleum Science and Technology*. 35, 1473–1480.
41. Chang, Y. T., Chen, Z. D., Zhang, Z. and Zhou, Z. G. (2017). Research on the performance of epoxy emulsified asphalt adhesive layer on asphalt pavement. *Journal of Wuhan university: engineering*, (50), 582. (In Chinese)
42. Zhang, Q., Xu, Y. H., and Wen, Z. G. (2017). Influence of water-borne epoxy resin content on performance of waterborne epoxy resin compound SBR modified emulsified asphalt for tack coat. *Construction and Building Materials*, *153*, 774-782.
43. Gaidis. J. M, Stierli. R. F, Tarver, C.C. (1976). Magnesium phosphate concrete compositions. *US Patents.*
44. Qiao, F., Chau, C.K., Li, Z. (2010). Property evaluation of magnesium phosphate cement mortar as patch repair material. *Construction and Building Materials,* 24 (5), 695-700.
45. Moseke, C., Saratsis, V., Gbureck, U. (2011). Injectability and mechanical properties of magnesium phosphate cements. *Journal of Materials Science-Materials in Medicine,* 22 (12), 2591-2598.
46. Chau, C. K., Qiao, F., Li, Z. (2012). Potentiometric study of the formation of magnesium potassium phosphate hexahydrate. *Journal of Materials in Civil Engineering,* 24 (5), 586-591.
47. Li, J., Xu, G., Chen, Y., and Liu, G. (2014). Multiple scaling investigation of magnesium phosphate cement modified by emulsified asphalt for rapid repair of asphalt mixture pavement. *Construction and Building Materials*, *69*, 346-350.
48. Issa, R., Zaman, M. M., Miller, G. A. and Senkowski, L. J. (2001). Characteristics of cold processed asphalt millings and cement emulsion mix, *Transportation Research Record*, 1767, 1–6.

49. Ma, T., H. Wang, Y.L. Zhao, and X.M. Huang. (2015). Strength Mechanism and Influence Factors for Cold Recycled Asphalt Mixture, *Advances in Material Science and Technology*, Vol. 2015, 181853.
50. Ferrotti, G., E. Pasquini, and F. Canestrari. (2014). Experimental Characterization of High-Performance Fiber-Reinforced Cold Mix Asphalt Mixtures. *Construction and Building Materials*, 57: 117-125.
51. Zhao, Y. X. and Zhang, L. (2007). Application of modified emulsified asphalt fiber sealing layer in pavement surface construction. *Journal of Liaoning communications college* (04), 27-28. (In Chinese)
52. Shanbara, H. K., Ruddock, F., and Atherton, W. (2018). A laboratory study of high-performance cold mix asphalt mixtures reinforced with natural and synthetic fibers. *Construction and Building Materials*, 172, 166-175.
53. Bueno, B., Da Silva, W. R., De Lima, D. C., and Minete, E. (2003). Engineering properties of fiber reinforced cold asphalt mixes. *Journal of Environmental Engineering*, 129(10), 952-955.
54. Wilson, T. P., and Romine, A. R. (1993). *Innovative materials development and testing. Volume 2: Pothole repair* (No. SHRP-H-353).
55. Prowell, B. D., & Franklin, A. G. (1996). Evaluation of cold mixes for winter pothole repair. *Transportation Research Record*, 1529, 76-85.
56. Smith, K. L., Peshkin, D. G., Rmeili, E. H., Dam, T. V., Smith, K. D., & Darter, M. I. (1991). Innovative materials and equipment for pavement surface repairs. Volume I: Summary of material performance and experimental plans (No. SHRP-M/UFR-91-504).
57. Dailey, J., Dave, E. V., Barman, M., & Kostick, R. D. (2017). Comprehensive field evaluation of asphalt patching methods and development of simple decision trees and a best practices manual (No. MN/RC 2017-25). Minnesota. Dept. of Transportation. Research Services & Library.
58. Zanko, L.M., and Hopstock, D.M. (2004). Minnesota taconite as a microwave-absorbing road aggregate material for deicing and pothole patching applications, University of Minnesota Duluth, Natural Resources Research Institute, and University of Minnesota Center for Transportation Studies, Minneapolis, MN.
59. Cox, B. C., Floyd, W. C., Rushing, J. F., Carr, T. A., & Rutland, C. A. (2020). Feasibility investigation of inductive heating of asphalt repair materials.
60. Ozbay, K., Parker, N. A., & Jawad, D. (2003). *Guidelines for life cycle cost analysis* (No. FHWA-NJ-2003-012).
61. AASHTO, T. (2007). 322; Standard Method of Test for Determining the Creep Compliance and Strength of Hot Mix Asphalt (HMA) Using the Indirect Tensile Test Device. *American Association of State Highway Transportation Officials: Washington, DC, USA*.
62. Abdalla, A., Faheem, A. F., & Walters, E. (2022). Life cycle assessment of eco-friendly asphalt pavement involving multi-recycled materials: A comparative study. *Journal of Cleaner Production*, *362*, 132471.
63. Hajj, R., and Y. Lu. (2021). Current and Future Best Practices for Pothole Repair in Illinois. Report No. FHWA-ICT-21-003. Illinois Center for Transportation/Illinois Department of Transportation, Springfield.

64. Ghosh, D., Turos, M., Hartman, M., Milavitz, R., Le, J. L., & Marasteanu, M. (2018). Pothole prevention and innovative repair. Minnesota Department of Transportation.
65. AASHTO, T. (2011). 283-07. Standard Method of Test for Resistance of Compacted Asphalt Mixtures to Moisture-Induced Damage*. American Association of State and Highway Transportation Officials, Washington, DC*, *USA.*
66. ASTM, D. (2020). 7870; Standard Practice for Moisture Conditioning Compacted Asphalt Mixture Specimens by Using Hydrostatic Pore Pressure. *American Society for Testing and Materials: West Conshohocken, PA, USA*.
67. Yu, S., Shen, S., Zhou, X., & Li, X. (2018). Effect of partial blending on high content reclaimed asphalt pavement (RAP) mix design and mixture properties. *Transportation Research Record*, *2672*(28), 79-87.
68. Han, S., Cheng, X., Liu, Y., & Zhang, Y. (2019). Laboratory performance of hot mix asphalt with high Reclaimed Asphalt Pavement (RAP) and Fine Reclaimed Asphalt Pavement (FRAP) content. *Materials*, *12*(16), 2536.
69. Shu, X., Huang, B., Shrum, E. D., & Jia, X. (2012). Laboratory evaluation of moisture susceptibility of foamed warm mix asphalt containing high percentages of RAP*. Construction and Building Materials*, *35*, 125-130.
70. LaCroix, A., Regimand, A., James, L. (2016). Proposed Approach for Evaluation of Cohesive and Adhesive Properties of Asphalt Mixtures for Determination of Moisture Sensitivity, *Transportation Research Record,* 2575: 61-69.
71. AASHTO, T. (2014). 108; Standard Method of Test for Determining the Abrasion Loss of Asphalt Mixture Specimens. *American Association of State Highway and Transportation Officials: Washington, DC, USA*.
72. Yang, C., Wu, S., Cui, P., Amirkhanian, S., Zhao, Z., Wang, F., ... & Xie, J. (2022). Performance characterization and enhancement mechanism of recycled asphalt mixtures involving high RAP content and steel slag. *Journal of Cleaner Production*, *336*, 130484.
73. Xu, L., Magar, S., Zhao, Z., Xiang, Q., & Xiao, F. (2023). Rheological and anti-moisture characteristics of rubberized reclaimed asphalt pavement with interfacial bond behavior*. Journal of Cleaner Production*, *391*, 136172.
74. Doyle, J. D., & Howard, I. L. (2011). Evaluation of the cantabro durability test for dense graded asphalt. In *Geo-Frontiers 2011: Advances in Geotechnical Engineering*. 4563-4572.
75. Chen, X., Wang, H., & Venkiteela, G. (2023). Asphalt Pavement Pothole Repair Using the Pre-Heating Method: An Integrated Experiment and Modeling Study*. Transportation Research Record*, 03611981231164066.
76. Christensen, D. W., Bonaquist, R., & Jack, D. P. (2000). *Evaluation of triaxial strength as a simple test for asphalt concrete rut resistance* (No. FHWAPA-2000-010+ 97-04 (19)).
77. Fang, Y., Zhang, Z., Wang, S., Yang, J., & Li, X. (2022). Determination of minimum dynamic modulus (E*) of high modulus asphalt concrete applied to semirigid base asphalt pavement. *Journal of Materials in Civil Engineering*, *34*(1), 04021378.
78. Li, S., Sun, Y., Xu, L., Yu, S., Liang, X., & Ye, J. (2022). Asphalt Layer Cracking Behavior and Thickness Control of Continuously Reinforced Concrete and Asphalt Concrete Composite Pavement. *Buildings*, *12*(8), 1138.

79. Bentz, D. P. (2007). Transient plane source measurements of the thermal properties of hydrating cement pastes. *Materials and structures*, *40*, 1073-1080.
80. Chadbourn, B. A., Luoma, J. A., Newcomb, D. E., & Voller, V. R. (1996). Consideration of hot mix asphalt thermal properties during compaction. *ASTM Special Technical Publication*, *1299*, 127-141.
81. Byzyka, J., Rahman, M., & Chamberlain, D. A. (2021). A laboratory investigation on thermal properties of virgin and aged asphalt mixture. *Construction and Building Materials*, *305*, 124757.
82. Jamshidi, A., Kurumisawa, K., Nawa, T., Mao, J., & Li, B. (2017). Characterization of effects of thermal property of aggregate on the carbon footprint of asphalt industries in China. *Journal of traffic and transportation engineering (English edition)*, *4*(2), 118-130.
83. Heddleson, R. A., & Doores, S. (1994). Factors affecting microwave heating of foods and microwave induced destruction of foodborne pathogens–a review. *Journal of Food Protection*, *57*(11), 1025-1037.
84. Chen, J., Wang, H., & Li, L. (2015). Determination of effective thermal conductivity of asphalt concrete with random aggregate microstructure. *Journal of Materials in Civil Engineering*, *27*(12), 04015045.
85. Benedetto, A., & Calvi, A. (2013). A pilot study on microwave heating for production and recycling of road pavement materials. *Construction and Building Materials*, *44*, 351-359.
86. Zhu, H., Yuan, H., Liu, Y., Fan, S., & Ding, Y. (2020). Evaluation of self-healing performance of asphalt concrete for macrocracks via microwave heating. *Journal of Materials in Civil Engineering*, *32*(9), 04020248.
87. Gallego, J., del Val, M. A., Contreras, V., & Páez, A. (2013). Heating asphalt mixtures with microwaves to promote self-healing. *Construction and Building Materials*, *42*, 1-4.
88. Chen, F., & Balieu, R. (2020). A state-of-the-art review of intrinsic and enhanced electrical properties of asphalt materials: Theories, analyses and applications. *Materials & Design*, *195*, 109067.
89. Chen, J., Wang, H., & Xie, P. (2019). Pavement temperature prediction: Theoretical models and critical affecting factors. *Applied thermal engineering*, *158*, 113755.
90. Vo, H. V., & Park, D. W. (2017). Application of conductive materials to asphalt pavement. *Advances in materials science and engineering*, *2017*.
91. Wang, H., Zhang, Y., Zhang, Y., Feng, S., Lu, G., & Cao, L. (2019). Laboratory and numerical investigation of microwave heating properties of asphalt mixture. *Materials*, *12*(1), 146.
92. Chang, C. M., Chen, J. S., & Wu, T. B. (2011). Dielectric modeling of asphalt mixtures and relationship with density. *Journal of Transportation Engineering*, *137*(2), 104-111.
93. Jaselskis, E. J., Grigas, J., & Brilingas, A. (2003). Dielectric properties of asphalt pavement. *Journal of materials in Civil Engineering*, *15*(5), 427-434.
94. Zhong, Y., Gao, Y., Zhang, B., Li, S., Cui, H., Li, X., & Zhao, H. (2021). Experimental study on the dielectric model of common asphalt pavement surface materials based on the LR model. *Advances in Civil Engineering*, *2021*, 1-8.

95. Porubiaková, A., & Komačka, J. (2015). A comparison of dielectric constants of various asphalts calculated from time intervals and amplitudes. *Procedia Engineering*, *111*, 660-665.
96. Leng, Z., Al-Qadi, I. L., & Lahouar, S. (2011). Development and validation for in situ asphalt mixture density prediction models. *NDT & e International*, *44*(4), 369-375.
97. Hosokawa, H., Kanzaki. Y., Gomi. A., and Kasahara, A. 2007. A Case Study of Work done by a HOT IN-PLACE RECYCLING (HIR) Machines. International Conference on Pavement Technology, Beijing, China, March.
98. Byzyka, J., Rahman, M., & Chamberlain, D. A. (2020). Thermal analysis of hot mix asphalt pothole repair by finite-element method. *Journal of Transportation Engineering, Part B: Pavements*, *146*(3), 04020029.
99. Diefenderfer, B. K., I. L. Al-Qadi, S. D. Reubush, and T. E. Freeman. Development and Validation of a Model to Predict Pavement Temperature Profile. Presented at 68th Annual Meeting of the Transportation Research Board, Washington, D.C., 2003.
100. Adwan, I., Milad, A., Memon, Z. A., Widyatmoko, I., Ahmat Zanuri, N., Memon, N. A., & Yusoff, N. I. M. (2021). Asphalt pavement temperature prediction models: A review. *Applied Sciences*, *11*(9), 3794.